ADDIS ABABA UNIVERSITY

SCHOOL OF EARTH SCIENCES

GRADUATE STUDY PROGRAMS

Partial fulfillment of the Degree of Master's Thesis in Mineral Exploration entitled:

THE GEOLOGY, TIMING EVENT AND ROLES OF QUARTZ PORPHYRY INTRUSIONS, IN VMS GOLD MINERALIZATION AT TERAKIMTI AREA, NORTH-WEST SHIRE, NORTHERN ETHIOPIA

Prepared by: Gashaw Wudie

Advisors

Dr. Worash Getaneh: Main Advisor

Dr. Mulugeta Alene: Co-Advisor:

@AAU ***June, 2016***

Declaration

I declare this thesis is my original work under supervision of Dr. Worash Getaneh and Dr. Mulugeta Alene at Addis Ababa University, College of Natural Sciences, School of Earth sciences, during 2015/2016 as partial fulfillment of the requirements for the degree of Master of Earth Science in Mineral Exploration. I further declare that this work has not been submitted to any other University or institution for award of any degree or diploma and all sources of materials used for this thesis have duly acknowledged.

Gashaw Wudie

Signature _____Date_____

June, 2016

Addis Ababa University
School of Earth Sciences Graduate Studies

Approval

This is to certify that the thesis prepared by **Gashaw Wudie**, entitled: *The Geology, Timing event and Roles of Quartz Porphyry intrusions on the VMS gold Mineralization at Terakimti area North West shire, Northern Ethiopia* submitted in partial fulfillment of the requirements for the Degree of Master of Earth Science (Mineral Exploration) complies with the regulations of the University and meets the accepted standards with respect to originality and quality.

Signed by Advisors and Examining Committees:

Dr Worash Getaneh (Main Advisor) Signature _____Date _____

Dr Mulugeta Alene (Co-Advisor) Signature _____Date _____

Prof. Tilahun Mamo (Examiner) Signature_____Date _____

Dr Zerihun Desta (Examiner) Signature _____Date _____

Dr Zemenu G/Yigzaw (Chairman) Signature_____ Date_____

Dr Balemwal Atnafu Signature_____ Date_____
(Chair Man of School of Earth Sciences)

Abstract

The volcanogenic massive sulfide gold and base metal mineralization at Terakimti area is part of the Southern Arabian Nubian Shield. This is one of the gold and base metal enriched area among many terrains in the shield and Northern Ethiopia. Many exploration companies and research groups are attracted to this area. The mineralization at Terakimti is intruded by several quartz porphyry intrusions. This work is conducted to determine the geology, the timing relation between the quartz porphyry intrusions with each other and with the VMS deposits and roles of the intrusions on the mineralization.

Different methods are adopted to complete this work. These are geological mapping and structural description; thin section and polished section description of the lithologies; analysis and interpretation of the trace and major elements of major host rock units. More over the precious and base metal element interpretations is conducted.

The major lithological units of the area includes basalts, rhyolits, some mafic and felsic volcanoclastics, several quartz porphyry intrusions, several quartz veins and gossans. The porphyry intrusions show homogenous characteristic of geological, mineralogical, structural and geochemical (major, trace, precious and base metallic) element. Based on the time of formation three types of mineralization are identified at Terakimti area. These are VMS deposits, mineralization in the quartz porphyry intrusions and supergene deposits

The mineralization and the metallic elements of the VMS systems at Terakimti are remobilized by the late coming quartz porphyry intrusions. As compared to the VMS deposits, the quartz porphyries are weakly mineralized and it interrupts the continuity of the VMS deposits. The remobilization and relocation of the massive sulfide deposits and mineralized bodies causes slightly scattered distribution of the VMS deposits. The gossan is related to the two types of mineralization especially the VMS. Generally this work described the basic relation between the mineralization of Terakimti area and could have contribution to the scientific community and the exploration groups.

Acknowledgment

First and for most I would like to acknowledge my supervisor Dr Worash Getaneh for his tremendous professional support, encouragement, persistent and continuous corrections of the work and scientifically writing the paper, limitless support providing materials and laboratory analysis. He helped me in making agreements with companies to work in the site and searching financial budget.

I would always give grateful thanks to my second supervisor Dr Mulugeta Alene for his great professional and technical contribution, technical methods of field data collection and laboratory works and correction of the final work.

I am grateful to Addis Ababa University giving this MSC scholarship and the sponsoring institution Bahir Dar University. It is also my pleasure to say thanks to the Ethiopian Geological Survey and Australian Laboratory Service for the laboratory works.

It is also my deep thanks to Dr Stephen Gardoll senior geologist at East African Metals Harvest Project. He gave me technical reports and material support including the accommodation service.

I would like to acknowledge Mr. Teketsel Tsige (country manager of the East African Metals project), Mr. Siyum (vice country manager) and Mr. Wubshet Kassay (Harvest project manager of the Tigray Resources Incorporated Plc). It is also my grateful to Mr. Asmerom, Mr. Haile and Mr. Mulualem and other co-workers for their unlimited help in the field and office works and other co workers. Finally it is my deep thanks to my families and my great friends for their limitless support and cooperative works.

Table of Contents

List of Figures

List of Tables

List of Acronyms

ALS: Australian Laboratory Service

ANS: Arabian Nubian Shield

DD: Diamond Drilling

EAO: East African Orogeny

EGS: Ethiopian Geological Survey

HREE: Heavy Rare Earth Element

ICP-AES: Inductively Coupled Plasma Atomic Emission Spectrometry

ICP-MS: Inductively Coupled Plasma Mass Spectrometry

LILE: Large Ion Lithophile Elements

LREE: Light Rare Earth Element

MOB: Mozambique Orogenic Belt

MSL Mean sea level

NMAE National Metrological Agency of Ethiopia

PAO Pan African Orogeny

PLC: Private Limited Company

PPL: Plane Polarized Light

PPM: Parts Per Million

PREP: Preparation

QPOR: Quartz Porphyry

RC: Reverse Circulation

REE: Rare Earth Element

VMS: Volcanogenic Massive Sulfide

XPL: Crossed Polarized Light

XRF: X-ray fluorescence

Chapter 1 Introduction

1.1 General background

The knowledge of where, when and how ore mineral deposits form and distributed has been worked out by geologists for many hundreds of years since the earliest on the subject by Agricola in the 16th century and before that time by natural philosophers. The growth of knowledge about formation of mineral deposits through this period of time and key indicator features for the future has resulted in continuous attempts at classification of ores. Successive attempts are building upon accumulated knowledge as ore bodies continue to be discovered. Detailed knowledge of geologic environments and processes has grown from research in the field and laboratory by different experts. Thus knowledge about the formation of ores, environment of formation and their classification categories based on different criteria has moved on parallel tracks. Hypothesis related to formation contribute to modification of existing system of classification and create new classifications based on the new discoveries. In the late 20th century, knowledge of the genesis of ores continues to expand at an alarming rate, and corresponding modifications of classification scheme continued (The International Study Group technical report, 2011).

The formation of mineral deposits in Africa as well as Ethiopia is related to the formation of East African Orogeny (EAO). The East African Orogeny developed due to the collision of East and West Gondwana, which finally formed the Gondwana Supercontinent (De Wit and Chewaka, 1981; Stern, 1994; Stern, 2002; Stern et al., 2005; Gray, 2005). The EAO represents one of the Earth's greatest collision zones. The tectonic evolution of the EAO involves the following successive processes. (1) Rodinia rifting and break-up; (2) seafloor spreading as well as arc and back-arc basin formation and terrane accretion; (3) continent-continent collision and (4) further crustal shortening, orogenic collapse and extension finally leading to the break-up of Gondwana which takes place at different times (Blasband et al., 2000; Dewit and Chewaka, 1981; Stern, 1994; Stern et al., 2006; Asfawossen Asrat et al., 2001).

The southern part of the EAO is represented by the Mozambique Orogenic Belt (MOB), resulted by collision between East Africa and East Gondwana – India. The polycyclic Proterozoic Mozambique Mobile Melt, a major geotectonic unit with a dominant northerly structural trend, extends for some 5000 km along the eastern margin of the African

Precambrian shields. The Mozambique Belt comprises high-grade gneisses, migmatites and schists (Asfawossen Asrat et al., 2001). This belt can be traced in southern, western, and eastern Ethiopia (Berhe, 1990; Asfawossen Asrat et al., 2001). A bifurcation in southern Ethiopia separates a northeastern branch extending from southern Kenya into the Horn of Africa and southern Arabia, from the main belt which continues into Western Ethiopia and the Sudan. The two branches i.e. the ANS and the MOB which are composed mainly of polymetamorphic continental lithosphere are separated by the Adola belt comprising crust of fundamentally different origin and mineralized rocks (Kasmin et al., 1978).

The Arabian Nubian Shield (ANS) is the northern half of the great collision zone called the East African Orogeny which is formed, when east and west Gondwana collided to form the supercontinent Gondwana (Vail, 1985; Stoeser and Camp, 1985; Johnson et.al., 2011; Johnson, 2014). It extends 2200 km along north-south and 1200 km east-west and is represented by Precambrian crystalline rocks exposed along the flanks of the Red Sea. It is generally believed that the Nakfa Terrane of the Eritrean basement has served as a linking terrane that connected the geology of northern Ethiopia particularly of Axum area to the rest of ANS in the north (Barrie et al., 2007; Asfawossen Asrat et al., 2001; Beyth, 1971). The geology of northern Shire is a linking terrane of the Axum area where those are the southern end of the Arabian Nubian Shield (Tarekegn Tadesse, 1997; Archibald et al., 2014).

1.2 Location and accessibility of the study area

The study area is located in the North West Shire, Northern Ethiopia, at particular place called Terakimti. The area is bounded by latitude of 1583000 N to 1587000 N and longitude of 413000E to 419000E which is at 1200 km from the capital city of Addis Ababa. The area covers 5km by 6km east-west and north-south respectively. The study area can be accessed by flights from Addis Ababa to Shire during the dry season or from Addis Ababa to Axum throughout the year. Accessibility in the area is through the paved roads, unpaved roads, foot trials and crossing the terrains through the bare ground.

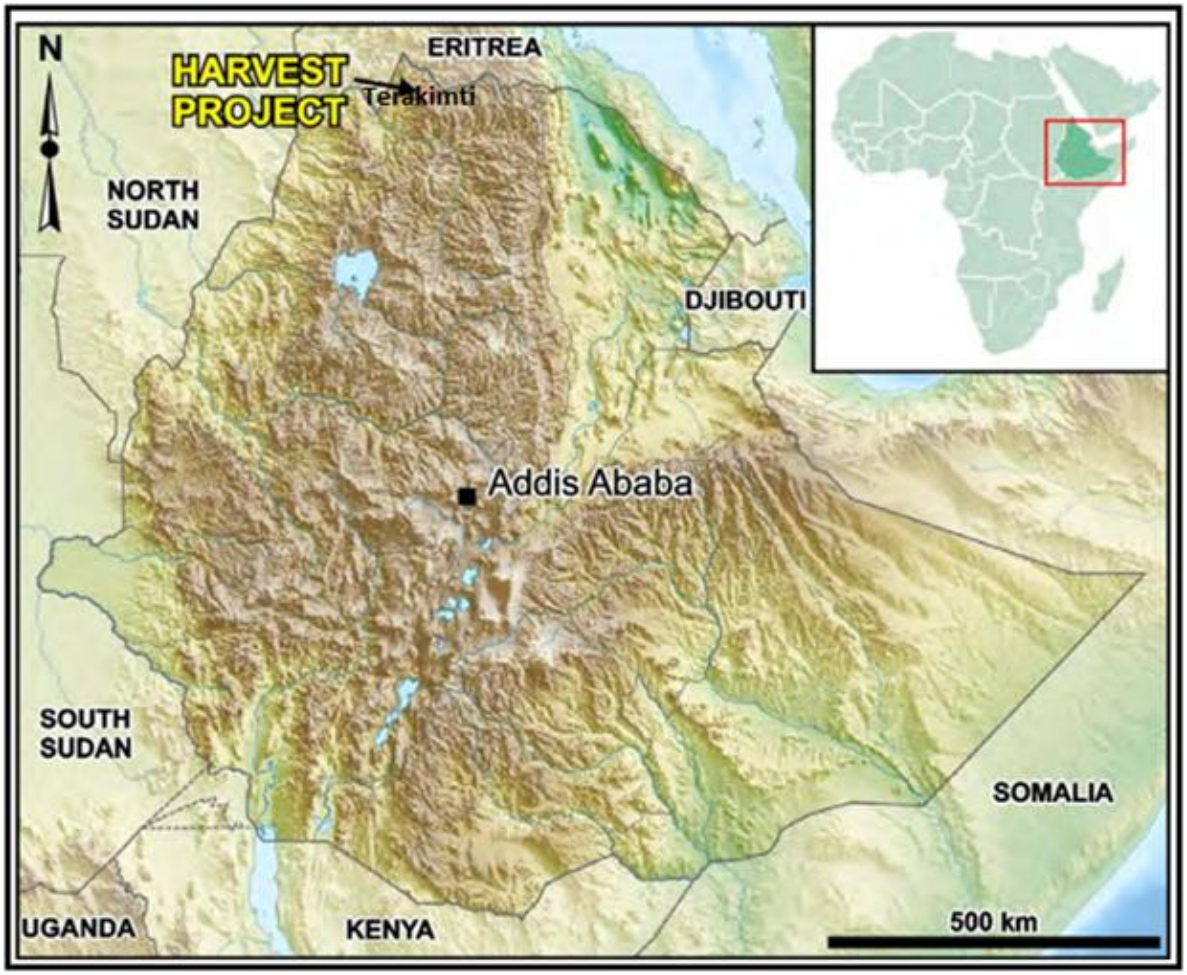

Figure 1.1 Location map of the study area.

1.3 Physiography of the study area

The topography of the study area is characterized by undulating chains such as hill terrains, domes and gentle surfaces. The nature of the drainage patterns are mostly dendrite where one river locally called Deba crosses the entire area and the others are tributaries of this river. The hilly terrains are covered by short trees and bushes.

1.4 Climate of the study area

The area is characterized by hot and cold climates of both dry and rainy seasons. According to National Metrological Agency of Ethiopia (2013) the rainy season extends from mid June to mid September with an average rainfall of 800mm to 1000mm per year. The minimum temperature reaches up to 13^{o}C in January and the maximum reaches up to 35 in April and may.

1.5 Population settlement

The population settlement in the area is sparsely populated where most of them are farmers. The main source of income for the local peoples is artisanal gold mining following the local rivers. In addition to this farmers also grow crops like teff, barely, wheat and others.

Figure 1.2 The local peoples collecting gold.

1.6 Objectives of the study

1.6.1 General objective

The general objective of the research is to study the geology of the area and to determine the relationship between the gold rich VMS deposits and the quartz porphyry intrusions.

1.6.2 Specific objectives

The specific objectives include:

- Preparing the geological map of the study area at 1:10,000 scale,
- Determine the relative timing of quartz porphyries and mineralization,
- Investigate the mineralogy, nature of mineralization and role of the quartz porphyry intrusions on the VMS mineralization.

Chapter 2 Methodologies and Analytical Procedures

Detailed literature review of the geology and tectonic setting, geological structures, the geochemical characteristics (rock, soil and sediment geochemistry) and geomorphology of the area are conducted. After these logical methods of data collection, analysis, synthesis and interpretations of the results is successfully conducted. The basic methodologies adopted to compile this research work involve detailed investigation in three important phase of activities namely pre-field work, field work and post field work phase. The detailed works at each phase are described as follows.

Pre-field work

In the pre-field work stage of the research different literatures from different sources were collected and reviewed. Important types of secondary data are collected. The laboratory and field instruments such as petrographic microscope, ore microscope, geochemical analytical equipments and others and their working procedures were identified and described. The different types of soft ware such as ARC GIS, global mapper, Google Earth, MapInfo, stereographic plotting software such as georient, geochemical soft ware like petrography are studied. More over the necessary materials and were collected and procedures are reviewed for field work and mapping.

Fieldwork

The fieldwork activity was conducted in two phases. The first phase was devoted for preliminary field work and reconnaissance survey of the area and to collect different secondary data. During this work 47 drill holes of quartz porphyry bodies are logged, and 8 core samples are collected. After this field eight thin sections and eight polished sections of the quartz porphyry intrusions and the massive sulfide bodies from the drill core samples are prepared at Addis Ababa University, School of Earth Sciences and the Geological Survey of Ethiopia respectively.

The second phase of the field work took one month. Logging the drill holes which were not completed in the first phase of the field work was conducted. Accordingly 112 drill holes including the first 47 holes were logged with their specific ground location. A total of more than 205 quartz porphyry bodies intersected by these holes are described as shown at appendix-2. These quartz porphyry intrusions are characterized. In addition to these criteria

the type of geologic units' overlaying and underlying the quartz porphyry bodies and the geologic unit intruded by the quartz porphyry intrusions are taken into consideration.

The geological mapping of the study area is completed at 1:10,000 scale. The field geological map is prepared and is digitized using ARC GIS. Detailed primary lithological, structural, mineralogical and deformational data are collected in the field at the second phase of the field work. Representative rock samples are collected from surface outcrops and from drilled core material to assess the geochemical value of the lithologies, for petrographical study of the rock units and to study the ore mineralogy. From these samples around 25 rock samples are brought to the office and from these, ten samples are selected for geochemical, thin section and polished section works.

Varieties of geological and structural data are collected from the quartz porphyry intrusions and host rock units at the outcrop and they are described and measured. The geological structures of the area and their orientations are measured using the available measuring instruments and they are plotted using soft ware. In addition to these the different types of secondary data such as technical reports, precious and base metal assayed values such as Au, Ag, Cu, Pb and Zn are collected from different sources. From the cross cutting relationships and the different secondary data the quartz porphyry intrusions and their relative timing with respect to each other and with respect to the host rock and the geological structures have been determined.

Post field work

As soon as the field work activities are completed the post field activities started immediately and the following important activities with appropriate and supporting instruments are performed. Data collected from the different sources such as primary data collected from field and secondary data collected from different sources are compiled, summarized and organized. Sixteen polished sections and eighteen thin sections are prepared for the representative rock samples collected in the field. More over ten samples were analyzed for major and trace elements using Inductively Coupled Plasma Atomic Emission Spectrometry (ICP-AES) and Inductively Coupled Plasma Mass Spectrometry (ICP-MS) respectively. This is conducted at standard geochemical laboratory (ALS Geochemistry in Ireland). Generally Table 2.1 shows the types of samples and the laboratory analysis made from these samples.

2.1 Geochemical analysis and methods

The sample preparations are completed at one of the ALS laboratory branch at Addis Ababa, Akaki Kaliti, Ethiopia and send for analysis to Ireland. The samples are crushed to that 70% of the crushed powders are less than 2mm size and these samples are pulverized and split to more than 85% passing the 75 microns. The rifle split off to the size of 1kg. This method is generally coded as PREP-31B. The preparation method is the same for all the major and trace element geochemical samples. The analytical process is conducted by fused bead using lithium borate fusion, acid digestion and finally analyzed by the Inductively Coupled Plasma Atomic emission spectrometry (ICP-AES) method for the major elements. The trace elements are prepared by the lithium borate fusion of the powdered samples prior to acid dissolution and analysis is done by inductively coupled plasma mass spectroscopy (ICP-MS). The rest of the metallic elements analytical works like gold, silver and other base metals such as Cu, Zn and Pb are completed by the Tigray Resources Incorporated PLC.

Table 2.1 Types of samples and laboratory analysis **(**The tick mark indicates that the sample analysis is conducted for the given method and the X sign is not analyzed)

Sample code	Sample location		Analysis type				Sample type	Rock unit
	Easting	Northing	Thin section	Polished section	Major element	Trace element		
GS001-A	416410	1583693	✓	✓	X	X	Core	VMS
GS001-B	416410	1583693	✓	✓	X	X	Core	VMS
GS002	416410	1583693	✓	✓	X	X	Core	porphyry
GS003	416410	1583693	✓	✓	X	X	Core	porphyry
GS004	416410	1583693	✓	✓	✓	✓	Core	porphyry
GS005	416409	1583693	✓	✓	✓	✓	Core	porphyry
GS006	416409	1583693	✓	✓	X	X	Core	porphyry
GS007	416395	1583711	✓	✓	X	X	Core	porphyry
T1L3	415475	1584470	✓	✓	✓	✓	Surface	Basalt
T1L4	415221	1584905	✓	✓	✓	✓	Surface	porphyry
T2L2	415350	1582286	✓	X	✓	✓	Surface	Rhyolite
T2L3	414744	1582538	✓	✓	X	X	Surface	Porphyry
T3L1	416540	1583755	✓	✓	X	X	Surface	Basalt
T3L3	416987	1583886	✓	X	✓	✓	Surface	Rhyolite
T3L4	417350	1584572	✓	✓	X	X	Surface	Rhyolite
T3L5	417112	1585370	✓	✓	✓	✓	Surface	Basalt
T3L6	416980	1585760	✓	✓	✓	✓	Surface	porphyry
T4L1	412560	1581660	✓	✓	✓	✓	Surface	Rhyolite
T4L2	413170	1583260	X	X	✓	✓	Surface	porphyry

Chapter 3 Geology of the study area

3.1 Regional Geology

The development of the Ethiopian basement is directly or indirectly related with the Arabian Nubian shield (ANS) and the Mozambique Orogenic Belt (MOB) both of which are related to the formation of the East African Orogene (EAO). The Axum formation of northern Ethiopia provides that the geology of the region is the southern part of the Arabian Nubian Shield (Tarkegn Tadesse et al., 1999; Tarekegn Tadesse, 1996 and 1997; Abdelsalam and Stern, 1996). The Arabian Nubian Shield extends from Jordan and southern Israel in the north to Eritrea and Ethiopia in the south and Egypt in the west to Arabia and Oman in the east (Blasband et al., 2000; Archibald et al., 2014). Most of the Precambrian volcano-sedimentary sequences and associated intrusions have been subjected to several orogenic episodes during the Pan African Orogeny, which is the cause for the formation of the Arabian–Nubian Shield terranes (Solomon Tadesse et al, 2003). The Arabian-Nubian shield hosts numerous VMS deposits, orogenic lode gold deposits and placer deposits practiced by artisanal workers (Barrie et al., 2007). The ANS hosts approximately sixty VMS) deposits in several districts found all over the shield most notably in Saudi Arabia, Sudan, Ethiopia and Eritrea (Barrie et al., 2007; Barrie and Hannington, 1999).

Geologically, the most promising regions in Ethiopia for gold and other metallic minerals are those Precambrian terrains, primarily volcanogenic belts of Proterozoic age. These regions are in Tigray (Northern Ethiopia), Welega and Benishangul Gumuz (Western Ethiopia) and Sidamo (Southern Ethiopia) (World Bank, 1988; Solomon Tadesse, 2009). The Northern metamorphic terrain of Ethiopia consists of a series of thick, inhomogeneous volcano-sedimentary assemblages that belong to the ANS of the Pan-African Orogeney (Asfawossen Asrat et al, 2004). Geology of Ethiopia is characterized by the occurrence of a very wide variety of rocks, different in age, origin and evolution. The Precambrian rocks were interested by the orogenic event known as Pan-African Orogeny (Getaneh Assefa et.al, 1981).

The Precambrian rocks of northern Ethiopia have experienced different phases of tectonic deformation. The tectonic structures include the folds; shear zones with sinistral sense of shear and fault systems (Tarekegn Tadesse et al., 1999).

More over detailed classification of the basement rocks in northern Ethiopia has been made by (Gauss, 1981; Asfawwossen Asrat et.al, 2001 and Shackle ton, 1986). Accordingly, the Neoproterozoic sequence of Tigray forms the southern end of the Arabian Nubian Shield (ANS). Basement rocks in the ANS, commonly found associated with the mafic-ultramafic rocks, are volcano-sedimentary sequences (Kazmin et al., 1978). In northern Ethiopia, low-grade, meta-volcanic, meta-volcanoclastic, and meta-sedimentary rocks are intruded by syn- to late tectonic granitoids where the meta-volcanic and meta-volcanoclastic rocks together forming the largest unit (Kazmin et al., 1978). According to Asfawwossen Asrat et al. (2001), it is suggested that the existence of three periods of granitic magmatism in both the ANS and the MOB, encompassing both syn- and post tectonic granitic bodies. The study area is part of the Arabian Nubian Shield at the southern end in the Adi Nebrid block which is a continuation of the Axum terrane (Abdelsalam and Stern, 1996; Tarekegn Tadesse, 1997).

The Northern domain extending northwards in Eritrea, composed of several meta-volcano-sedimentary belts and sub-belts, bounded by mafic–ultramafic rocks, host gold and base metal occurrences. A good example for this is the Adi Zeresenay gold (Solomon Tadesse et.al, 2003). Beyond that the geology of the Adyabo area which is neighboring to Terakimti is analogous to the host rocks for gold-rich VMS deposits located at Bisha and the Hassai districts, which occur within the Adi Nebried back arc basin (Archibald et.al, 2015).

According to Tarekegn Tadesse (1997) the northern part of the Ethiopian geological domain particularly the Axum formation block is divided in to six tectono-stratigraphic, structural bounded geological blocks. These are the Mai Kenetal block, the Adwa block, the Chila block, the Adi Nebrid block, the Adi Hageray block, and the Shiraro block.

According to Geological Survey of Ethiopia (1999) the geology of the study region is characterized by the different rock units. These are (1) undifferentiated metasediments with intercalations of siltstone, chert, phylitic schist and minor sandstone; (2) phylitic and graphitic schists, quartzite and metagreywake; (3) sericite-quartz-feldspar schist, metarhyolite with lenses of quartzite, graphite and phyllitic schist; (4) meta-agglomerate and intermediate metavolcanics, epidotized agglomerate with mafic and felsic clasts interlayered with intermediate metavolcanics; (5) Granitoids, biotite tonolite, granodiorite and diorite; (6) strongly deformed metavolcanics which contain mega-xenoliths.

The diversity of lithologies present on the region including the study area is resulted as a function of the collapsed back-arc basin. This geological setting is postulated due to the presence of cycles of mafic and felsic volcanic and volcanoclastic rocks, synvolcanic intrusions and the occurrence of deep and shallow water sediments of the Adi Nebrid Block. The region underwent significant deformation and shearing during destruction of the back-arc basin. The major structural feature in the northern Ethiopia is the northeast-southwest striking and variably southeast and northwest dipping composite foliation (Tarekegn Tadesse, 1996 as sited by Gebreyohanis Gebrehiwot, 2014). Figure 3.1 shows the regional Geological Map particularly the geology of the Adi Nebride block in the region including the Terakimti area (Geological Survey of Ethiopia, 1999).

The Terakimti area which is part of the Shiraro plain is located in an elongated tectonic depression bounded by the low escarpment in the North West (Beyth, 1971). The rocks of the study area belong to the Upper Complex of the Ethiopian basement specifically the Tsaliet Group (Tarekegn Tadesse et al., 1999; Gebreyohannes Gebrehiwet, 2014). The ANS also includes basement outliers well exposed in the southern Ethiopia and Kenya (Stern, 2004). The area is found in connection with the highly prospective Eritrea mineral belt of Asmera in the southern part of Arabian Nubian Shield (Archibald, et al, 2015; Stern, 2004).

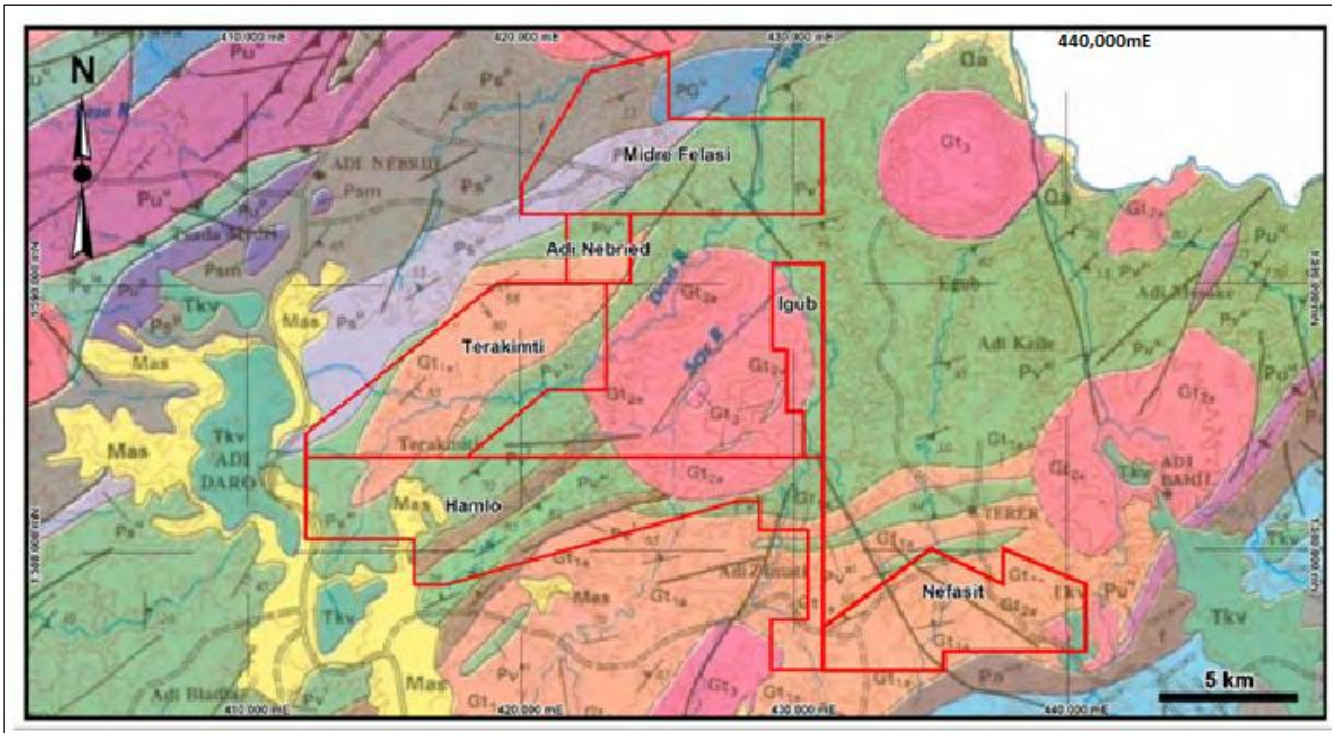

PALEOZOIC-MESOZOIC

Mas — Reddish Sandstone, laminated siltstone, conglomerates and minor Paleozoic boulder bed (tillite)

NEOPROTEROZOIC

ADI NEBRID BLOCK

Ps^u — Undifferentiated meta-sediments; intercalations of siltstone, chert, phylitic schist and minor sandstone

Ps^p — Phyllitic and graphitic schists, quartzite and metagreywake

Pv^i — Sericite-quartz-feldspar schist: (metarhyolite) with lenses of quartzite, graphite and phyllitic schist.

Pv^{ai} — Meta- agglomerate and intermediate meta volcanics: epidotized agglomerate with mafic and felsic clasts interlayered with intermediate metavolcanics.

CHILA BLOCK

Pa^{am} — Amphibolite schist with marble bands.

Pa^{pc} — Phillite and quartzite with calcareous bands

GRANITIC INTRUSIVES

Gt_3 — Granite: coarse grained, pink biotite granite and hornblend biotite granite; commonly contains laths of large potassium feldsare

Gt_{2a} — Granitpoid: course grained xenolithic granodiorite, diorite, tonolite and granite. Distinct marginal foliation and zone of hybridization is characteristic.

Gt_{2b} — Large feldspar granite (Shire granite).

Gt_{1a} — Granitoid: biotite tonolite,; granodiorite and diorite; strongly deformed and contains meta-volcanic mega-zenoliths

MAFIC AND ULTRAMAFIC INTRUSIVES AND ASSOCIATED BANDS

Pu^m — Meta-gabbro: melanocratic , medium grained, massive and marginally sheared.

Pu^u — Undifferentiated gabbroic rocks; coarse grained leucocratic to mesocratic, locally layered gabbros

Pu^u — rocks: talc schist, tremolite-chlorite schist, altered pyroxinites, metavolcanics and ultramafic mélange.

Figure 3.1 Regional Geological Map of the different blocks. (Adopted from Geological Survey of Ethiopia, 1999)

3.2 Local Geology

The Terakimti area is part of the structurally bounded tectono-stratigraphic Adi Nebrid block of the Axum geologic formation that has its own stratigraphy and structural trend. The geology of the Terakimti particularly the study area as part of Terakimti is characterized by mafic to felsic rocks, mafic volcanoclastics, felsic volcanoclastics, several quartz porphyry intrusions, large number of quartz veins and gossans. The quartz porphyry intrusions are dominantly intruding the rhyolite and basaltic units. Petrographic study of the major types of host rock units shows different mineralogical composition, textural characters and structural variation. On the other hand most of the quartz porphyry intrusions have analogous textural, structural and mineralogical characteristics. The outcrop and petrographic study of the different types of samples are described as follows

3.2.1 Basalts

This rock unit is found in the central, south eastern and north western part of the area. The unit is highly sheared parallel to the NE-trending regional foliation. It is intruded by several quartz porphyry intrusions and branched quartz veins. The basalts exhibit chlorite, silica and epidot alteration to varying degrees and exhibiting pyrite enrichment. The modal composition of the minerals in this unit consists of 36% quartz, 14% feldspar (both alkali and plagioclase), 4% muscovites, 30% chlorites, 9% epidotes and 7% opaque minerals

These units have medium to small sized crystal of quartz arranged in a sorted way. The chlorites are characterized by interconnected crystal grains with mutual boundaries. It is intensely sheared together with the quartz and feldspar minerals and muscovite grains. In addition elongated and small grains of muscovite crystals are found together with the ground mass matrix. These minerals show a characteristic feature of intensely shearing together with the quartz and chlorite grains. There are also epidote minerals of small sized crystals distributed over these rock units. Very large grains of these minerals are broken into medium sized crystals. The thin section and outcrop images of the basalt units are shown in (Fig 3.2).

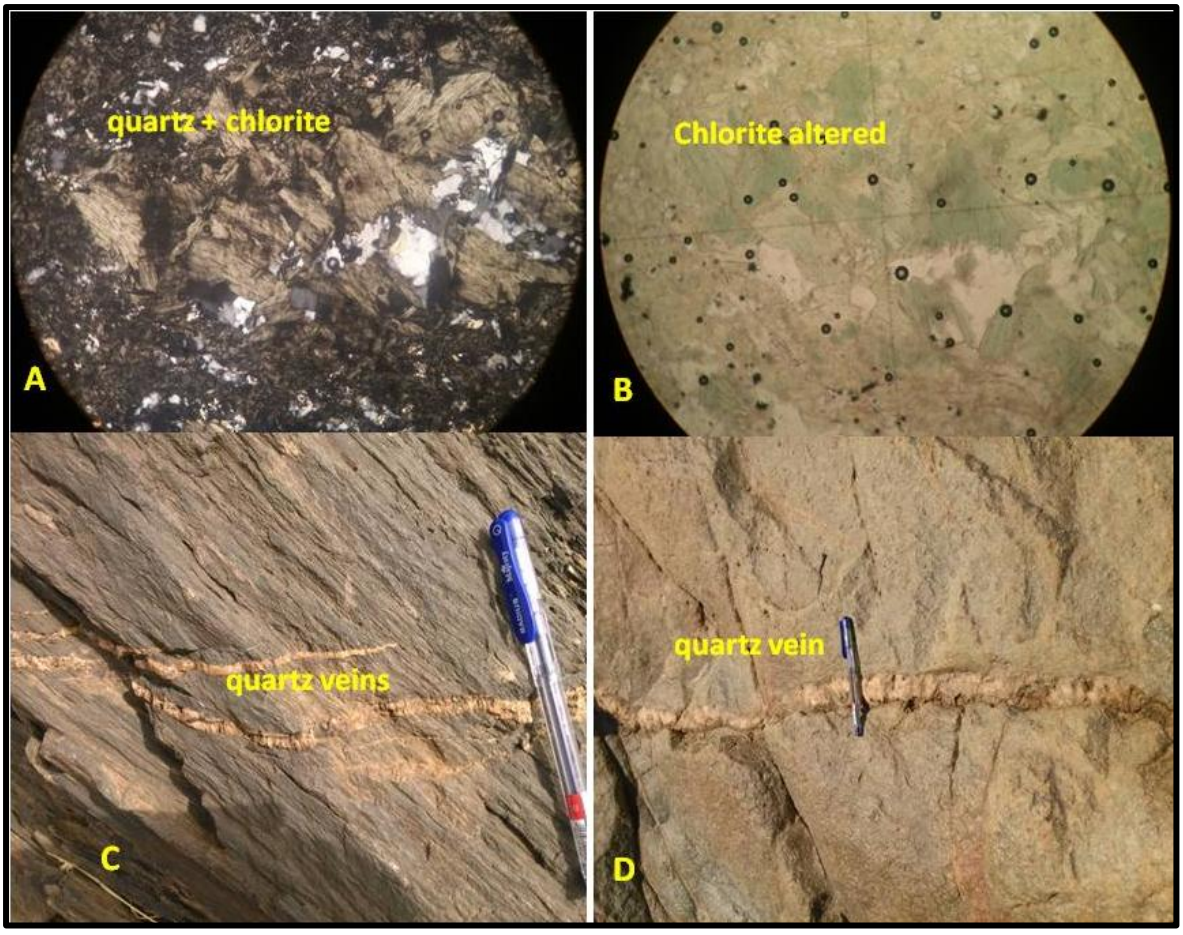

Figure 3.2 Thin section and outcrop images of the basalt units. The units at the outcrop are cut by quartz veins. (A) Thin section image of basalt which is chlorite dominated (XPL view, 10x magnification); (B) The same images as in 'A' (ppl view 10x magnification); (C) Intensely sheared basalt cut by branched quartz vein along the fractures; (D) Chlorite altered Basalt outcrop image

3.2.2 Rhyolites

This unit is characterized by intense weathering and intruded by several quartz porphyry intrusions. At some locations this rock unit is attributed by highly sericitic alteration. It is intruded by parallel aligned quartz veins and covered by weathered gossanous material with different size fragments of quartz. It is characterized by banded forms of felsic minerals with medium to large sized phenocrysts forming a porphyritic texture. It is covered by soil gossans. The dominant minerals in this unit are silica and feldspar. The minerals found in these units included quartz, feldspars, micas and some chlorite and alteration of these minerals. The modal percentage of these minerals indicates 68% quartz, 7% feldspars, 10% muscovites and 15% opaque minerals.

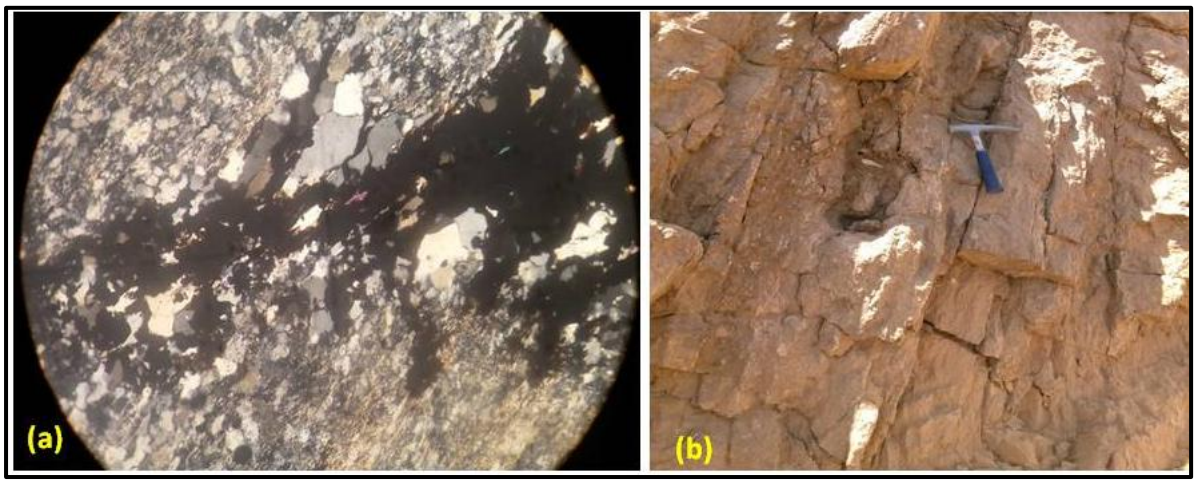

Figure 3.3 Thin section and outcrop images of the rhyolite units. The unit is intensely sheared, altered and weathered. (a) Thin section images of sheared rhyolites contain largely quartz and mica minerals (XPL 10X magnification). (b) Rhyolite at outcrop affected by intense weathering and shearing

3.2.3 Mafic volcanoclastics

This unit covers very small area and not represented in the geological map. It is cut by quartz porphyry intrusion. Possibly the primary mafic volcanoclastic deposits could predominantly of phreatomagmatic origin, as observed from the outcrop and as indicated by the clast assemblages. The mafic volcanoclastic rocks are generally consisting of basaltic clasts characterized by non vesicular to poorly-vesicular with quartz particles probably derived surface fragments of quartz veins and quartz porphyry intrusions

3.2.4 Felsic volcanoclastics

These rock units are characterized by fine to medium grained texture composed of quartz and feldspar minerals. The felsic volcanoclastic rocks are intruded by parallel aligned quartz veins along the regional shear. Chlorite or epidote alteration is associated with this unit. This unit covers very small area.

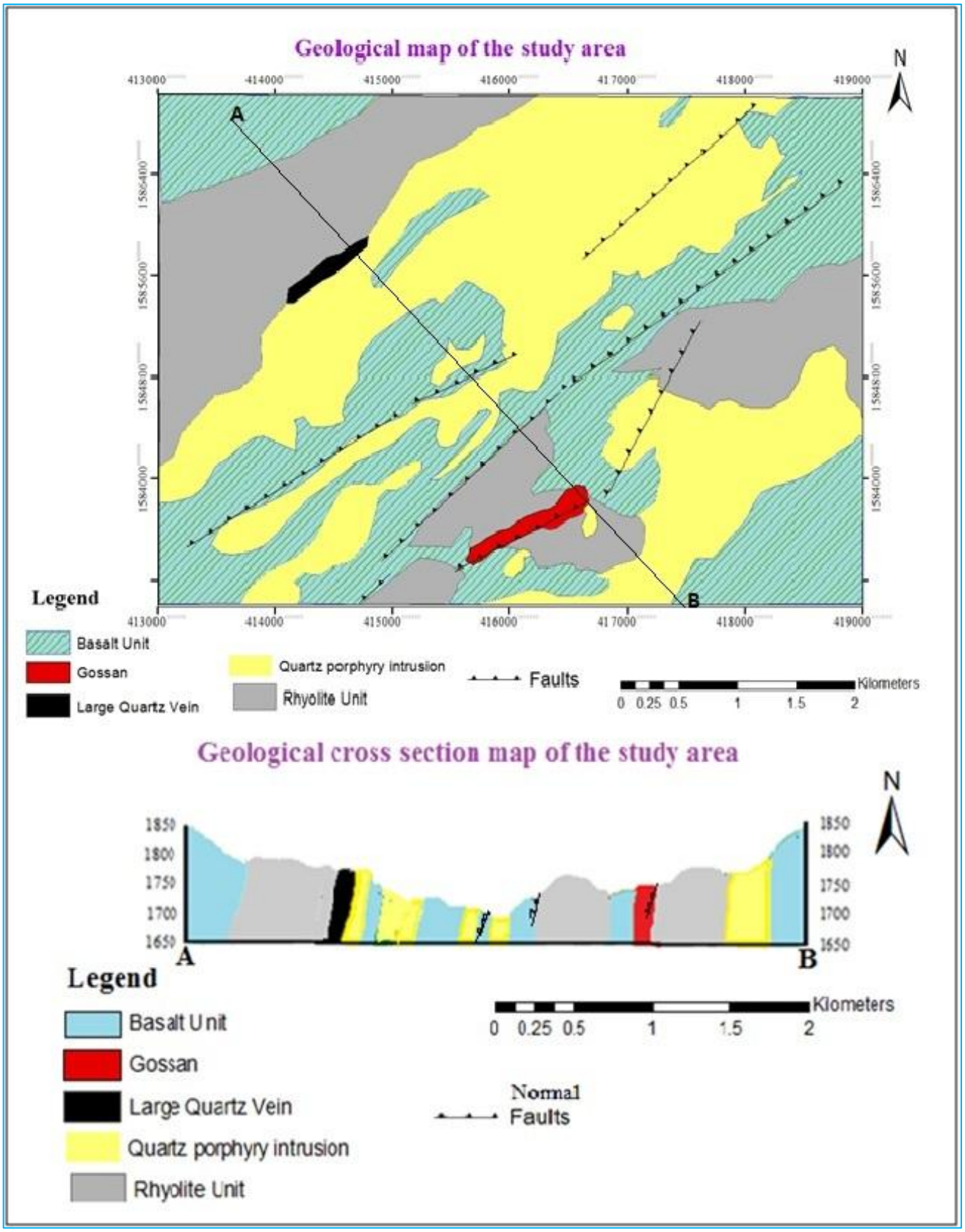

Figure 3.4 Geological map and cross section of Terakimti area.

3.2.5 Quartz porphyry

There are several quartz porphyry intrusions in the study area. These are characterized by grey to green color in the study area emplaced in mafic and felsic volcanic units. They cover small to large area at different localities. These intrusions are also found at a depth of 175 meters and beyond (Appendix-2). The intrusions are affected by weathering of different intensity from the surface to depth which can be categorized as highly weathered, moderately weathered and fresh porphyry intrusions. These have large grains of quartz a maximum of more than 2cm, pyrite and chalcopyrite minerals. The intrusions form hilly outcrops and cut by several quartz veins. The porphyries are coming to the surface following the faults and they are late intrusion events cutting the volcanogenic massive sulfide deposits. Some parts of the intrusions are intensely affected by chlorite and epidote alteration. The intrusions are affected by weathering with small to large sized quartz fragments covering the surface and shear deformation parallel to the regional shear.

3.2.5.1 Texture of the quartz porphyry

The quartz porphyry contains large porphyroblasts of quartz, feldspars such as plagioclase and alkali feldspar a fine grained matrix. Some quartz porphyroblasts contain inclusion of other epidot and muscovite minerals. In most of the samples the porphyroblasts are wrapped around by the foliation. The phenocrysts show anhedral to subhedral shapes. At some samples the ground mass matrix containing the muscovite, small quartz grains, feldspar, and the chlorites are intensely foliated and aligned themselves in response to the stresses

3.2.5.2 Mineral assemblages of the quartz porphyry

The mineral paragenesis of the quartz porphyry intrusions is characterized by quartz, feldspars, muscovite minerals and alteration products of the chlorite minerals, variable sizes of epidote grains and fine grains of ground mass matrix. Progressive change of one mineral type to the other type is commonly observed phenomena under the thin section samples. The modal compositions of these minerals contain 71%quartz, 10% feldspars, 8% muscovite, 5% chlorite, 2% epidote minerals and 4% opaque minerals,

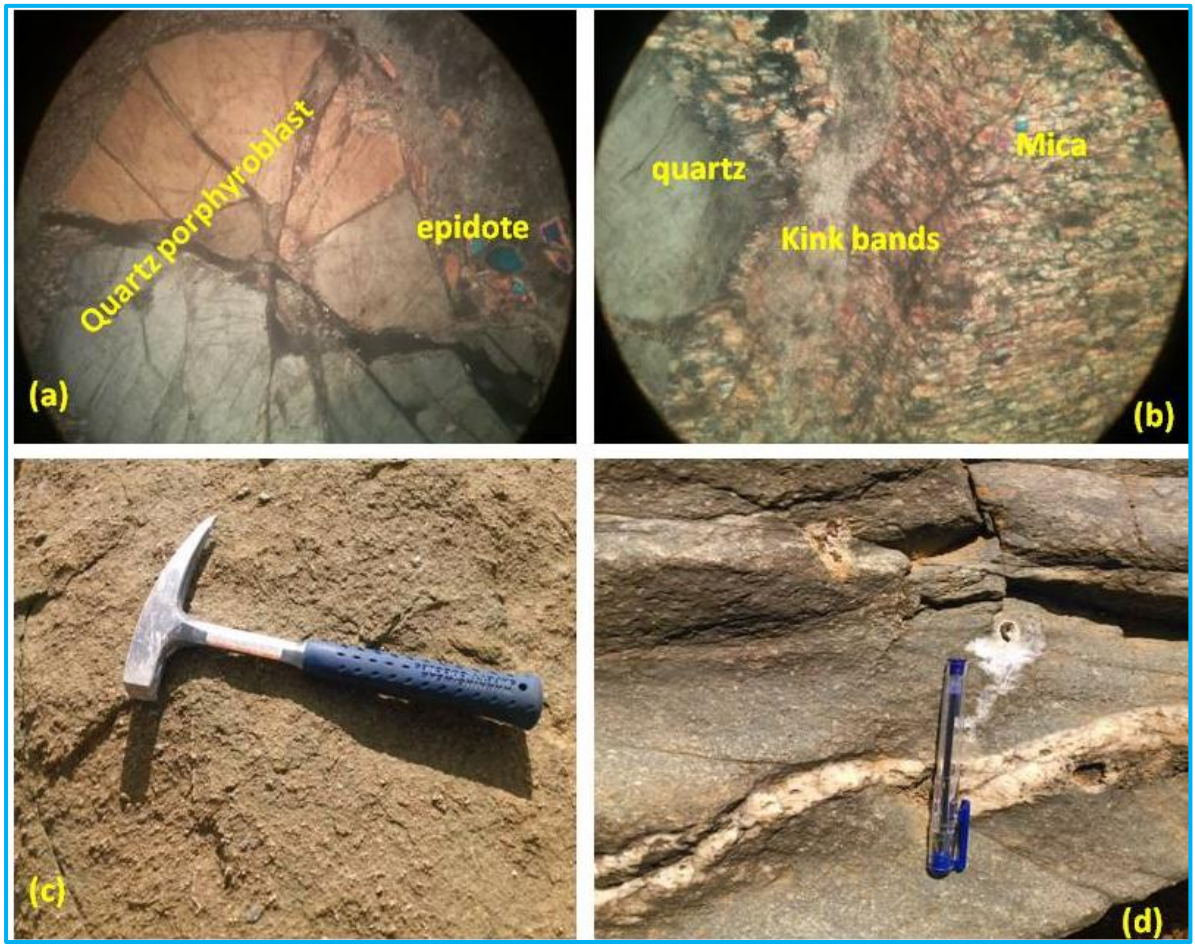

Figure 3.5 Thin section and outcrop images of the quartz porphyry intrusions (a) Large porphyroblast of quartz with epidote minerals at the right (blue color under XPL view with 10x magnification); (b) Quartz porphyroblasts with muscovite. The muscovite's show kink bands (10 x magnifications); (c) Quartz porphyry intrusion (large quartz grains are clearly visible); (d) Chlorite altered quartz porphyry intrusions cut by quartz veins.

3.2.6 Pegmatite

This unit is characterized by very fine grains to large sized fragmented pegmatite boulders. It is coming through the contact of the rhyolite and the quartz porphyry intrusion. The pegmatite unit is less affected and deformed by the regional shear deformation. It is highly fragmented and weathered at the surface (Figure 3.6c). These units are probably formed together with the quartz veins.

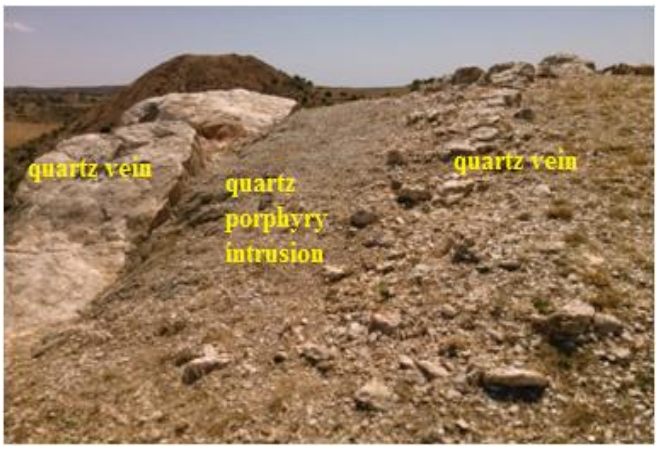

a. Cross cutting relation between quartz porphyry intrusions (weathered) and quartz veins

b. Quartz porphyry intrusions cutting the host rocks and exposed by the Deba River

c. Pegmatite unit outcrop image

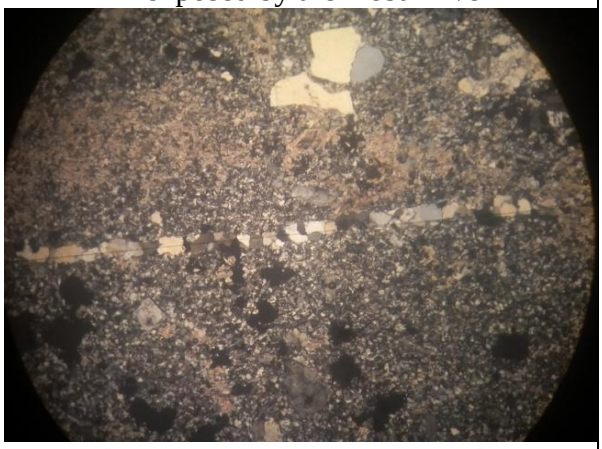

d. Micro Quartz veins. (under XPL view 4x magnification)

e. Large quartz vein intruding the host rocks

f. Gossans (hematite rich)

Figure 3.6 Outcrops and thin section photographs of the rock units

3.2.7 Quartz veins

The occurrence of most of the veins is following the orientations of the shear zones except some veins coming through the regular fractures. The maximum width of the veins reaches 5-7m and more, in places the veins are highly fragmented. The width between two successive parallel veins varies from one location to other location. These units are cut by the faults structures together with the host rocks at different locations. The size of this unit varies from large (mappable scale) to very small at microscopic size.

3.2.8 Gossan

This gossan body is found at the central part. It is characterized by enrichment of hematite and magnetite minerals (Figure 3.6h). The hematite rich gossans is red to red brown color and the magnetite rich shows banding of black and brown weathered surface. The gossans are associated with massive sulfides such as pyrites and chalcopyrites enriched in the metallic elements such as Au-Cu-Pb-Zn and rarely siliver.

Chapter 4 Geological Structures and Metamorphism

4.1 Introduction

There are different types of brittle and ductile deformational structures in the study area where both of these structures show macro and micro sized descriptive features. These show slight difference from the same rock types found at different location. This variation is possibly due to the result of the intensity of the deformational stress and stress field. For example the intensity of shear deformation of the several quartz porphyry intrusions varies from the surface to depth. According to Tarekegn Tadesse (1997) and Beyth (1971) the regional shear deformational structures in the Adi Nebrid block has a north east to south west striking which dips to the south east. This is also the characteristic trend of the shear structures in the study area except the local shears are dipping to the North West. This could be due to the existence of more than one deformational episode. These structures are described into two categories of brittle and ductile structures. The brittle structures such as faults and fracture are dominant at Terakimti.

4.2 Ductile deformational structures

These are the first categories of deformational structures found in the study area. These structures found in the Adi Nebride block are related to the regional shear deformational process of the northern Ethiopia (Tarekegn Tadesse, 1997). The quartz porphyry intrusions and the host rock units are affected by these types of structures. There are two groups of these types of structures. These are shear foliation and folded deformational structures identified at micro level and not visible at the outcrops of the area.

4.2.1 Shear foliations

These structures are highly distributed all over the entire study area and affect all types of lithological units. The quartz veins which are late coming are not affected by the shear foliations. According to Tarekegn Tadesse (1997) the orientation of the regional shear deformation is dominated by the north east to the south west strikes. The orientations of the shear deformational structures at Terakimti are analogous with the regional shear deformations with some variation of the strike angle and dip direction. The intensity of these structures at the quartz porphyry intrusions found at different locations show almost similar features. This tells the porphyries are affected by the same deformation. But the orientation

direction and dips of these structures shows slight variation of the strike and dip angle from one location to the other. Table 4.1 shows the orientation of the shear foliations at Terakimti.

Table 4.1 Location and orientation of the shear foliations at Terakimti area and the host rocks affected by these shear foliations.

Location points		Elevation above MSL	Orientation of foliation plane		Azimuth	Structure type	Rock type
Easting	Northing		Strike	Dip			
415666	1583622	1760	S70W	70NW	250	Shear foliation	Meta-rhyolites
415268	1585440	1730	S40W	65NW	220	Shear foliation	Chloritized QPOR
414923	1585131	1745	S70W	70NW	250	Shear foliation	Quartz porphyry
415350	1582286	1827	S35W	80NW	215	Shear foliation	Rhyolite
415350	1582286	1827	S60W	75NW	240	Shear foliation	Quartz porphyry
417112	1585370	1661	S55W	45NW	235	Shear foliation	Basalt
417112	1585370	1661	S55W	45NW	235	Shear foliation	Basalt
412560	1581660	1695	S60W	85NW	240	Shear foliation	Contact of QPOR
413170	1583260	1738	S35W	77NW	215	Shear foliation	Basalt
413060	1584040	1762	S52W	42NW	235	Shear foliation	Quartz porphyry
414040	1582990	1770	S60W	75NW	240	Shear foliation	Quartz porphyry

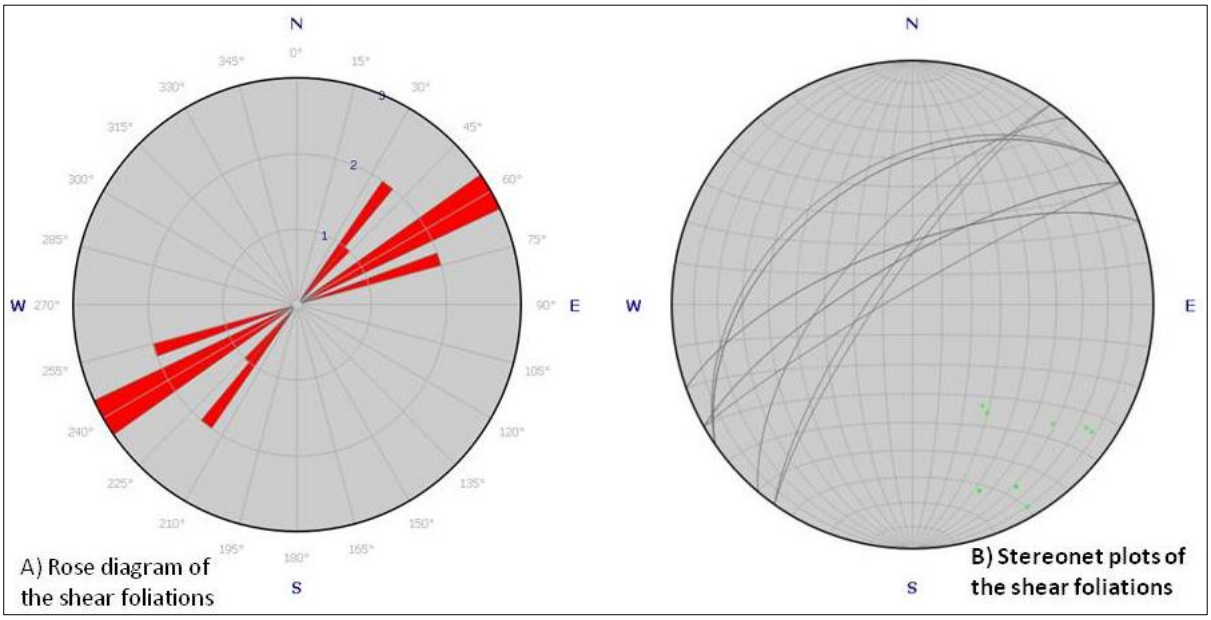

Figure 4.1 Rose diagrams and stereonet plots of the shear foliations

The rose diagram (Figure 4.1a) shows the direction of the types of the shear foliations. Most of them shows that they are overlapped each other on the plot. The figure shows that the shear foliations occurred at high frequency. The equal area net at (Figure 4.1b) shows the great circles of the shear foliations touch the stereonet at the same quadrant. These are

oriented in NE to SW direction dipping to the NW. This shows the parallel to sub parallel orientation of the measured foliations.

4.2.2. Micro folds

These structures are only visible at microscopic scale. The micro fold varies from one sample to the other as a result of variation of the stress field from one locality to the other. In addition this could be due to the variation of the response of the rocks to stress. According to Archibald et.al, (2014) the presence of folded quartz and epidotic veining to the neighboring terrain of the study area suggest the presence of ductile deformation. The microscopic quartz veins cutting the quartz porphyry intrusions show slight folds as shown at Figure 4.2a & d. Similarly the folded structures are identified at the host rock units at a microscopic scale where the different minerals especially the micas are folded at the matrix.

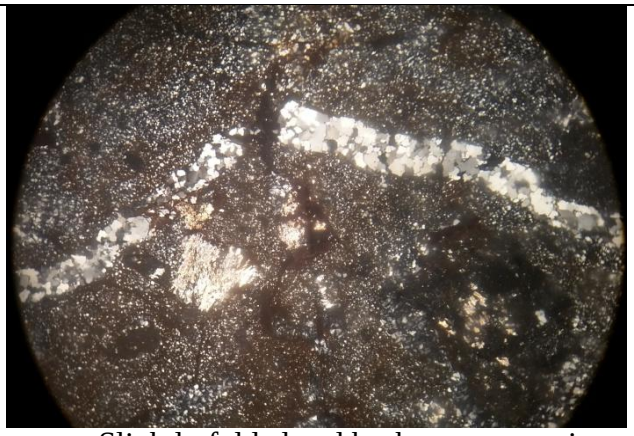

a. Slightly folded and broken quartz vein at the microscopic scale under (XPL view, 4x-magnification)

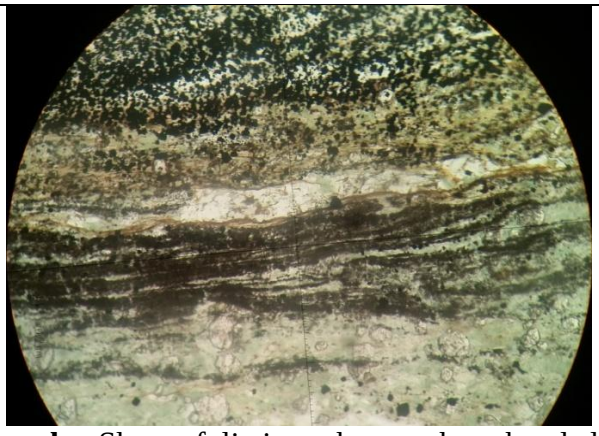

b. Shear foliation that makes banded layers of the black and white minerals under ppl view micro photograph (4x magnification)

c. Mica minerals showing kink bands (XPL view 4x magnification)

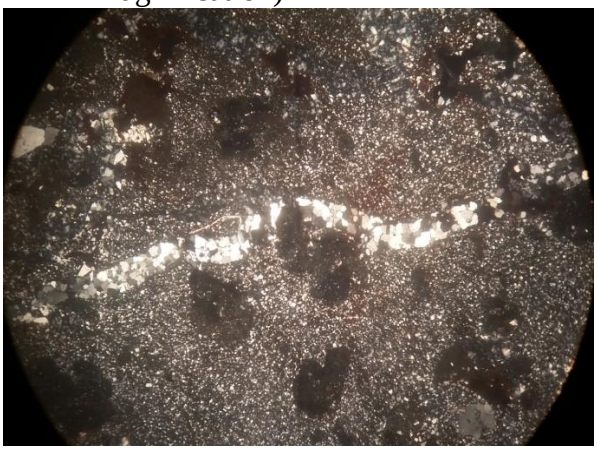

d. Slightly folded micro quartz vein. (XPL view 4x magnification)

Figure 4.2 Micro folds and banded layer structures of the intrusions and the host rocks

4.3 Brittle geological structures

Faults and joints are the dominant brittle geological structures found at different locations in the study area. The different types of geologic units found at different locations in the area are affected by these geological structures. The brittle structures associated with the regional shear zone are the one that have a significant role for the formation of the different quartz veins. Faults and other fractures are the dominant types of structures under this group.

4.3.1 Faults

These structures are found at different locations in the study area. These are small to large regional faults. Large faults observed at the outcrop causes displacement of the mafic and felsic geological units as well as the quartz porphyries. The quartz veins are affected by this geological structure where they are interrupted from their original continuity. These geological structures are dominated at the contact regions of the different lithologic units. They are dominantly striking along the north east to south west direction which is parallel to semi parallel to the direction of the regional shear. The rose diagram plots and the equal area stereographic projections of the fault structures shown at Figure 4.2 clearly show the frequency of the occurrence of the fault structures and their orientation relationships.

Table 4.2 Location and orientation of the fault structures

Location		Orientation of fault plane			Structure type	Rock type
Easting	Northing	Strike	Dip	Azimuth		
416667	1584480	S75W	87NW	255	Normal fault	Rhyolite
417332	1584791	S20W	72NW	200	Normal fault	Rhyolite
415100	1583279	S49W	65NW	229	Normal fault	Contact zone
415500	1583680	S47W	79NW	227	Normal fault	Rhyolite and basalt contact
417334	1585280	S45W	75NW	225	Normal fault	Basalt
415250	1584160	S65W	84NW	245	Normal fault	Contact of basalt & QPOR
417329	1586080	S41W	65NW	221	Normal fault	Altered QPOR and basalt

The following two figures are the plots for the fault structures. From the rose diagram it is visible that the faults occurred high frequently in the area with some of them showing nearly the same orientation where one plot is overlapped over the other. The second equal area stereonet also shows that the great circles of the faults touch the stereonet at the same quadrant. The great circles at the equal area net connect to the stereonet circle at the first and

third quadrant. These shows the fault structures have nearly similar orientation with some strike and dip angle variation.

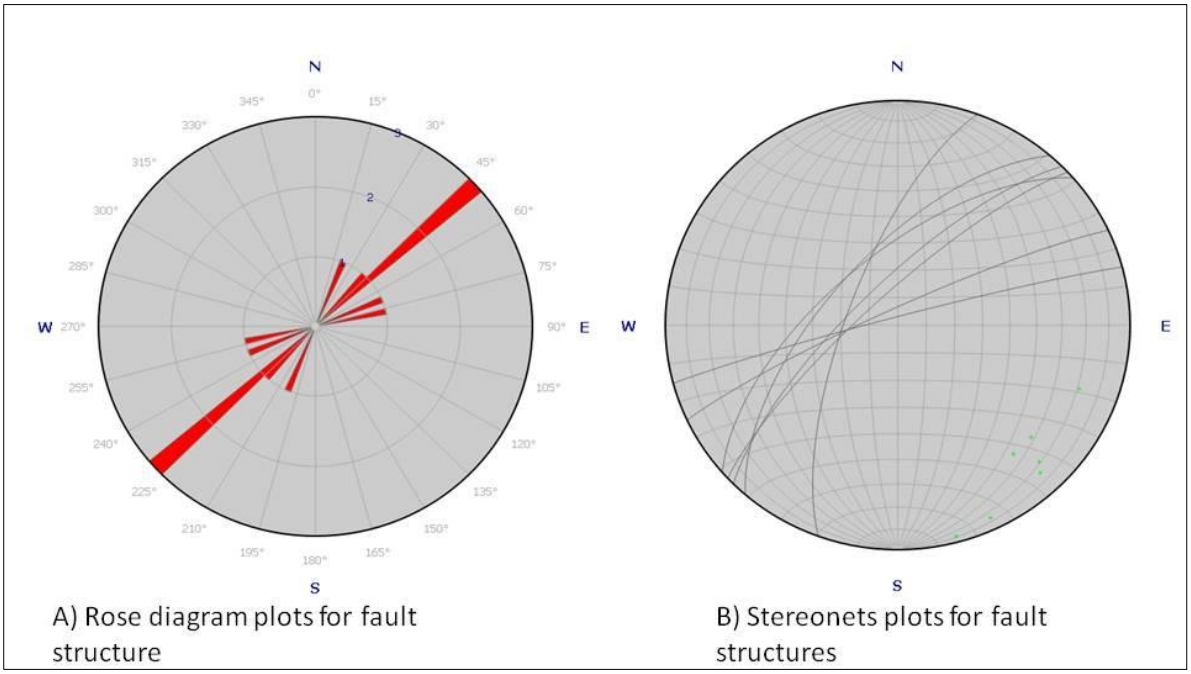

Figure 4.3 Rose diagrams and stereonet plots of the faults

On the other hand the surface host rock of the intrusions such as the rhyolite units and the basalts are generally show that they are affected by such type of brittle deformational structures. Similarly the surface outcrops of the quartz porphyry intrusions are generally affected by these structures. Quartz porphyries that intrude the mafic and felsic rocks are affected by the fault structures and displaced from their original position.

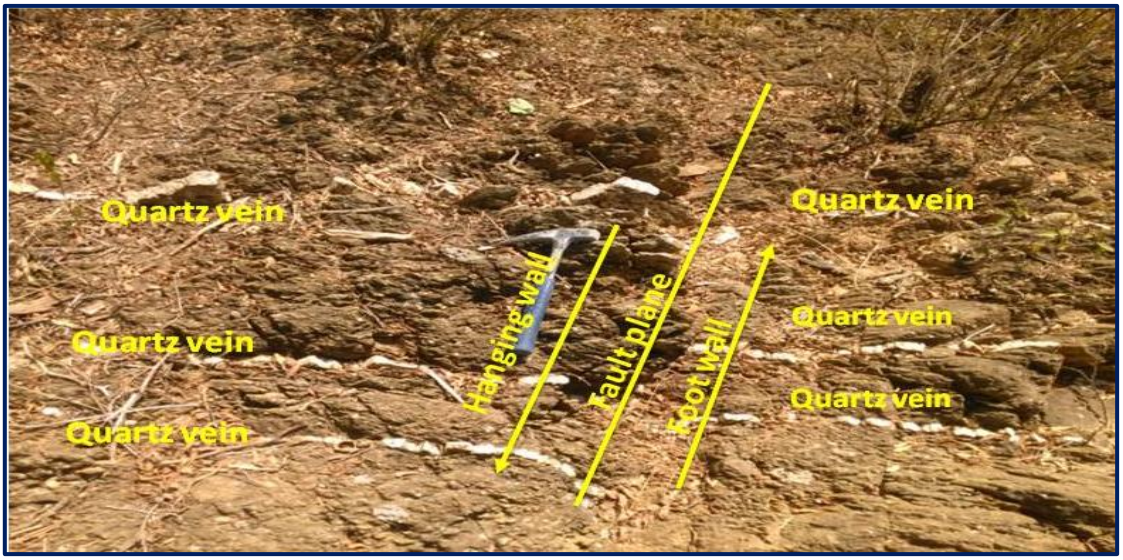

Figure 4.4 Outcrop photographs of fault structures

4.3.2 Joints and general fractures

These are the second brittle geological structures found in different types of geological units with different sets of orientations. The orientation shows strong variation at the same rock units and at the same outcrops. In some of the units more than three sets of fractures are found and they are cross cut each other. These fractures are in filled by late coming quartz veins. For example the joints at the chloritized basaltic unit are in filled by the branched quartz veins affected by the shear deformation stress.

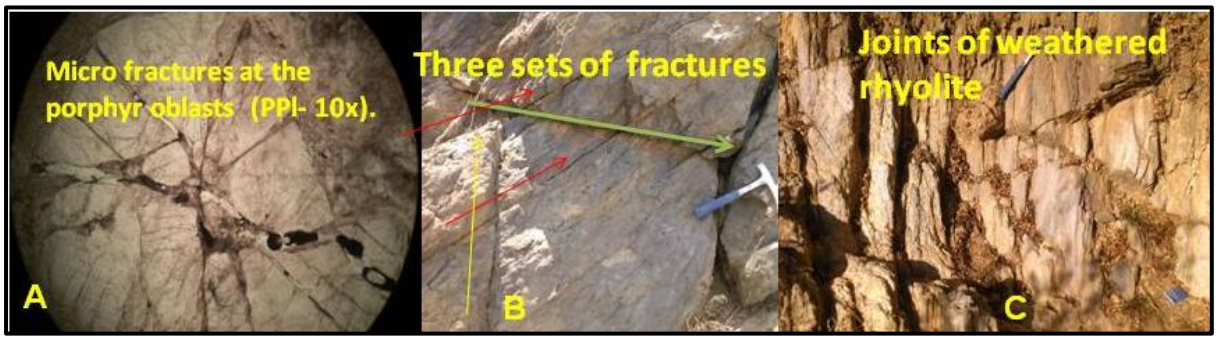

Figure 4.5 Images of general fractures and simple joints at Terakimti area.(A) Joint structures of affected by the shear stress and weathering; (B) Three sets of fractures (C) Micro fractures at the quartz porphyry intrusion samples (10 x magnifications). Filled by quartz veins

Table 4.3 Location and orientation of quartz veins and fractures

Structure location		Elevation above MSL	Orientation of fracture plane		Azimuth	Type	Rock type affected
Easting	Northing		Strike	Dip			
414923	1585131	1745	S20E	25SW	160	Fractures	Quartz porphyry
415156	1584560	1693	S15E	90NW	165	Quartz vein	Basalt
415734	1582700	1777	S30W	70NW	210	Quartz vein	Rhyolite
414744	1582538	1796	S20W	60NW	200	Fractures	Quartz porphyry
414744	1582538	1796	S50E	75SW	130	Fractures	Quartz porphyry
414744	1582538	1796	S10W	53NW	190	Quartz vein	Quartz porphyry
414040	1582990	1770	S10W	87NW	190	Quartz vein	Quartz porphyry
416540	1583755	1746	S40W	75SE	240	Quartz vein	Quartz porphyry
416773	1583744	1756	S60W	75NW	240	Quartz vein	Rhyolite
417350	1584572	1796	S20W	65NW	200	Quartz vein	Rhyolite
417350	1584572	1796	S83W	10SE	163	Fractures	Rhyolite
417350	1584572	1796	S15W	85SE	195	Fractures	Rhyolite
417350	1584572	1796	S20E	90NE	160	Fractures	Rhyolite
417350	1584572	1796	S10W	80NW	190	Quartz vein	Rhyolite
417350	1584572	1796	S35E	85NE	145	Fractures	Rhyolite
413060	1584040	1762	S17W	64NW	197	Quartz vein	Quartz porphyry

The following two figures are rose diagrams and stereonets plotted for the fractures cutting the different lithologic units.

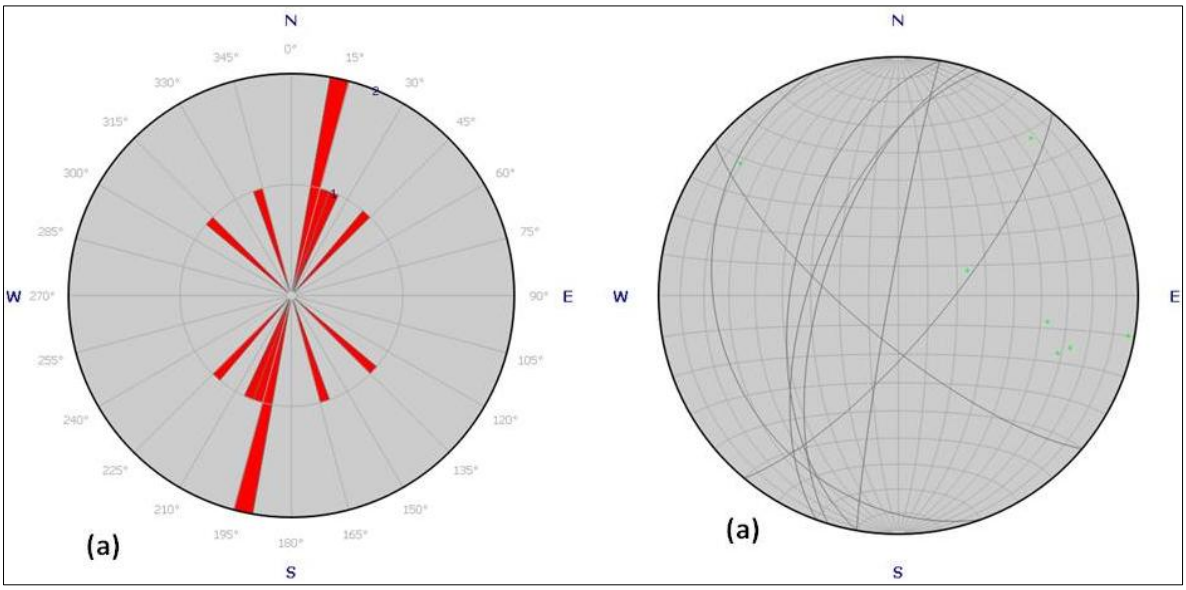

Figure 4.6 Stereonets and rose diagrams for fractures. (a) Rose diagram of joints and quartz veins cutting the quartz porphyry intrusions; (b) Stereographic projections of joints and quartz veins cutting the quartz porphyry intrusions.

The orientation of the fractures varies from one location to the other location (Table 4.3). The rose diagrams in Figure **4.6** shows the plot of the quartz veins and fractures commonly found within the quartz porphyry intrusion and shows different orientation. At the rose diagram (Figure 4.6a) the veins have different orientations which some directed to the NE to the SW quadrant and others are NW to SE. More over at the stereonet plot (Figure 4.6b) these veins touch the stereonet at different points. These indicate the quartz veins formed along the fractures in the area have different orientation and cross cut each other. Those veins show parallel to sub parallel orientations are formed along the shear deformational weak zones.

4.4 Cross cutting relations

The different types of the units in the study area governed by the law of cross cutting relations where this is directly related with the timing event of the lithologic units. This relationship is identified both at the outcrop and at the thin section samples. The general relationship of the units is described sequentially as follows. The different quartz porphyry intrusion bodies are formed intruding the felsic and mafic rocks as well as the VMS deposits. On the other hand these intrusion bodies are cut by the different sized and parallel aligned as well as cross cutting quartz veins. This cross cutting relation implies that the quartz porphyry

intrusions are formed after the formation of the mafic and felsic rock and the VMS deposits. The different quartz veins are formed cutting all types of other lithological units.

4.5 Tectonics of the study area

The Terakimti area is located within the Pan African, Neoproterozoic, southern Arabian-Nubian Shield (ANS). This belt of rocks comprises a composite set of granitoid-greenstone terranes located in north east Africa, and extends through Eritrea, Egypt, Sudan, Ethiopia, and western Saudi Arabia (Abdelsalam and Stern, 1996). For the purpose of this work the tectonic effects are describe in terms of the timing event of the lithologic units based on the relationship between the out crop characteristics of the units and micro tectonic features.

4.5.1 Tectonic features and timing relations

According to Yardley et al. (1990) there are three categories of time relationship between deformation of external foliation and internal foliation of the porphyroblasts. The prophyroblasts of the quartz porphyry intrusions have a characteristic feature of internal schistocity. In some of these situations the external foliation shows a rotational feature around the porphyroblasts. There are pre tectonic porphyroblasts in the quartz porphyry intrusions. At (Figure 4.7a and c).the internal foliations are oblique to the external foliations. From the figure the ground mass matrix show some rotational foliation around the porphyroblasts. According to Yardley et al (1990) these indicates pre-tectonic porphyroblast.

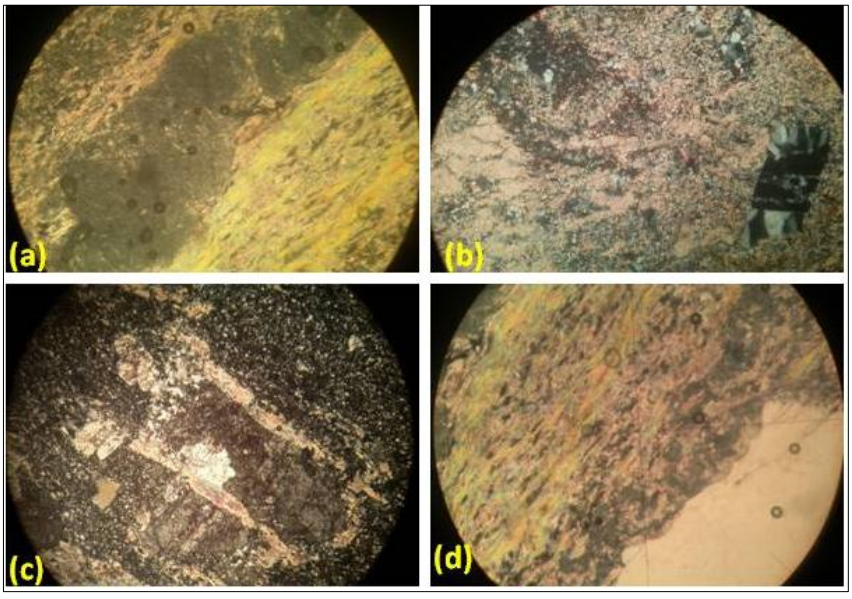

Figure 4.7 Tectonic relations of the porphyroblasts and matrix foliation.(a).Pre-tectonic foliation fabric. The internal foliations are oblique to the external; (b) Syn-tectonic foliations at the upper left side of the image for the host rock units; (c) Feldspar porphyroblast showing an other pre-tectonic crystal of the porphyries and (d) Post tectonic porphyroblast of quartz at the host rocks the internal foliations are parallel to the external (Note that all images are under XPL view with 4x magnification)

At the samples of the host rock units all three types of pre-tectonic, syn-tectonic and post tectonic crystals are observed. The less deformed large crystal of quartz at the host rock units shows the internal fabrics that are at some parallel alignment to the external foliations (Figure 4.7d). According to Yardley B., Mackenzie W. and Guilford C. (1990) these porphyroblastic crystals are grouped under the post tectonic groups of the crystals. At some of the samples the porphyroblasts grow with the internal foliation fabric in a parallel fashion with the external foliations. This tells that the prophyroblasts are post tectonic crystals (Figure 4.7d). On the other hand at another thin section samples the internal foliation is at an oblique angle to the matrix foliation. In most of the samples the crystals of the ground mass particularly the mica minerals are rotated around the porphyroblasts and make an external rotational fabric without any effect on the internal foliation.

But as compared to the matrix foliation the internal foliation is more rotated. On the bases of Yardley eta al (1990) principle such type of porphyroblast and matrix foliation relation indicates that there is syn-tectonic growth of porphyroblasts in the host rock units.

4.6 Metamorphism of the study area

According to Tarekegn Tadesse (1997) the tectonostratigraphic structural bounded geological blocks of the northern Ethiopia are characterized by their deformational history and metamorphism. The study area contains different types of mafic and felsic metavolcanic lithological units. The mafic metavolcanic rock units are dominated by the meta-basalts and the felsic meta-volcanic units are dominated by the meta-rhyolites with their own characteristic mineral assemblages and geochemical characteristic. These rock units which cover large area of the surface environment are the basic geologic bodies hosting the VMS gold deposits and other base metal mineralization.

4.6.1 Meta basalts

The area is characterized by very low metamorphosed and intensely deformed basalts with intense chlorite alteration. Under the petrographic description the metabasaltic unit is characterized by the assemblages of the minerals like quartz, muscovite, chlorite, plagioclase feldspar, alkali feldspar, epidote plus opaque minerals like sulfides and oxides. This association of minerals indicated that the host rocks are under the progressive metamorphic process.

4.6.2 Meta rhyolites

These geologic formations are very abundant covering large area of the study with a characteristic feature of intensive shearing parallel to the regional deformation direction. Under the petrographic microscope these units are characterized by low grade metamorphism with the mineral assemblages such as quartz which is the most abundant, muscovite second abundant, chlorite for some samples and alkali feldspar. This implies that these rock units are at the grade of lower green schist metamorphic facies.

4.7 Timing of the quartz porphyry intrusions

The samples of the quartz porphyry intrusion bodies collected and described at depth are slightly affected by chlorite alteration as compared to the surface outcrops. The quartz porphyry intrusions intruding the felsic volcanic rocks are also affected by the chlorite alteration. From these effects it is observed that these alterations are possibly occurred after the formation of the intrusions.

Texturally all the samples taken from the quartz porphyry intrusions are characterized by analogous porphyroblast and ground mass matrix relationships except the size of the crystals which decrease for the outcrop samples as compared to the drill core samples. This condition indicates that the intrusion bodies have almost similar characteristic features. The grain size variation of the samples could be the result of the variation in the growth of the crystals at depth and at the surface for the same types of units.

On the other hand the quartz porphyry intrusions are characterized by the shear deformations observed both at the hand specimen and thin section. The intensity of deformation is almost the same for all the intrusion samples collected. In addition to this the orientations of the shear deformation at the quartz porphyry intrusion bodies is striking in the SW to NE direction with slight variation of the strike and dip angle

The size of the intrusion varies from one location to the other location both at the surface and at depth. These intrusion bodies show branching of one unit from the other unit where the area between them is covered by other types of rock units and the VMS deposits. These units are continuing along the direction of the regional shear zone where they are interlock each other at the sutured areas. This branching and mixing feature of the intrusions are also observed at the depth of the intrusions cutting the VMS deposits. Both the surface geologic

maps (Fig. 3.4) and the subsurface sectional maps (Fig. 4.8) clearly indicate that several quartz porphyry intrusions observed at one location are interlock and becomes one unit at the other areas. This situation also indicates that several quartz porphyry intrusions could have the same origin and formed at the same time. They become branched as they come to the surface following the favorable path ways.

There are also some eye spot like features of these intrusions found at the outcrop and at depth. All the intrusions are coming to the surface by cutting the massive sulfide bodies and other host rock units as shown in the section and in the geological map. They are less affected by the deformation than the volcanogenic massive sulfide bodies. These situations tell that the intrusions are late in the event than the VMS deposits.

The following Figure 4.8 shows the relation between the quartz porphyry intrusion and the VMS deposits at depth. The figure clearly shows that the intrusions are late coming in the event cutting the VMS deposits. At the right part of the figure they are separate and forms individual intrusions. There are four branches of the intrusions observed at this part of the sectional map. These different intrusion bodies which cut the massive sulfide are mixed and become one unit at the upper left side of the subsurface sectional map. This relationship possibly implies that these intrusions are formed at the same time and becomes branched as they are coming to the surface. The other two drill core sample images just below the section map at Figure 4.8 shows the clear contact region where the quartz porphyry intrusions are cutting the massive sulfide deposits.

On the other hand the relationship between the quartz porphyry intrusions found at different locations in the study area are described that they have analogous textural and structure features. They have the same mineral assemblages except some intrusions are affected by chlorite alteration. This tells that these intrusions are formed at the same time in the event and related each other whereas the alterations are late coming after their formation. In addition as observed from Figure 5.1 all the intrusion samples fall in the VAG field concentrating at the same region. This indicates all the intrusions are formed at the back arc setting environment. Generally the outcrop juxtaposition of the different quartz porphyry intrusions and their relation with the host rock units and the VMS deposits indicate they are late coming in the event. On the other hand several intrusions located at different localities are formed at the same time.

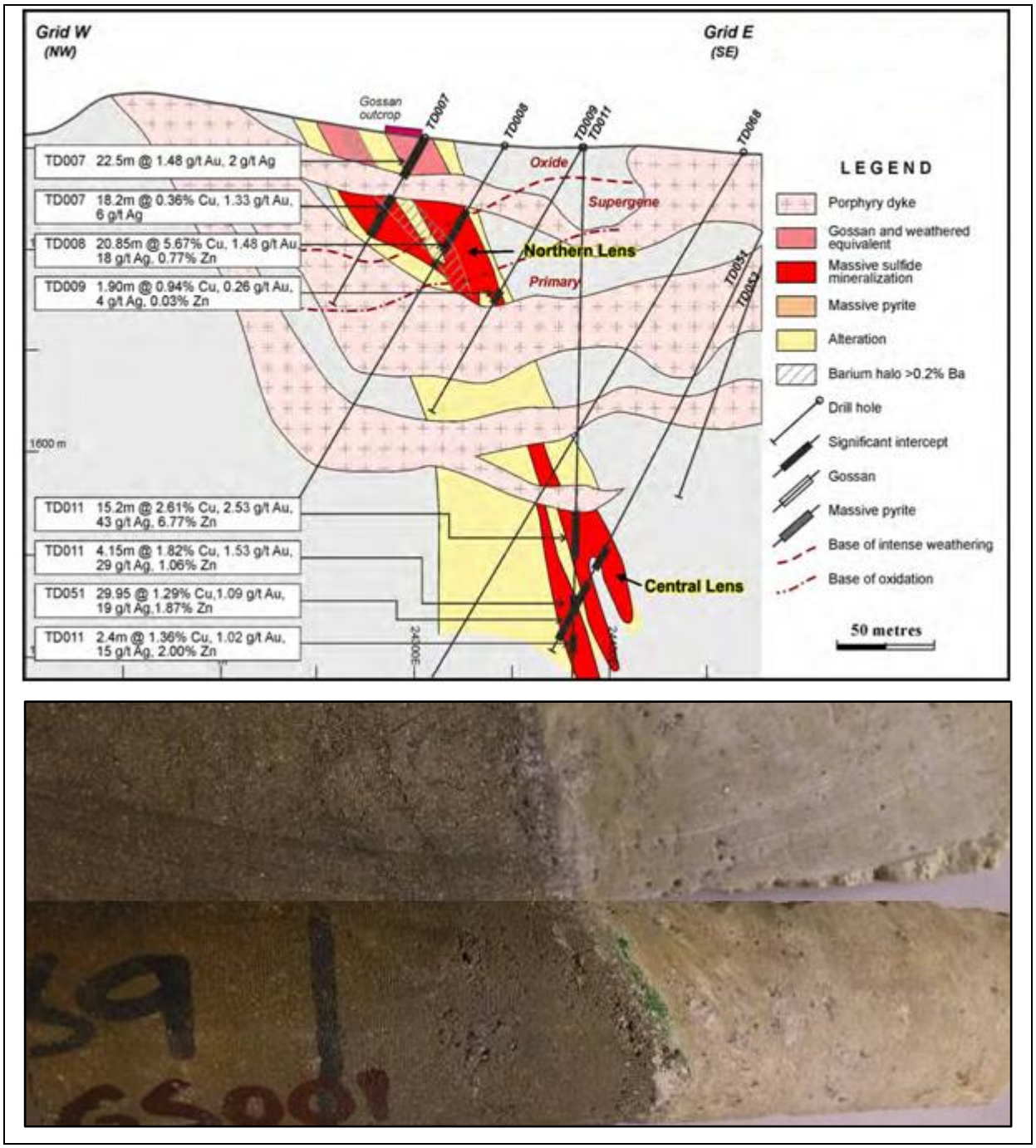

Figure 4.8 Sub surface relation of quartz porphyry intrusions and VMS deposits. The analytical results on the map are for only the massive sulfides at different depth interval. This figure shows the subsurface sectional view of the study area which shows the relationship between the quartz porphyry intrusions and the volcanogenic massive sulfide deposits and the relationship between the different quartz porphyry intrusions (Adopted from Archibald et al., 2013 technical report)

Chapter 5 Geochemistry and geochemical interpretation

5.1 Introduction

The geochemical study of the stream sediments, rocks and soil gold geochemistry studies are conducted for the entire concession area of Terakimti and other neighboring concessions of the nearby properties (Archibald et al., 2014). Accordingly the initial soil geochemical studies are conducted at Terakimti area for the mineralized gossan zone using portable XRF (handheld) Thermo Scientific Niton XRF analyzer. The different elements analyzed using this portable XRF instrument by the company include As, Bi, Ba, Ca, Co, Cr, Cs, Cu, Fe, Hg, K, Mn, Mo, Ni, Pb, Rb, S, Sn, Sr, Te, Th, Ti, U, V, W, Zn and Zr. Detailed surveys over the mineralized areas at Terakimti were conducted by different exploration groups working in the area at different times. From the separate study of the gold soil geochemistry significant concentration of gold is obtained. The major and trace element geochemical description of both the quartz porphyry intrusions and the host rock units is given below.

5.2 Geochemistry of the quartz porphyry intrusions

There are many quartz porphyry intrusions in the area intruding the mafic and felsic host rocks. A total of five samples are analyzed for the major and trace element geochemistry characterization of the intrusions.

5.2.1 Major element geochemistry of the quartz porphyry intrusions

Table 5.1 Major elements analytical result of the quartz porphyries

Methods of analysis	Analyzed trace elements	Samples and percentage (%) concentration values of the elements				
		GS004	GS005	T1L4	T3L6	T4L2
ICP-AES	SiO2	72.1	72.5	75.2	69.9	76.7
ICP-AES	Al2O3	15.9	16.65	12.3	14.25	13
ICP-AES	Fe2O3	0.96	1.03	2.99	3.85	2.33
ICP-AES	CaO	0.06	0.08	0.97	1.77	0.09
ICP-AES	MgO	0.08	0.07	1.03	2.44	0.63
ICP-AES	Na2O	4.15	3.3	4.44	4.83	3.58
ICP-AES	K2O	1.03	0.98	0.85	0.78	2.31
ICP-AES	Cr2O3	0.01	0.01	<0.01	0.01	0.01
ICP-AES	TiO2	0.18	0.19	0.2	0.25	0.15
ICP-AES	MnO	0.01	0.01	0.06	0.11	0.04
ICP-AES	P2O5	0.03	0.06	0.06	0.09	0.05
ICP-AES	SrO	<0.01	<0.01	<0.01	0.01	<0.01
ICP-AES	BaO	0.04	0.04	0.04	0.02	0.06

The major elements are the one that dominates any rock at the analysis where their concentration is expressed in percentage (Rollinson, 1993). Table 5.1 above shows the result in percentage of the major elements for the five samples of the quartz porphyry intrusions both at depth and at the surface. The first two samples (GS004 and GS005) are from the drill core and the other three are the surface outcrop samples.

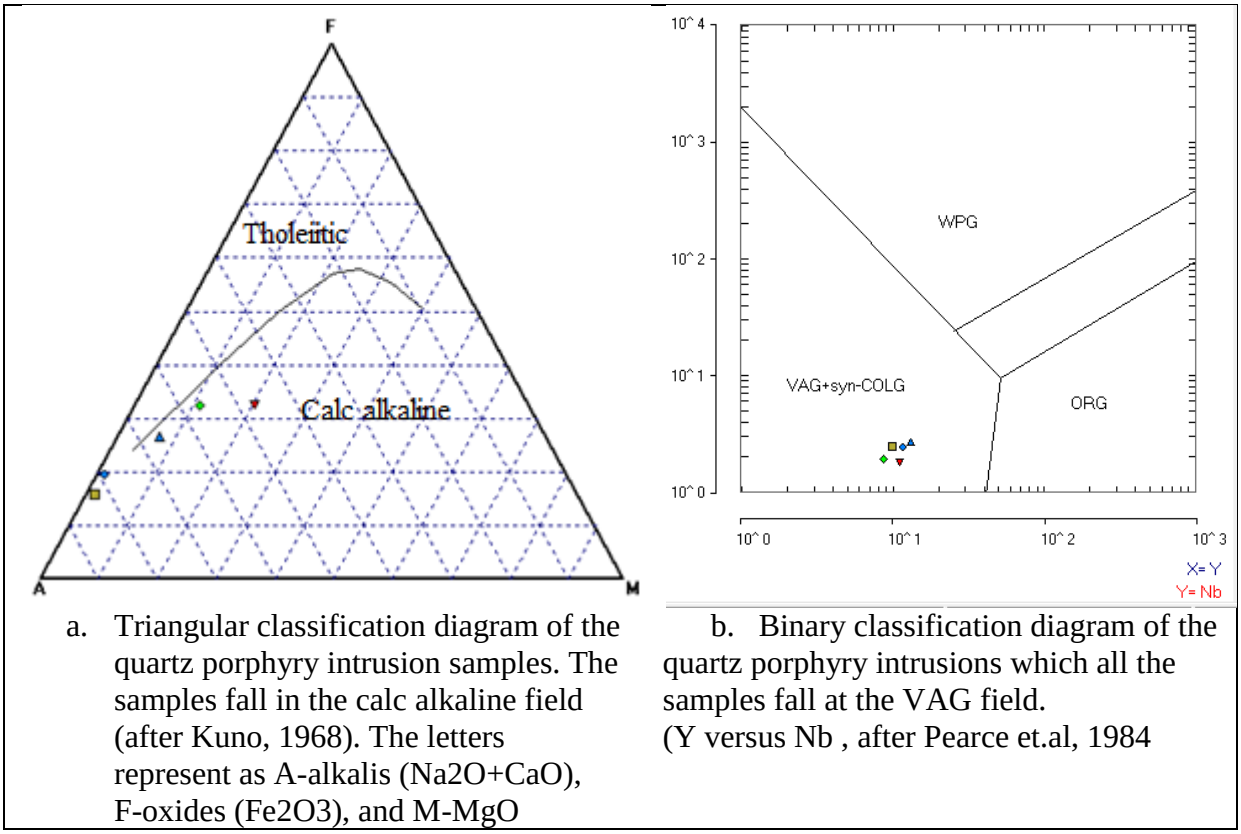

a. Triangular classification diagram of the quartz porphyry intrusion samples. The samples fall in the calc alkaline field (after Kuno, 1968). The letters represent as A-alkalis (Na2O+CaO), F-oxides (Fe2O3), and M-MgO

b. Binary classification diagram of the quartz porphyry intrusions which all the samples fall at the VAG field. (Y versus Nb , after Pearce et.al, 1984

Figure 5.1 Chemical classification diagrams for the quartz porphyry intrusions. The symbols representing the samples in both figures are: GS004- Brown square; GS005- Blue diamond; T1L4- Green diamond; T3L6- Red and inverted triangle; T4L2- Blue triangle

The analytical result plots for the quartz porphyry intrusions in AFM diagram (Fig. 5.1a) show that the quartz porphyry intrusions fall in the calc alkaline field (after Kuno, 1968). The figure shows that all the samples of the intrusions are concentrated at the same region with a positive slop which indicates that they could have relatively the same characteristics. This could be at the volcanic arc setting as described by trace element plot (after Pearce et.al, 1984). This is indicated in Figure 5.1b where Y is plotted against Nb.

On the other hand the following Harker variation diagrams Figure 5.2 show the plots of SiO2 versus the different major elements for the quartz porphyry intrusion sample. The figure shows the main compositional trend of the porphyry intrusion samples.

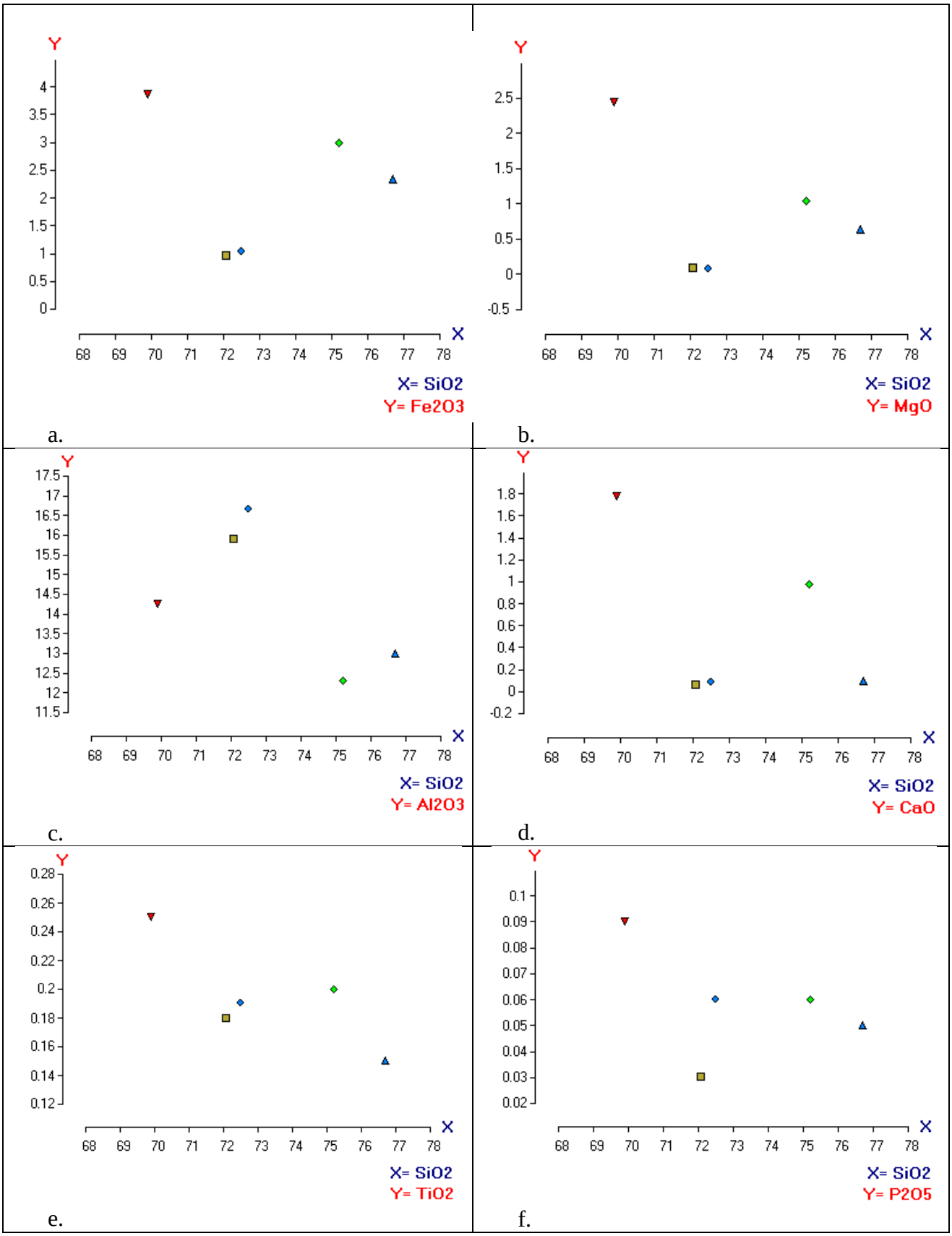

Figure 5.2 SiO2 versus major elements plot for the quartz porphyry intrusion. The symbols representing the samples in both figures are: GS004- Brown square; GS005- Blue diamond; T1L4- Green diamond; T3L6- Red and inverted triangle; T4L2- Blue triangle.

According to Rollinson (1993) and Fawzy et al. (1997) the scattered nature of the samples over the whole types of the SiO2 versus major element plots indicate that the quartz porphyry intrusions have accumulation of large number of phenocrysts. Accordingly this is also caused by the intensive alteration. In other cases these conditions are occurred by element mobility which takes place during weathering, metamorphism and/or as a result of interaction with hydrothermal fluids (Rollinson, 1993). The quartz porphyry intrusions are dominated by the large quartz porphyroblasts and intensive chlorite alteration. Therefore the most likely cause for these trends on the variation diagrams could be accumulation of the porphyroblast phenocrysts and alteration. In addition weathering could have some roles for these patterns.

5.2.2 Trace elements of the quartz porphyry intrusions

Both compatible and incompatible trace elements are detected from the analytical results of the quartz porphyry intrusion samples. There are 31 trace elements and REE for each of the samples which show analytical results of different ranges of concentration values. The following table 5.2 shows the analytical results of the trace element and REE values of the quartz porphyry intrusions both for the surface and subsurface samples. The elements are arranged based on their atomic number which increases from the top to bottom in the table.

Table 5.2 Trace element analytical results of the quartz porphyry intrusions

Methods of analysis	Trace Element	Atomic number	Analyzed Samples and their concentration values in ppm				
			GS004	GS005	T1L4	T3L6	T4L2
ICP-MS	Be	4	1	1	1	1	1
ICP-MS	V	23	23	38	48	69	0.49
ICP-MS	Cr	24	10	10	<10	10	10
ICP-MS	Ga	31	13	14.4	10.8	12.8	16.3
ICP-MS	Rb	37	22.9	19.2	16.4	12.8	51.5
ICP-MS	Sr	38	102	213	45.1	210	49.9
ICP-MS	Y	39	9.8	11.6	8.6	10.9	12.9
ICP-MS	Zr	40	75	79	76	69	78
ICP-MS	Nb	41	2.6	2.5	2	1.9	2.8
ICP-MS	Sn	50	1	1	1	1	1
ICP-MS	Cs	55	0.22	0.15	0.17	0.28	0.55
ICP-MS	Ba	56	355	385	333	194.5	580
ICP-MS	La	57	6.3	12.3	4.6	4.9	6.2
ICP-MS	Ce	58	12.8	25.6	10.2	10.3	12.5
ICP-MS	Pr	59	1.51	3.16	1.32	1.54	1.67
ICP-MS	Nd	60	7.1	13.3	5.7	7.5	7.6
ICP-MS	Sm	62	1.46	3.11	1.29	1.74	1.58
ICP-MS	Eu	63	0.51	0.85	0.4	0.42	0.47
ICP-MS	Gd	64	1.4	2.33	1.49	1.86	1.66
ICP-MS	Tb	65	0.23	0.31	0.26	0.26	0.29
ICP-MS	Dy	66	1.59	2.04	1.35	1.7	1.88
ICP-MS	Ho	67	0.39	0.4	0.31	0.36	0.42
ICP-MS	Er	68	1.12	1.29	1.05	1.11	1.25
ICP-MS	Tm	69	0.18	0.21	0.16	0.17	0.19
ICP-MS	Yb	70	1.18	1.32	0.81	1.02	1.61
ICP-MS	Lu	71	0.22	0.23	0.15	0.17	0.28
ICP-MS	Hf	72	1.9	2.2	2.2	2.1	2.3
ICP-MS	Ta	73	0.1	0.1	<0.1	0.3	0.2
ICP-MS	W	74	3	2	1	1	2
ICP-MS	Th	90	0.96	1.23	0.92	0.81	1.12
ICP-MS	U	92	0.65	0.47	0.42	0.74	0.49

The following trace element variation diagrams show the plot of the highly incompatible trace elements such as Th versus Ta, Th versus La, La versus U and La versus Nb. These elements are assumed to be insensitive to fractional crystallization (Dereje Ayalew et al, 1999). The patterns of the plot at Figure 5.3d show that they are slightly correlated. In addition the plots Th versus La and La versus Nb shows increasing correlation. The Th versus Ta plot shows decreasing correlation. Sometimes this happens due to source heterogeneity. But the quartz porphyry intrusions have almost similar characteristic features. According to Dereje Ayalew et al. (1999), Dereje Ayalew and Sally (2009) and Rollinson (1993) this

variation and scattering nature possibly suggests accumulation of phenocrysts and element mobility. This could be the most likely cause for those elements at the quartz porphyry intrusion samples.

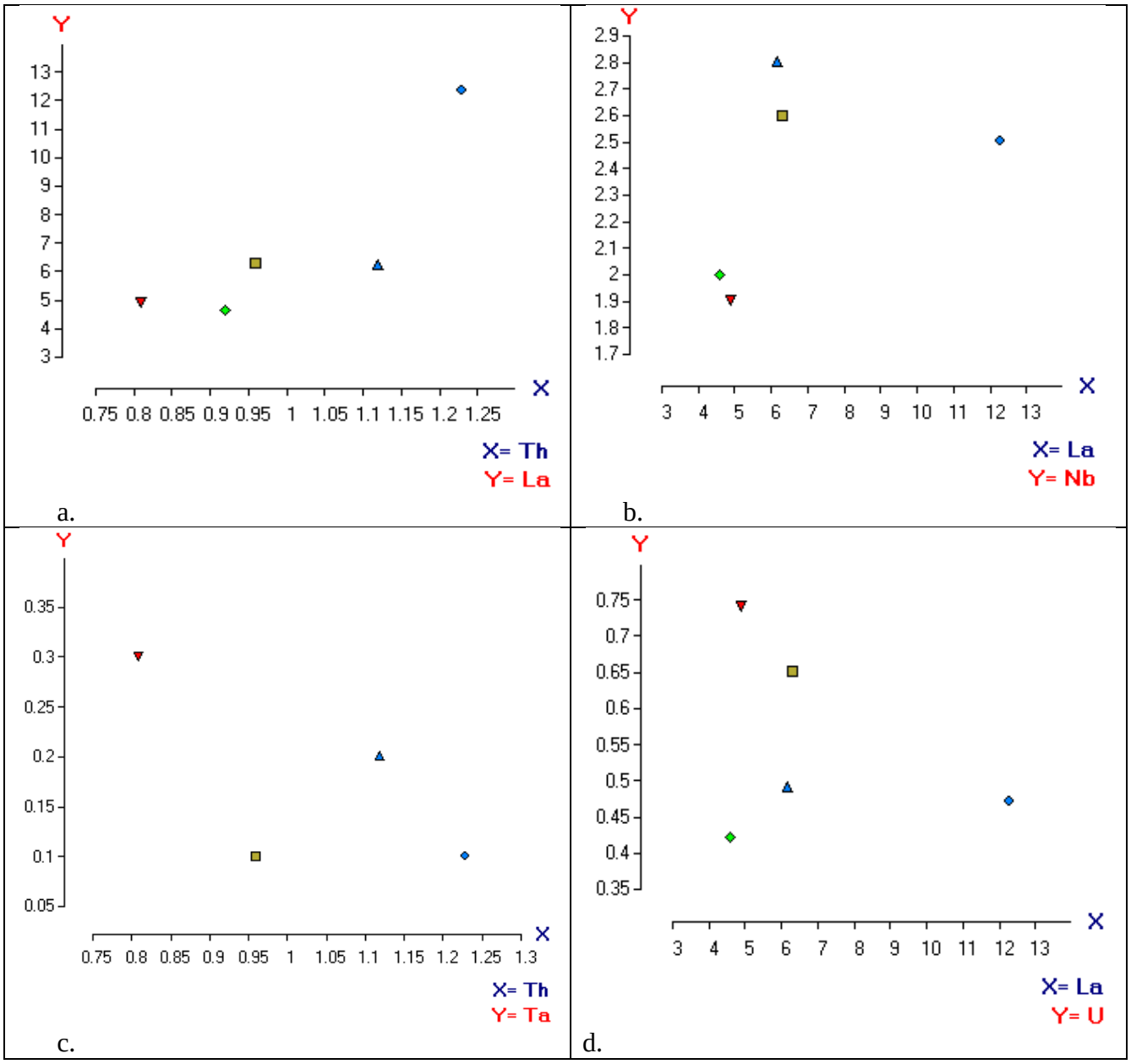

Figure 5.3 Trace element variation diagrams of the quartz porphyries intrusion. The symbols representing the samples in both figures are: GS004- Brown square; GS005- Blue diamond; T1L4- Green diamond; T3L6- Red and inverted triangle; T4L2- Blue triangle.

The rock/chondrite normalized rare earth element pattern in (Figure 5.4) of the quartz porphyry intrusions shows relatively flat heavy rare earth element patterns. The plotted pattern shows negative slop relatively decreasing towards the HREE up to the element Dy and from Dy to Tm it becomes flat pattern for all the samples. The patterns of all the

analyzed intrusion samples show analogous graphic pattern. The similarity of the pattern of the graphs for the porphyries indicates that the formations of the quartz porphyry intrusions are at the same event in the juxtaposition and they have homogenous characteristics.

The second (Figure 5.5) shows the primordial mantle normalized trace element pattern of the quartz porphyry intrusion samples. The pattern of the graph shows that the samples are characterized by relative enrichment of the highly incompatible trace elements. The graph shows crusts at rubidium, barium and potassium. On the other hand the normalized graph shows a pattern of low anomalous value or a trough for the elements such as cesium, niobium and titanium for all of the quartz porphyry intrusion samples. This pattern suggests that existence of opaque minerals fractionation (Rollinson, 1993; Dereje Ayalew et al., 1999).

On the other hand the graph shows that an average value of the more mobile large ion lithophile elements (LILE) of strontium. According to Rollinson (1993) this condition might be an intermediate fractionation of the plagioclase mineral

From the graph it is observed that the high field strength elements like titanium, niobium and tantalum show very low anomalous value for all of the intrusion samples. This indicates the fractionation undergoes less or no involvement of the minerals like illmenite, rutile or sphene (Rollinson, 1993). The negative Nb anomaly as compared to the other elements indicates a characteristic of continental crust and suggests that there is probably involvement of the continental crust in its formation.

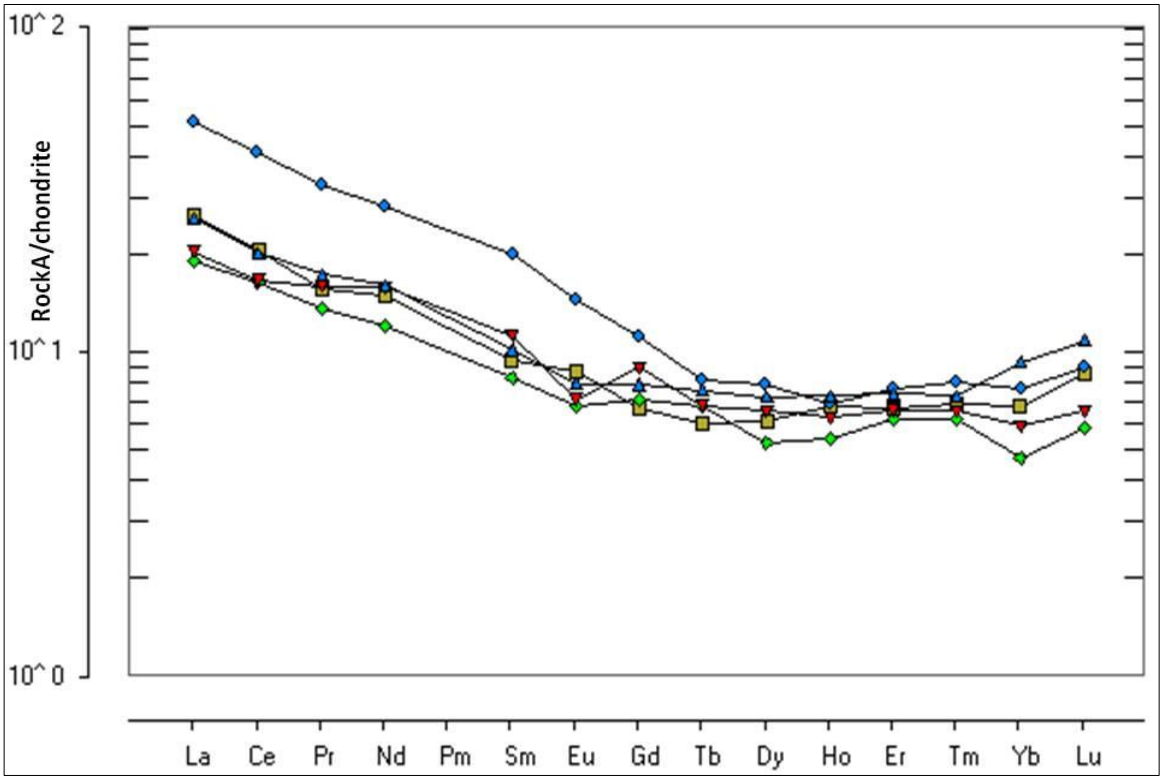

Figure 5.4 Chondrite normalized REE plot of the quartz porphyry intrusions The symbols representing the samples in both figures are: GS004- Brown square; GS005- Blue diamond; T1L4- Green diamond; T3L6- Red and inverted triangle; T4L2- Blue triangle

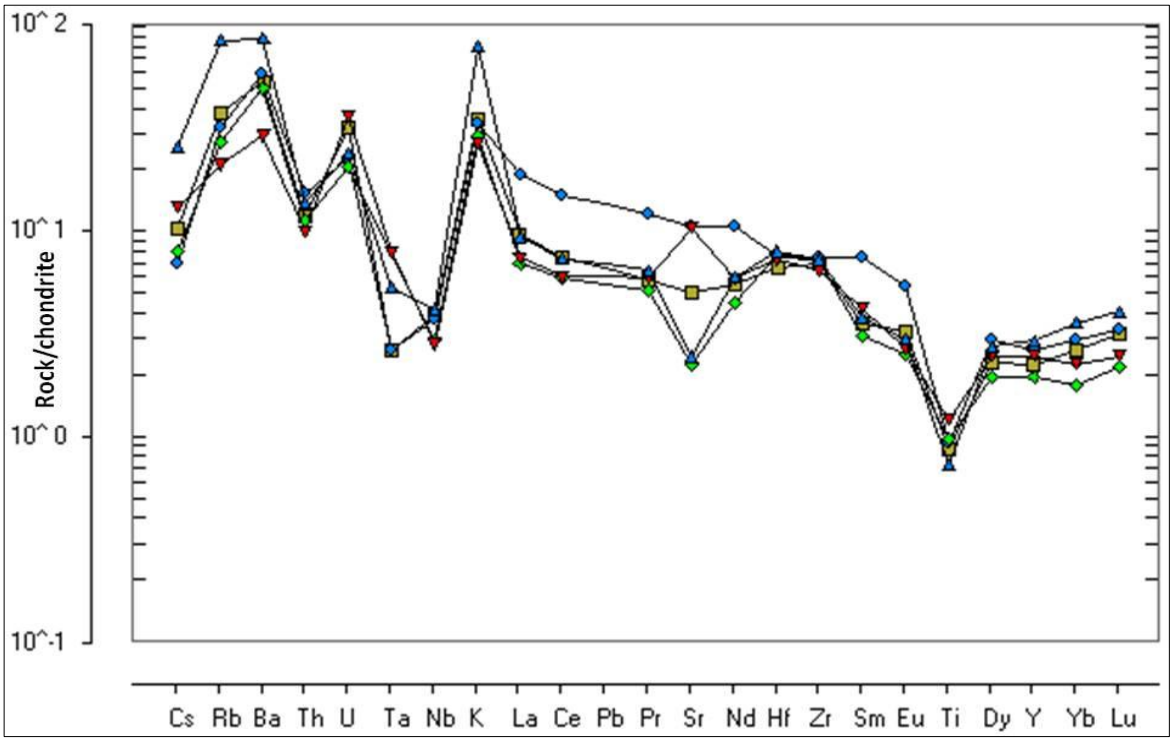

Figure 5.5 primitive mantle normalized trace element plot of the porphyry intrusions The symbols representing the samples in both figures are: GS004- Brown square; GS005- Blue diamond; T1L4- Green diamond; T3L6- Red and inverted triangle; T4L2- Blue triangle

5.2.3. Genesis of the quartz porphyry intrusions

The means by which the rock or mineral is formed and becomes stable varies from one rock type to the other rock type. It depends on the source of the original material, the agents responsible for the formation of the rocks, the transportations agent. In addition it is depending on the transportation path way as well as the environmental condition at the time of formation and after formation (Bucher, 2011).

Several quartz porphyry intrusions are distributed and outcropped over the entire part of the Terakimti area. Naturally in most volcanic rocks high anomaly of Eu at spider plots generally tells that the fractionation of magma is at depth shallower than 40 kilo meters (Winter, 2011). But there is no Eu anomaly observed on the spider diagram of the quartz porphyry intrusion samples. According to winter (2011), this condition indicates that the depth of fractionation may be beyond 40km limit.

In addition chromium is highly compatible element in nature. The tabulated data shows that this element has limited concentration which is 0.03 for the surface sample T2L2, 0.02 for the sample T1L3 and 0.01 or less than 0.01 for the other samples. According to Green (1980) as sited by Winter (2011) this value is very small as compared to the mantle source rocks of chromium and the source of the samples may not be mantle origin and it might possibly be the lower crustal source.

5.3 Geochemistry of the host rocks

The widely distributed and different rock units affected by the quartz porphyry intrusions and the host rocks of the VMS gold and other base metal minerals are dominated by basalts and rhyolites. The rocks are characterized by different textures, structures and mineralogical associations.

5.3.1 Major element geochemistry of the host rock units

The different major elements analyzed using ICP-AES method of the 13 element package include SiO2, Al2O3, Fe2O3, CaO, MgO, Na2O, K2O, Cr2O3, TiO2, MnO, P2O5, SrO and BaO. The analytical results of the major element values of the host rock units samples are listed in Table 5.3.

Table 5.3 Major element analytical results of the host rock units

Method of analysis	Types of major element	Sample codes and concentration % values of the major elements of the host rock units for the intrusions				
		T1L3	T2L2	T3L3	T3L5	T4L1
ICP-AES	SiO2	49.6	65.8	84.5	35.4	76.7
ICP-AES	Al2O3	2.34	23.9	7.31	19.7	13
ICP-AES	Fe2O3	37.4	0.51	3.13	18.7	2.33
ICP-AES	CaO	3.77	0.04	0.03	0.28	0.09
ICP-AES	MgO	1.44	0.04	0.69	13.55	0.63
ICP-AES	Na2O	0.2	0.21	0.24	0.6	3.58
ICP-AES	K2O	0.11	0.04	2.82	0.03	2.31
ICP-AES	Cr2O3	0.02	0.03	0.01	0.01	0.01
ICP-AES	TiO2	0.08	0.85	0.17	1.13	0.15
ICP-AES	MnO	0.66	<0.01	0.45	0.19	0.04
ICP-AES	P2O5	2.74	0.02	0.03	0.2	0.05
ICP-AES	SrO	<0.01	<0.01	<0.01	<0.01	<0.01
ICP-AES	BaO	<0.01	<0.01	0.12	<0.01	0.06

As shown at (Figure 5.6) the samples concentrated at one region in the lower left part of the figure are the quartz porphyry intrusions samples. All the diagrams below at Figure 5.6 show that the basalt sample T3L5 has high magnesium value which is 13.55% as compared to the other host rock samples. According to Dereje Ayalew et al. (1999) this condition suggests that the sample is fractionated mafic phases. The two basalt samples i.e. sample T1L3 and T3L5 have different value of magnesium number which is 1.44% and 13.55% and they shows scattered trend in the graphs as plotted magnesium versus other oxides. According to (Rollinson, 1993) this considerable scattered implies that it would be due to the source heterogeneity for those mafic rocks.

The other samples taken from the basaltic units and the rhyolite units' show scattered trends in the plot of MgO versus other major elements. This situation indicates that the magma may be from heterogeneous source or changing fractionation assemblage at the time of crystallization (Rollinson, 1993). Best example is shown at (Figure 5.6) for the basalt samples i.e. the one at the upper right and the lower diamond shaped samples which are sample T3L5 and sample T1L3 respectively. This could be due to changing fractionation assemblage or source heterogeneity for those samples. The trend of the samples also proves that the geology of the host rocks in the area is generally having a characteristic of bimodal volcanism and composition with the mafic to felsic suit.

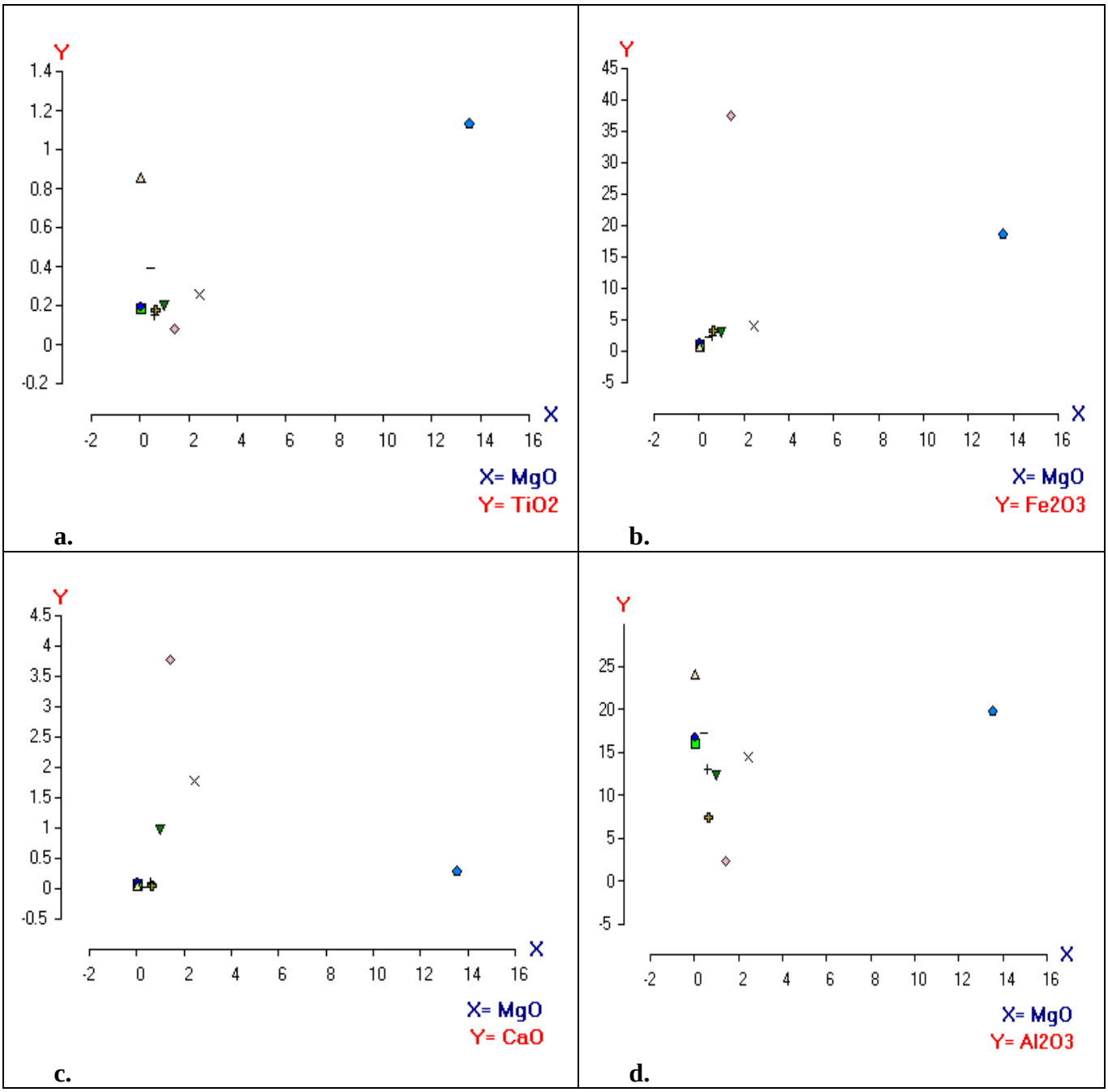

Figure 5.6 MgO versus major element plot of the quartz porphyries and host rocks. The samples and the symbols in the plot represented as: (T1L3- Purple diamond; T2L2- Brown triangle; T3L3- Brown cross; T3L5- Blue booth; T4L1- Green inverted triangle; T3L6- X-sign; T4L2- Plus(+) sign; GS004- Green square; GS005- Blue diamond.

On the other hand the magnesium value of quartz porphyry intrusion samples shows little variation and they are accumulated at the small area of the graphs. Some of them are overlapped each other that have the same value of the oxides. This possibly refers that they are subject to the same processes of formation at the same geologic time as well as the same sources. From the last plot (MgO versus Al2O3) the alignment of the samples shows almost

in a vertical pattern. The value of Al2O3 varies from one to the other without or little variation in the value of the MgO for the felsic samples including the quartz porphyry intrusions. This indicates the enrichment of Al2O3 might be a latter surface processes after the formation of the intrusions (Rollinson, 1993).

5.3.2 Trace element geochemistry of the host rock units

Table 5.4 Trace element analytical results of the host rock units

Methods of analysis	Trace Element	Atomic number	Analyzed Samples and their concentration values in ppm				
			T1L3	T2L2	T3L3	T3L6	T4L2
ICP-MS	Be	4	<1	1	1	1	2
ICP-MS	V	23	843	281	45	572	16
ICP-MS	Cr	24	100	160	10	20	10
ICP-MS	Ga	31	7.5	18.9	13	23.9	15.4
ICP-MS	Rb	37	3.5	0.8	61.4	0.4	29.7
ICP-MS	Sr	38	45	69.5	8.6	59	25.5
ICP-MS	Y	39	141.5	2.4	17.6	14.4	22.5
ICP-MS	Zr	40	44	43	66	42	124
ICP-MS	Nb	41	2.9	1.7	2.2	1.4	4.3
ICP-MS	Sn	50	4	1	1	1	1
ICP-MS	Cs	55	0.12	<0.01	0.25	0.01	0.15
ICP-MS	Ba	56	39.9	26.5	1055	20.5	986
ICP-MS	La	57	104.5	25.9	24.9	5.1	21
ICP-MS	Ce	58	41.9	21.4	43.8	11.6	35.9
ICP-MS	Pr	59	22.6	1.64	4.94	1.54	3.81
ICP-MS	Nd	60	101	5.4	20.3	7.9	14.8
ICP-MS	Sm	62	18.1	0.72	4.34	2.29	3.06
ICP-MS	Eu	63	4.15	0.12	1.33	0.75	0.8
ICP-MS	Gd	64	20	0.65	3.89	2.73	3.18
ICP-MS	Tb	65	2.88	0.11	0.6	0.37	0.6
ICP-MS	Dy	66	18.85	0.58	3.15	2.63	3.83
ICP-MS	Ho	67	4.36	0.09	0.7	0.55	0.83
ICP-MS	Er	68	11.95	0.27	1.97	1.75	2.69
ICP-MS	Tm	69	1.63	0.05	0.27	0.21	0.41
ICP-MS	Yb	70	8.6	0.36	2.11	1.5	3.34
ICP-MS	Lu	71	1.18	0.08	0.35	0.25	0.56
ICP-MS	Hf	72	0.6	1.2	1.7	1.4	3.5
ICP-MS	Ta	73	1.1	0.2	0.1	<0.1	0.2
ICP-MS	W	74	1	2	2	2	2
ICP-MS	Th	90	1.28	0.78	1.88	1.38	3.85
ICP-MS	U	92	1.51	0.59	0.92	0.41	0.98

Figure.5.7 below show the Chondrite normalized rare earth element abundances plots and the distribution pattern of the host rocks where the normalization values are (after Sun & McDonough, 1989). Figure 5.8 also shows the Primitive mantle-normalized trace element concentration plot (spider diagram) for the same host rock units. In this case the normalization values are from (Sun and McDonough, 1995).

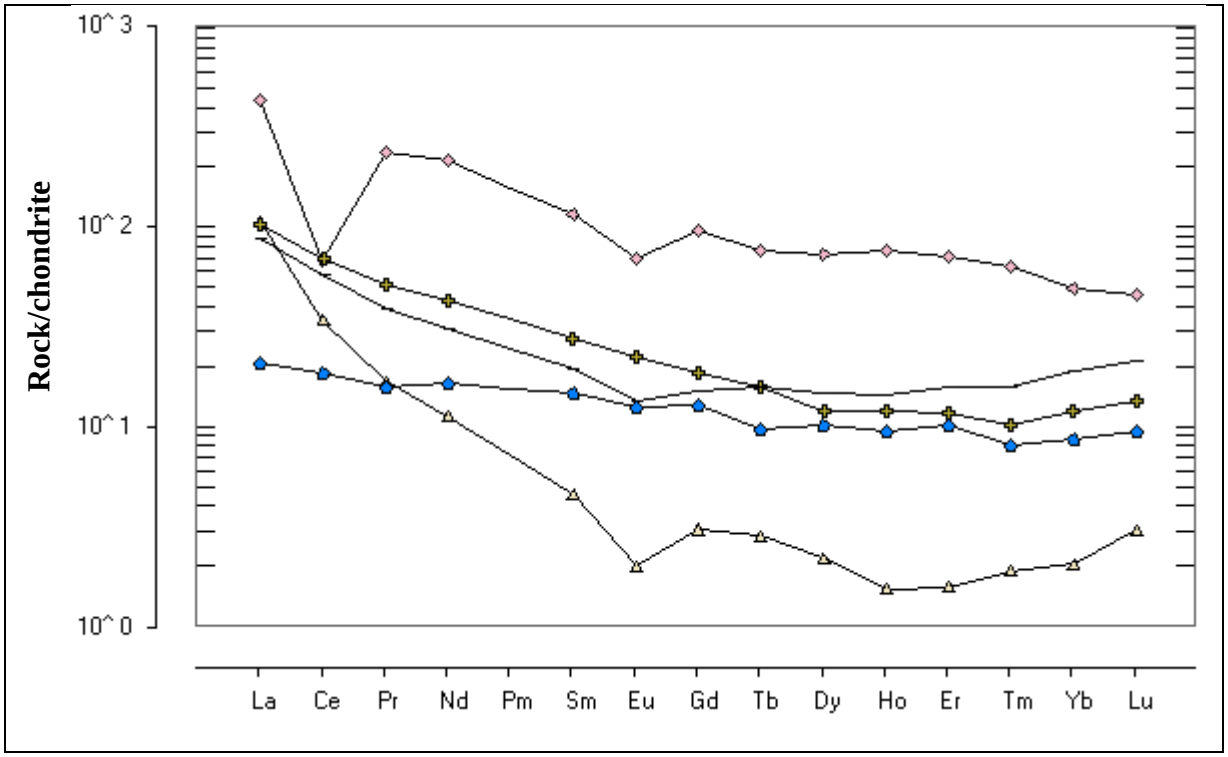

Figure 5.7 Chondrite normalized rare earth element plots of the host rocks. Normalization values are from (Sun and McDonough, 1995). The symbols represent (T1L3- Purple diamond; T2L2- Brown triangle; T3L3- Brown cross; T3L5- Blue booth; T4L1- Minus sign

From the chondrite normalization diagram plotted pattern it is observed that the two basalt samples i.e. sample T1L3 and sample T3L5 show wide difference value of lanthanum which is 104.5 and 5.1. This may be due to the result of source heterogeneity for the mafic samples (Rollinson, 1993). On the other hand the rare earth element chondrite normalized diagram shows that one of the rhyolite samples (sample, T2L2) show relatively low value of Eu which is 0.12. From the graph this sample shows a trough at the value of this element. The other samples show non anomaleous value of this element. In nature for magmatic melts that takes place at high oxygen activities the Eu element behalves like the other elements and it never show any anomalous pattern in the chondrite normalization pattern of the graphs. According to Rollinson (1993) and Dereje Ayalew et al. (1999) this anomalous nature of the element at

the T2L2 rhyolite sample at the plotted graph implies that the magmatic melt may takes place at low oxygen activities.

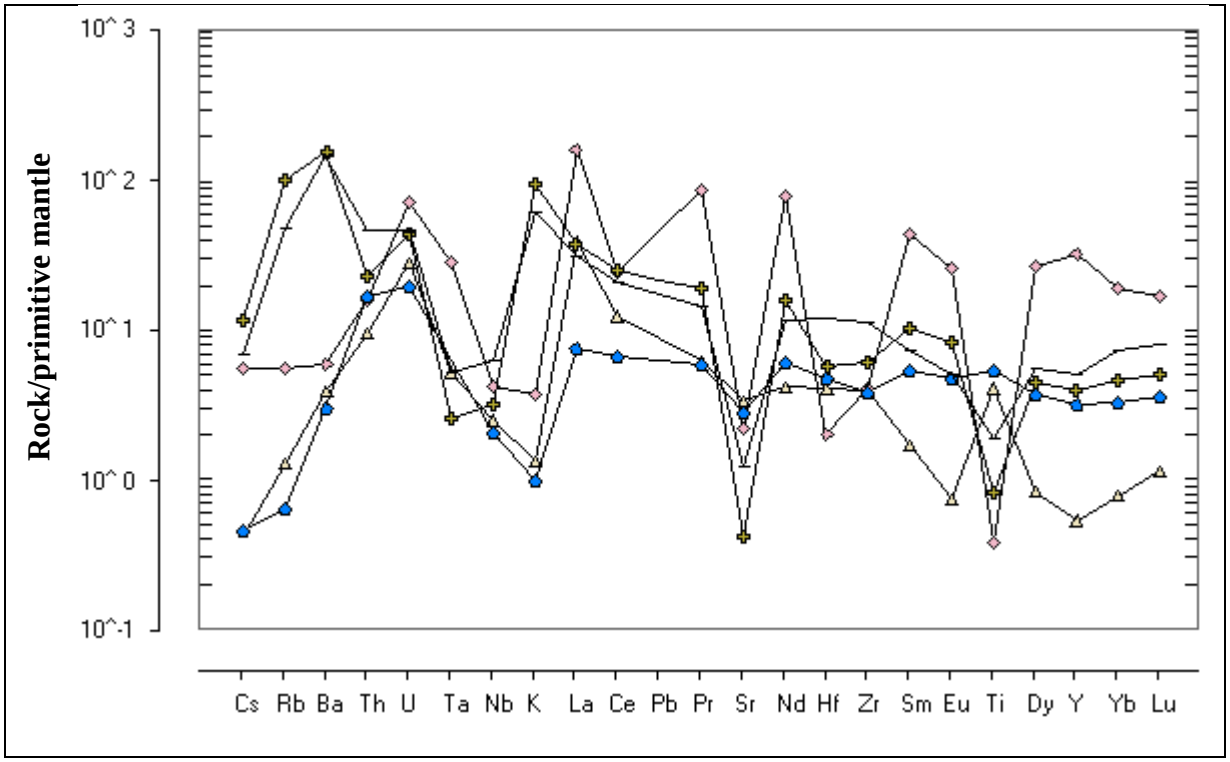

Figure 5.8 Spider diagram plot of the trace element for the host rocks. Normalization values are from (Sun and McDonough, 1995). The symbols represent (T1L3- Purple diamond; T2L2- Brown triangle; T3L3- Brown cross; T3L5- Blue booth; T4L1- Minus sign

As compared to the quartz porphyry intrusion samples the trace element spider diagram of the host rocks show high anomalous value of the elements. These show trough at some elements and crust at other elements. The anomalous nature of the elements is different at different samples. According to Rollinso (1993) and Dereje Ayalew et.al (1999) this proves the source heterogeneity for the same rock samples and bimodal volcanic nature of the host rock units.

Chapter 6 Mineralization and the roles of quartz porphyry intrusions

6.1 Introduction

The Arabian Nubian Shield is a significant orogenic body where numerous gold deposits and both artisanal and other mining activities are performed (Groves et al., 2003). Accordingly the gold deposits are hosted in a variety of rocks. These ranges from graphitic mica schist to ultramafic rocks for the Legedembi Ethiopian deposits and granite intrusion bodies for the Sukhay Barat-East- Saudi Arabia. The others are within granite contact facies in the El Sid and Umm Rus- Egypt. According to Samuel Abraham et al. (2006) among the different types of the gold deposits in the region VMS types are interesting for many researchers and exploration groups. This is due to the fact that VMS deposits of the region have poly metallic content and massive character.

6.2 Types of Mineralization

Three types of mineralization are recognized at Terakimti areas that are formed sequentially. The first is the volcanogenic massive sulfide (VMS) type enriched in poly metallic elements like (Cu, Zn, Pb silver and Au). The second type is the porphyry related mineralization characterized by weak mineralization and low value of the metals. The third is the supergene type of mineralization derived from the VMS and the porphyry metallic elements. These types of mineralization are described below.

6.2.1 Volcanogenic massive sulfide Mineralization

The VMS deposit at Terakimti area is associated with the mafic and felsic rocks with typical characteristic mineral assemblages such as pyrites, chalcopyrite, covelites and galena. The VMS is the main part of the deposit hosting the exploitable quantity of gold and other base metal elements. According to Archibald et al. (2014) this mineralization is characterized as a poly metallic type consisting of the metallic elements such as Au, Ag, Cu, Pb and Zn. The tabulated data of the different drill holes and the metallic element values are shown at appendix-1. The drill holes are tabulated based on the azimuth and dip of the drill holes, the depth intervals and the analytical values of the above metallic elements. The VMS bodies show that they have high concentrations of the metallic elements. The maximum value reaching up to 7.49% of Cu at a drill hole of TD008, 27.17g/t of Au at drill holes TD053, 300g/t of Ag at drill hole 10HTD002 and 23.03% of Zn at drill hole TD040. These data are

obtained from samples analyzed at depth intervals of 40.70 to 54.45 for Cu, 10.88m to 17.00m for Au, 28.80m to 42.00m for Ag and from 239.20m to 242.70m depth for Zn. The following graphs (Figure 6.1) show the concentration values of the four elements for the VMS samples taken at different depth intervals

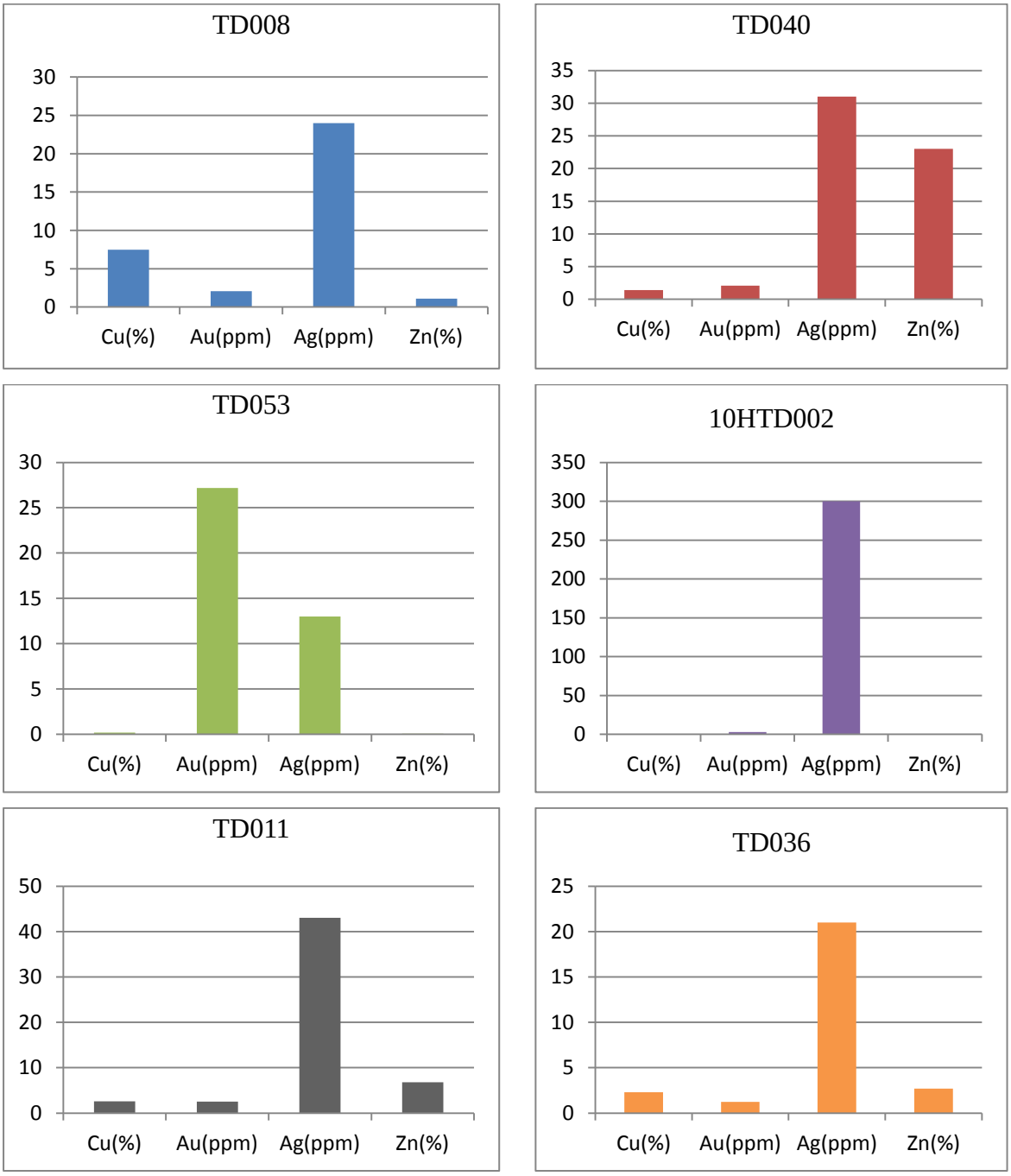

Figure 6.1 Graphs of selected drill holes for the VMS deposits. Note that as shown at appendix-1 TD represents the diamond drilling. The depth intervals for these drill holes include (TD008: from 40.7m-54.45m; TD040: from 239.2m-242.7m; TD053: from 10.88m-17.00m; 10HTD002: from 28.80m-42.00m; TD011: from 181.75m- 196.95m; TD036: from 81.4m-89.10m

6.2.1.1 The sulfides

The VMS deposits are more enriched with the sulfides than the quartz porphyry intrusions and the supergene deposits. The major sulfide minerals include the pyrites, pyrhotites and covelites. The pyrites are characterized by the textures of large sized grains. The pyrhotites are found as an inclusion in the large galena mineral. Dark zones are common at the boundary of some of these minerals which are results of alterations. The other mineral covelite is found in contact with the pyrites. These are slightly deformed showing some rotational features around the grains of pyrites and chalcopyrites. These minerals are very abundant at the drill core samples than the surface. The other mineral is galena characterized by small to large sized anhedral crystals found in most of the VMS samples. Most of the galena minerals are affected by alteration changing the minerals to reddish dark color. Most of the VMS deposits are enriched by these minerals with a characteristic of some indented black spots in the ground mass of foliated silicates. Replacement of galena by the covelites is common at most of the VMS samples.

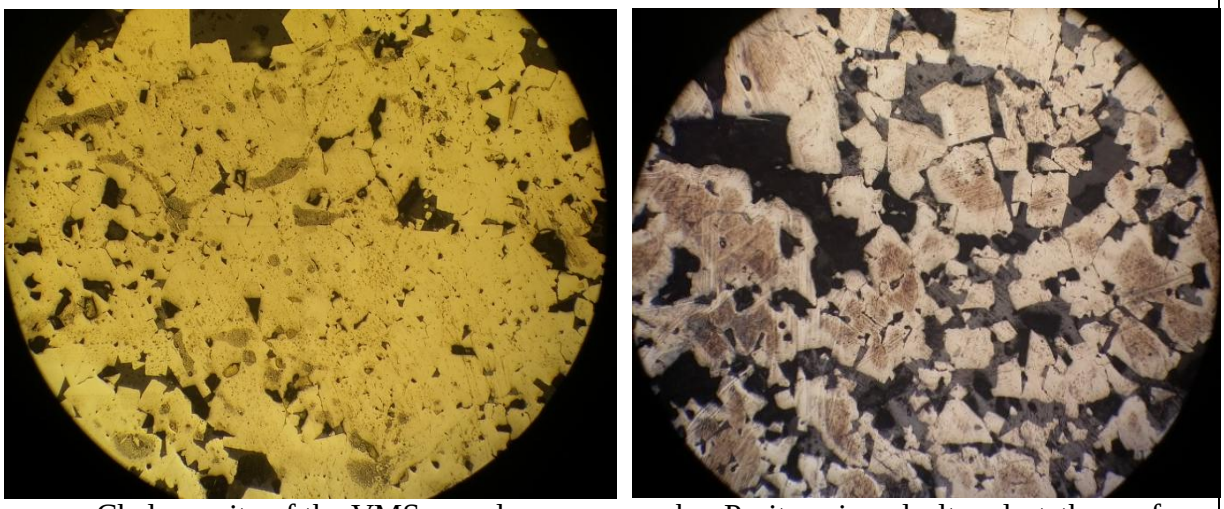

a. Chalcopyrite of the VMS samples. This mineral covers most of the field of views (XPL view, 10x magnification)

b. Pyrite mineral altered at the surface (ppl view (10x magnification)

Figure 6.2 Images of sulfide minerals from VMS deposits.

6.2.1.2 VMS mineralization model

The Arabian Nubian Shield hosts several volcanogenic or volcanic hosted massive sulfide deposits where they are manifested at different localities in different countries in the shield including the northern and western Ethiopian regions (Asfawossen Asrat et al., 2001,

Tarekegn Tadesse., 1997, Kasmin et al., 1978; Barrie et al., 2007; Beyth, 1971). According to Ohmoto (1996) all types of VMS deposits are assumed to be formed at extensional tectonic settings like mid oceanic spreading centers, arc back up spreading centers, and interacontinental rifts. The VMS mineralization in the Adi Nebried back arc basin has been variably described as bi-modal type (Hannington, 2009). The mineralization is hosted within volcanic and met sedimentary rocks. On the other hand the mineralization of the VMS deposits at Terakimti is bi-modal volcanic type. According to Hannington (2009) the surfacial manifestations of the VMS bodies are the formation of oxide gossans like hematite, magnetite or goethite gossans which are common in the study area. The following (Figure 6.3) shows the simple model of the VMS mineralization in the area.

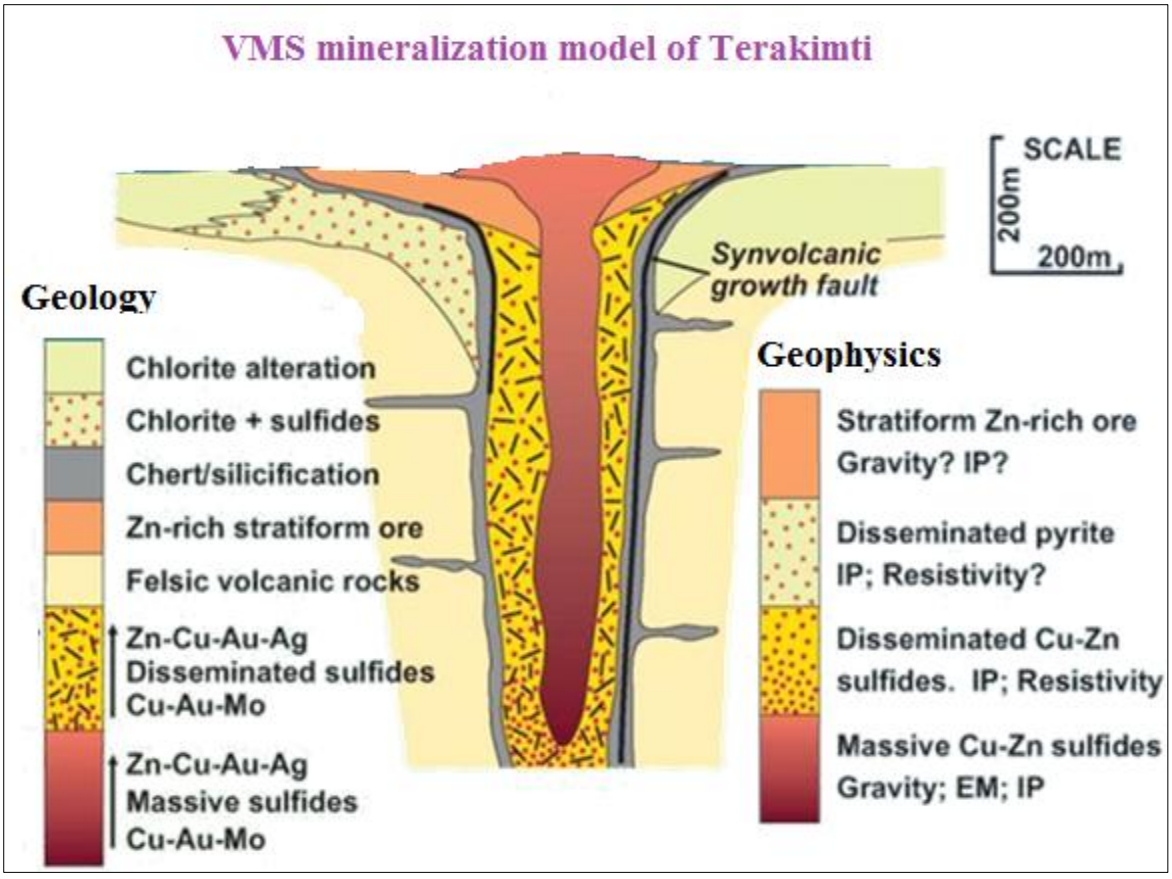

Figure 6.3 Mineralization model of the Terakimti VMS mineral deposits.

This shows the Idealized model of the Terakimti VMS mineralization showing the different zones of the mineralized bodies, the host rock bodies, some alteration features some structural features which is obtained by modeling the combined results of the geological and geophysical works Adopted from Steve et al. (2015) unpublished technical report and Archibald et al. (2014) technical report.

6.2.2 Mineralization of the quartz porphyry intrusions

The samples of quartz porphyry intrusions show different mineral associations where each mineral have distinct textural, structural and other characteristics. The most dominant ore minerals of the quartz porphyry intrusions include pyrite, chalcopyrite, covellite and galena. To study the characteristic of each quartz porphyry intrusions these minerals are described separately below.

6.2.2.1 Pyrites

These are the most dominant and abundant sulfide minerals of the quartz porphyry intrusions. These minerals cover most of the areas occupied by sulfides in each sample. The pyrites show white yellow color, very high reflectance with some altered surface, sub-hederal to euhedral triangular and rectangular shape. These minerals are dominant at the contact zones of the intrusions with the VMS deposits

6.2.2.2 Chalcopyrite

Chalcopyrites are the second abundant sulfide minerals in the quartz porphyry intrusions. The chalcopyrite are found in contact with the pyrite grains and distributed over the entire silicate ground mass commonly called chalcopyrite disease. They are characterized by high scratched surfaces than the pyrite minerals and highly indented surfaces. Most of the grains have anhedral habits and they are surrounding the pyrite crystals. At some samples the chalcopyrite grains are found as an inclusion in the pyrite and pyrhotite. For example (Fig. 6.4b) shows an association of the pyrite, chalcopyrite and covellite minerals where the pyrites and chalcopyrite's are in grain contact with each other. The covelites are forming a replacement texture at the grain boundaries of the pyrites and the chalcopyrites.

6.2.2.3 Galena

These are the other minerals found in association with the pyrites and chalcopyrites. These minerals are characterized by the hypautomorphic to xenomorphic crystals with triangular to circular black and some rectangular indents on the tabular surfaces. On the other hand some of these minerals are found as surrounding the other sulfide minerals like the pyrites, chalcopyrite's and the covelites. Some of the grains are broken into small fragments.

6.2.2.4 Covellite

These minerals are characterized by blue colors mostly found at the grain boundaries of other minerals. It is very small in abundance and found only at mineral boundaries of some samples. The covelite grains are found replacing the pyrites, galena and chalcopyrites at most of the samples which changes these minerals to an altered blue and dark color. On the other hand the covelite replacement of the sulfides might possibly be they are later formed than the sulfides as a result of alteration and replacement. In some cases covellites are surrounded by the chalcopyrites and pyrites which indicate the covelites replacement of the pyrites and chalcopyrites.

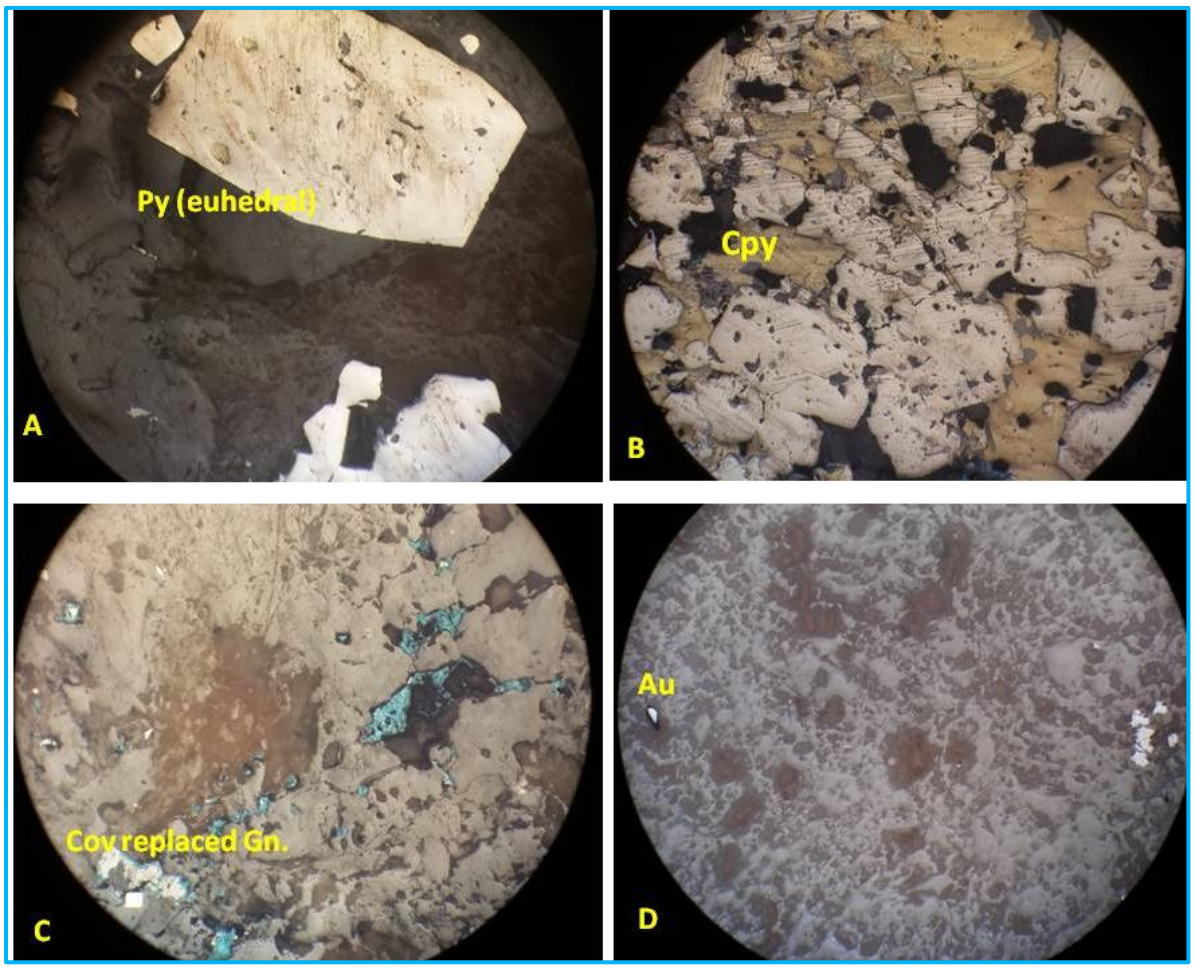

Figure 6.4 Ore minerals of the quartz porphyry intrusions. (A) Pyrite minerals of the quartz porphyry intrusions; (B) Chalcopyrite (yellow one) mutual grain contact with pyrite minerals (white grey color); (C) Covellite minerals (blue) replacing the galena mineral. Some of the galena minerals are totally replaced by the covellites (grey color). (D) Small gold grain within the silicates (at the left upper part). The one at the right part is galena. (Note that all images are under ppl view with 10x magnification)

6.2.3 Supergene mineralization

The supergene mineralization is the third type of mineralization formed latter and affects both the VMS and the quartz porphyry intrusion mineralization. This is dominantly found at and around the gossan zones of the Terakimti area. Surficial weathering results in the primary sulphides forming secondary, supergene minerals such as chalcocite, covellite, digenite, and bornite (Archibald et al., 2014). The surface manifestations of this supergene mineralization system at Terakimti area are the leaching of metals leaving silica and iron to produce a hematite and magnetite gossan. In addition the subsurface section map at Figure 4.8 shows this mineralization is dominant above the base of oxidation zone. The figure shows concentration of the metals at the supergene zone.

According to Groves et al. (2013) the supergene processes affect the surface and near surface parts of the Terakimti mineralization systems which leads for the formation of four vertical mineral zonations. These are the gossans zones, the silver enrichment transition zone, the supergene copper zone and the primary mineralized zone. The gossan is characterized by enrichment of the oxide minerals and gold without the presence of sulfide minerals which could possibly be the result of chemical weathering combined with the effect of circulation of meteoric water. The other silver enriched transition zone with variable gold is characterized by the absence of most primary ore sulfides except the pyrites and covellites. At this mineralized zone high gold and silver (up to 300 g/t Ag) are present with covellite and pyrite preserved as sulfides. The third important mineralized zone is the Supergene Copper Zone. This zone is characterized by weak development and is composed of abundant primary sulphide minerals and approximately 5 to 20% secondary copper minerals which include predominately covellite and minor amounts of chalcocite which occurs with primary chalcopyrite minerals. Accordingly the last significant mineralized zone is the primary zone characterized by the presence of copper, gold, silver and zinc which is composed of massive to sub-massive sulfide minerals.

6.3 Roles of the quartz porphyry intrusions in the VMS mineralization

The different quartz porphyry intrusion bodies have cross cut with the different host rocks of VMS deposits. The VMS deposits are also intruded by several late quartz veins. In addition the analytical results at appendix-1 shows the VMS deposits are highly mineralized than the quartz porphyry intrusions. From the analytical results of the metallic elements such as Au,

Ag, Cu, Pb and Zn the massive sulfides have concentrated value of elements whereas most of the samples from the quartz porphyry intrusions show only anomalous values.

More over the VMS ore samples shows that they are dominated by the association of the sulfide minerals like pyrite, chalcopyrite, covellite, galena and other oxide minerals. However the quartz porphyry intrusions even though they contain these minerals they are less abundant where they are dominated by the different gangue silicate minerals. In addition the maximum value of gold obtained from the analysis of the quartz porphyry intrusions is 3.4g/t as shown at Table 6.1 and the minimum value is that many barren samples without gold and others are weakly mineralized (Appendix-2 and table 6.1). As compared to the gold values of the VMS bodies with a maximum value of gold 27.17g/t, the porphyry bodies are weakly mineralized. The different section maps show that the VMS deposits are detached one from the other due to the late coming multiple quartz porphyry intrusions. The continuity of the VMS deposits is interrupted by the intrusions. On the other hand the VMS deposits are found within the large quartz porphyry intrusions. The core logs show that some massive sulfide bodies are bounded above and below by quartz porphyry intrusion.

In addition the VMS deposits of the area have characterized by high concentration and association of the Zn and Ag elements in the presence galena mineral. According to Mavogenes et al. (2001) these characteristic relations show that the massive sulfides are possibly remobilized by the late coming quartz porphyry intrusions. In addition according to Tomkins et al. (2004) and Frost et al. (2002) the presence of the globular masses of the galena minerals and microveinlets of sulfides in the different silicates of the quartz porphyry intrusions indicate that they are remobilized by the late coming silicate intrusions. There are also associations of the massive sulfides with different alteration zones both above and beneath the massive sulfides at depth (Appendix-2 and Figure 4.8). This relation is an important line of evidence to identify remobilization of massive sulfide bodies and associated elements (Tomkins Et al., 2007; Peter et al., 2010).

More over the scattered trend observed on the major and trace element variation diagrams is a good indicator of elements mobility (Rollinson, 1993). According to Rollinson (1993) the presence of the minerals that show metamorphism is started is also an indicator that there is a greater possibility of element mobility. All these possibilities are common features that the elements of the VMS bodies are remobilized by the late coming intrusions.

The remobilization of the massive sulfide bodies and contained minerals with the role of the quartz porphyry intrusion bodies could have both advantageous and disadvantageous features. Partial remobilization of the sulfide deposits results an increase in grain size and purity of the minerals which makes the libration easier and less costly (Vokes, 1969; Vokes, 2000; Marshall et al., 2000; Gauthier and Chartrand, 2005; as sited by Cynthia, 2010). In addition to these the selective mobilization or remobilization of the massive sulfide bodies results local enrichment of the significant metallic elements. Either all of the important metallic elements such as Au, Ag, Cu, Pb and Zn or some of them are highly concentrated in the VMS.

On the other hand the massive sulfide deposits in the area show distribution in relation with the quartz porphyry intrusions where one sulfide bodies is detached from the other. According to Cynthia (2010) and Mosier (2009) this remobilization of the VMS deposits will make the scattered distribution of them.

Table 6.1 Abundance of metallic elements in the quartz porphyry intrusions (gold, copper, lead and zinc). These are only for some selected drill holes at specific depth interval.(adopted from Archibald et al, 2014) technical report

Hole ID	From (m)	To (m)	Interval (m)	Copper %	Gold g/t	Silver g/t	Zinc %	Local azimuth	dip
10HTD001	71.70	79.30	7.60	2.07	4.01	36	2.59	275	-70
TD003	135.75	142.90	7.15	0.29	0.20	2	0.06	270	-60
TD004	57.45	131.30	73.85	3.77	1.31	14	0.72	270	-60
TD007	31.20	49.40	18.20	0.36	1.33	6	0.00	270	-60
TD018	135.63	154.80	19.17	3.68	1.40	13	2.37	270	-58
	138.89	154.80	15.91	4.07	1.35	13	2.83		
TD027	0.04	88.90	7.80	0.93	0.77	6	0.02	270	-63
TD034	0.00	29.00	29.00	0.14	3.40	11	0.08	270	-61
TD036	17.10	25.75	8.65	0.21	2.18	6	0.07	270	-80
TD039	86.15	105.90	19.75	2.39	1.81	13	1.99	270	-60
TD056	90.45	104.35	13.90	1.87	0.97	18	3.55	270	-60
TD057	140.90	143.70	2.80	2.12	3.00	33	0.72	270	-60

Chapter 7 Results and Interpretation

The lithology of the quartz porphyry intrusions are characterized by the presence of large quartz and feldspar porphyrobasts and other mica minerals. Basic to acidic host rock units hosting the VMS gold mineralization are common in the area. Field observations, textural characteristic features and structural evidences as well as mineralogical relation of the VMS deposits and the intrusions show that intrusions are late coming as compared to the VMS deposits. This is shown at the surface and subsurface maps. The subsurface sectional map (Figure 7.1) shows that the quartz porphyry intrusions are cutting the highly mineralized VMS deposits.

On the other hand the quartz porphyry intrusions have common textural, structural and mineralogical features. All quartz porphyry intrusions show that they have similar textural, mineralogical and micro structural features. In addition the field data collected show that the intrusion bodies have similar characteristic features except some of them show that they have local chlorite alteration together with the other mafic host rock units. Some grain size increase from surface samples to the samples at depth. This is related to the crystallization history at the time of formation of the intrusions.

The intrusions are also characterized by similar mineralogical assemblages except the alteration features which affect both the quartz porphyry intrusions and the other host rock units. These and other characteristic features of the quartz porphyry intrusions possibly tell that they have formed at the same. The ore mineral characteristics of the quartz porphyry intrusions observed at the polished section samples and under the thin section samples shows that most of the sulfide crystals and the oxides are replaced by the silicates where some of the grains are totally replaced by the silicates.

In addition there are also geochemical characteristics that relate one quartz porphyry intrusion to the other. The SiO2 content of the five intrusion samples listed at Table 5.1 shows variations between 69% and 77%. This is due to the variation of the quartz porphyroblast phenocrysts distribution in the analyzed samples. The samples are concentrated near each other in the other major element variation plotted diagrams as in (Figure 5.2). Not only the SiO2 content most of the major element contents of the intrusion samples are near each other and shows only slight variation. According to Dereje Ayalew et al. (1999) and Rollinson (1993) such characteristic features of the geochemical values for the samples imply that they

have genetic relation with each other. The triangular AFM diagram of the intrusion samples shows that all are concentrated at the VAG field. The primitive mantle-normalized trace element concentration plot patterns (spider diagram) of the quartz porphyry intrusions (Sun and McDonough, 1995) clearly show that they have the same fashion and parallel alignment. This possibly implies they have exposed to the same geological process of formation and timing. Two samples such as sample GS005 and T2L6 from the plot show that they have high value of Sr element that the plot falls at the same point for the two samples. According to Dereje Ayalew et al. (1999) and Asfawossen Asrat et al. (2004) such situations might be occurred as a result of crustal contamination

The field juxtaposition also shows that the quartz porphyry intrusion bodies are cut by late coming several quartz veins which are the latest of the formation units in the area. Based on the general cross cutting law, textural evidences and other geochemical results show that the general successive timing events of the units from older to younger in the area includes host rock units, massive sulfide deposits, the quartz porphyry intrusions and late coming and parallel aligned quartz veins and finally the gossan.

Other core point of the study is the role of the quartz porphyry intrusions in the occurrence of the VMS mineralization. Concentration of the different metallic elements such as the precious metals (Au and Ag) and the base metals (Cu, Pb and Zn) varies from the VMS to the quartz porphyry intrusions. The drilling log information of the quartz porphyry intrusions indicates the VMS deposits are cut by the intrusions. The analysis of the above metallic elements from intrusion samples show that most of the results are poorly enriched and only the anomalous values of the metals are observed. As compared to the massive sulfides they are very weak. Most of the massive sulfide bodies show that they are enriched in these metallic elements. From these characteristic features and metal values it is clearly visible that the intrusions are poorly mineralized. On the other hand mineralogical and other geochemical evidences show that they are remobilized the VMS mineralization. According to Vokes (1969 and 2000); Marshall et al. (2000); Gauthier and Chartrand (2005); Cynthia (2010); Mosier (2009) and Jensen and Bateman (1981) the processes of remobilization could possibly due to the effect of the intrusions cutting the earlier formed massive sulfide deposits and relocates at the new site of deposition.

The most important point which indicates the role of the quartz porphyry intrusion bodies in the VMS gold mineralization is the geochemical analytical results for gold and other base metal elements. The value of gold for the quartz porphyry intrusions is only show anomalous values with the exceptions of some samples at specific depths intervals (Appendix-1 and Table 6.1). On the other hand the VMS have high concentration of gold. Figure **4.6** and appendix-1 shows the analysis value of gold, silver and other base metals for the volcanogenic massive sulfide deposits. This indicates the intrusions are weakly mineralized and only stops the continuity of the VMS deposits

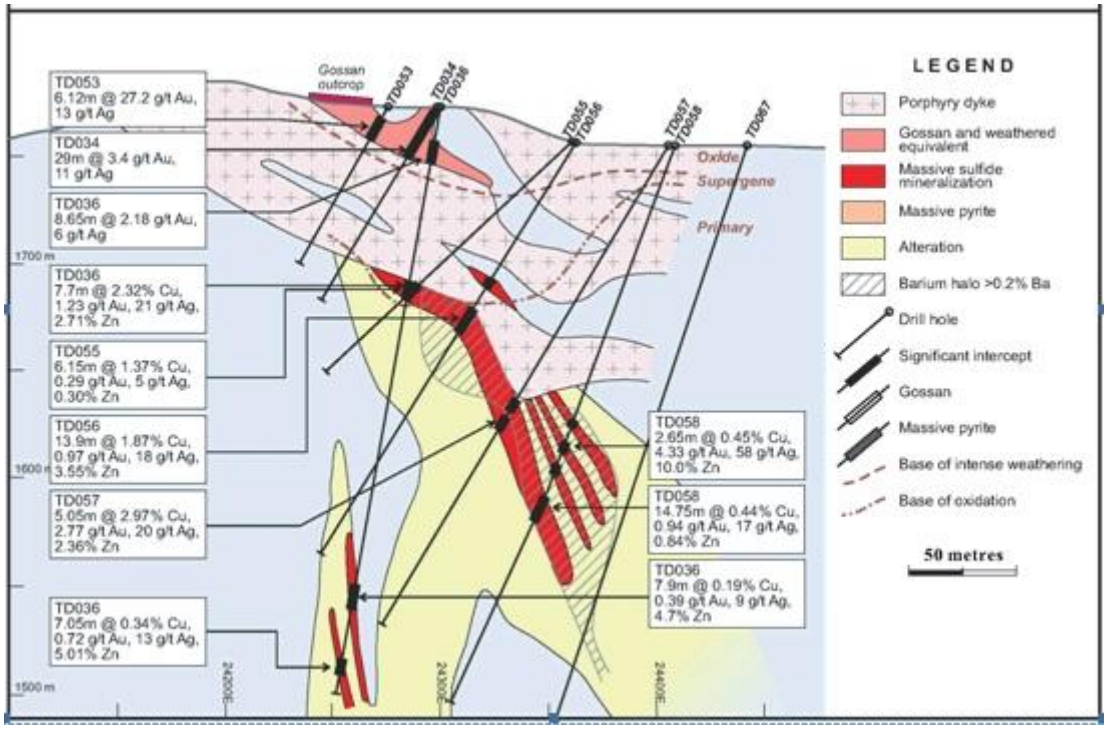

Figure 7.1 Metallic element concentration of VMS deposits at depth. This figure shows the assayed value of the massive sulfide units at specific depth intervals and subsurface cross cutting relationships with the quartz porphyry intrusions. (Adopted from Tigray resources incorporated plc 2012 unpublished technical report).

7.1 Research output

The core and significant findings that are elaborated and fully and/or partially resolved points includes that the geological map of the study area is completed at large 1:10,000 scale. Small units are made to be clear and visible. The structural relationship, mineralogical assemblages and textural characteristics of the quartz porphyry intrusions and the host rock units are described. The relative difference between the mineralization of the porphyries and the massive sulfide deposits are described. Based on these descriptions the relative timing

relationship between the different host rock units, the VMS deposits and the timing relation of the quartz porphyry intrusions found in the area are resolved. The three type of mineralization (VMS, porphyry and supergene are described and interpreted. More over this work basically resolves and clarifies the roles of several quartz porphyry intrusions on the VMS mineralization. The three types of mineralization in the area are described.

Chapter 8 Conclusions and Recommendations

8.1 Conclusions

The Terakimti area is covered by different types of lithological units. Based on thin section study, polished section study and geochemical analytical results it is concluded that the area is dominated by mafic (basalt) and felsic (rhyolite) volcanic suits.

Different field and laboratory results are obtained about the geology of the area and related to the regional geology. The field geological and structural relation between the different types of rock units show that they are not occurred at the same time. The field cross cutting relationship, textural characteristics, mineralogical compositions and geochemical evidences indicates that the quartz porphyry intrusions are cutting the other units. The quartz porphyry intrusions are cut by the late coming quartz veins which are the youngest of the units. On the other hand there are several quartz porphyry intrusions characterized by homogenous textures, mineralogical assemblage, geochemical features and structures. More over these intrusions show related patterns of both trace and major element plots that are good evidences that they are formed at the same time.

There are three types of gold and base metal mineralization sequentially formed at Terakimti area. These are the VMS, the porphyry and supergene deposits. The other important point is the role of the several quartz porphyry intrusions for the formation of the VMS gold and other base metal mineralization. The precious and base metal value of the different samples taken from the quartz porphyry intrusions show that they are weakly mineralized. On the other hand the geochemical analytical results of the VMS deposits show that the sulfides are enriched and have concentrated value of the metallic elements. In addition the subsurface section maps of the massive sulfides show that the VMS deposits are cut by the intrusions and misplaced from their continuity. More over the alterations and enrichment of silver as well as grain size variations are commonly observed to these sulfide units. These situations are evidences that the VMS deposits are remobilized by the intrusions.

Generally the distribution of the ore deposits, ore host rock relations the geological structures and the geochemical analytical results it is concluded that the intrusions are late coming after the VMS deposits. The cross cutting relation, out crop descriptions, micro texture,

microstructure and geochemical evidences combined with mineralogical characters show that the different quartz porphyry intrusions are formed at the same time in the juxtaposition.

8.2 Recommendations

Based on the different field and laboratory results and the interpretations, it is recommended that exact isotopic studies of the quartz porphyry intrusions will better determines the exact timing relation of the quartz porphyry intrusions. This may be the future works of other researches and this can be conducted for other intrusion units in the neighboring prospects and their regional relationships. The other important point is exactly where the VMS are remobilized and relocated. This can also conducted in addition to the Terakimti area for all other concessions in the region where several types of quartz porphyry intrusions are found in association with the VMS deposits. This is because of the problems observed that the massive sulfides are disturbed and some are relocated by the late coming quartz porphyry intrusions and found together in disordered manner. More over detailed works of the supergene deposits will improve the mineralization potential of the area.

References

Abdelsalam, M. and Stern, R.J. (1996). Sutures and shear zones in the Arabian–Nubian Shield. Journal of African Earth Science. **23:** 289–310.

Archibald, M. and Christopher, M. (2014). Mineral Resource Estimate at the Mato Bula Trend, Harvest Project technical report, Blue Coast Research, 207pp

Archibald, M., Christopher, M. and David G. (2014). Mineral Resource Estimate at the Terakimti Prospect, Harvest Property, Unpublished Technical Report, 207pp

Archibald, M., Christopher, M. and David G. (2015). Mineral Resource Estimate at the Mato Bula Trend, Adyabo Project northern Ethiopia, unpublished Technical Report, 202pp

Asfawossen Asrat and Pierre Barbey. (2003). Petrology, geochronology and Sr–Nd isotopic geochemistry of the Konso pluton, South-Western Ethiopia: implications for transition from convergence to extension in the Mozambique Belt. International Journal of Earth Science, Geol Rundsch **92**: 873–890

Asfawossen Asrat, Barbery, P. and Gleizes, G. (2001). The Precambrian geology of Ethiopia. Africa Geosciences review **8**: 271-288.

Asfawossen Asrat, Barbey, P. Ludden J. N, Reisberg L., Gleizes G. and Ayalew D. 2004. Petrology and Isotope Geochemistry of the Pan-African Negash Pluton, Northern Ethiopia: Mafic-Felsic Magma Interactions during the Construction of Shallow-level Calc-alkaline Plutons. Journal of Petrology, Oxford University press **45**: 1147–1179

Barrie, T.C., William N.F. and Claude A.H. (2007). The Bisha Volcanic Associated Massive Sulfide Deposit, Western Nakfa Terrane, and Eritrea. Society of Economic Geology. **102**: 717–738.

Barrie. C.T. and Hannington, M.D. (1999). Volcanic-associated massive sulphide deposits, Processes and examples in modern and ancient settings, Reviews in Economic Geology, Society of Economic Geology and Geological Association, Canada, **8**: 398-408.

Berhe, S.M. 1990. Ophiolites in North-East and East Africa, implications for Proterozoic crustal growth. Journal of Geological Society of London. **147**: 647-657.

Beyth, M. (1971). The geology of Central – Western Tigray, Rheinche Friedrich– Wilhems Universitate, Bonn, Germany, 95pp.

Beyth, M. (1972a). The geology of central – western Tigray, PhD. Thesis, Rheinche Friedrich– Wilhems Universitate, Bonn, Germany, 147pp.

Beyth, M. (1972b). Paleozoic-Mesozoic sedimentary basin of Mekele Outlier, Northern Ethiopia. AAPG Bull. **56**: 2426-2439.

Blasband, S.W, Brooijmans, H., Boorder, D. and Visser, W. (2000). Late Proterozoic extensional collapse in the Arabian Nubian Shield, structural geology, geodynamics research institute, the University of Utrecht, Netherland. **157pp**

Chewaka, S. and. Dewit, M.J. (1981). Precambrian base metals, Plate tectonics and metallogenesis, some guidelines to Ethiopian Mineral Deposits, Ethiopian Institute of Geological Surveys. **2**: 65-82.

Cousens, B.L. and Piercey, S.J., (2009) Submarine Volcanism and Mineralization. Geological Association of Canada, Mineral Deposits Division, **19**: 91-146.

Cynthia, D.B. (2010). Petrology of Metamorphic Rocks Associated with Volcanogenic Massive Sulfide Deposits, Volcanogenic Massive Sulfide Occurrence Model Scientific Investigations Report. U.S. Department of the Interior, U.S. Geological Survey, 146pp.

Dereje Ayalew and Gibson A. (2009). Head-to-tail transition of the Afar mantle plume: Geochemical evidence from a Miocene bimodal basalt–rhyolite succession in the Ethiopian Large Igneous Province. Elsevier publication, **112**: 461–476.

Dereje Ayalew, Gezahegn Yirgu and Raphael. (1999). Geochemical and isotopic (Sr, Nd and Pb) characteristics of volcanic rocks from southwestern Ethiopia, Journal of African Earth Sciences, Great Britain **29**: 381-391,

Fawzy, F and Abu E.E. (1997). Geochemistry of an island arc plutonic suite: Wadi Dabr intrusive complex, Eastern Desert, Egypt, Elsevier Science Ltd, Great Britain, Journal of African Earth Sciences, **24**: 473-496.

Frost, B.R, Mavogenes J.A. and Tomkins AG. (2002). Partial melting of sulfide ore deposits during medium- and high-grade metamorphism. Canadian Mineralogist **40**: 1–18.

Gass, I.G. (1981). Pan African (Upper Proterozoic) plate tectonics of Arabian-Nubian Shield. Precambrian plate tectonics. Elsevier, Amsterdam, 387-405.

Gauthier, M. and Chartrand, F. (2005). Metallogeny of the Grenville Province revisited: Canadian Journal of Earth Sciences, **42**:1719–1734.

Gebreyohannes Gebrehiwet. (2014). Geology, geochemistry and geochronology of Neoproterozoic rocks in western Shire Northern Ethiopia. Unpublished Msc Thesis, 88pp

Getaneh Assefa, Giovanni, M., Paola, D. and Roberto, V. (1981). Plate Tectonics and Metallogenic processes in Ethiopia. Unpublished Preliminary Report. 861-867

Gray, D.A., Meert, J.G., Goscombe, B.D., Armstrong, R., Trouw R.A. and. Passchier, C.W. (2005). A Damara Orogen perspective on the assembly of Southwestern gondwana, Institute for Geoswissenschaften, Johannes Gutenburg University, **89**: 456-468.

Green, T. H. (1980). Island arc and continent-building magmatism: A review of petrogenetic models based on experimental petrology and geochemistry. Tectonophys., **63**:367-385.

Greg C. (2009). Anatomy of Porphyry-Related Au-Cu-Ag-Mo Mineralized systems, Corbett Geological Services, North Queensland, 123pp.

Groves, I. M., Gardoll, S. J., Cavan, S. K., Warren, H. L., Carmen, C. E., Groves, D. I. (2013). The Terakimti Volcanogenic Hosted Massive Sulfide Cu-Au-Ag-Zn Deposit, Tigray Region, Northern Ethiopia. Internal company report, 56pp.

Hannington, M.D. (2009). Modern submarine hydrothermal systems – a global perspective on distribution, size and tectonic settings, Geological Association of Canada, 121pp.

Hiroshi Ohmoto. (1996). Formation of the volcanogenic massive sulfide deposits, the Kuroko perspective, Elsevier B.V, Kuroko, **10**: 135-177

International Study Group. (2011). Minerals and Africa's Development, United Nation Economic Commission for Africa, Addis Ababa, 230pp.

James, R. (2001). Ore-Mineral Textures and The Tales They Tell, The Canadian Mineralogist. **39**: 937-956

Jensen, L. and Bateman, M, (1981). Economic Mineral Deposits. John Wiley & Sons Canada. 49pp

Johnson, P.R. (2014). An Expanding Arabian-Nubian Shield Geochronologic and Isotopic Data set: Defining Limits and Confirming the Tectonic Setting of a Neoproterozoic Accretionary Orogen. The Open Geology Journal, **8**: 3-33.

Johnson, P.R., Andresen, A., Collins, A.S., Fowler, A.R., Fritz, H., Ghebreab, W., Kusky, T. and Stern, R.J. (2011). Late Cryogenian–Ediacaran history of the Arabian–Nubian Shield: Journal of African Earth Sciences. **61**: 167-232.

Kazmin V., Shiferaw A. and Balcha T. 1978. The Ethiopian basement and possible manner of evolution. Geologische Rundschau. **67**: 531-546.

Kroner A. and Stern, R .J. (2005). Africa/Pan-African Orogeny Encyclopedia of Geology Rift Valley University, Germany Amsterdam.**1:** 758pp

Kurt B. (2011). Petrogenesis of Metamorphic Rocks, Springer, Freiburg University Germany Berlin, 441pp.

Mackenzie W.S., Donaldson, C.H. and Guilford, C. (1982). Atlas of igneous rocks and their textures, Longman Scientific and Technical, Great Britain, England, 85pp.

Marshall, B., Vokes, F.M. and Laroque, C.L. (2000). Regional metamorphic remobilization: Upgrading and formation of ore deposits, Reviews in Economic Geology **11**: 19−38.

Mavogenes, .J.A., Mac, I.W., Ellis D.J. (2001). Partial melting of the Broken Hill galena sphalerite ore: experimental studies in the system PbS-FeS-ZnS-Ag2S. Econ Geol **96**: 205–210.

Mosier, D.L., Berger V.I. and Singer D.A. (2009). Volcanogenic massive sulfide deposits of the world; database and grade and tonnage models. U.S. Geological Survey Open-File Report 1034 pp

Mulugeta Alene, Jeniken, G.R.T., Leng, M. J. and Darby shire, F.D.P. (2006). The Tambien Group, Ethiopia: An early Cryogenian (ca. 800 - 735 Ma) Neoproterozoic sequence in the Arabian-Nubian Shield, Precambrian Research. **147**: 79-99.

Mulugeta Alene, Ruffini R and. Sacchi, R. (2000). Geochemistry and Geotectonic Setting of Neoproterozoic Rocks from Northern Ethiopia (Arabian-Nubian Shield). International Association for Gondwana Research, Japan. **3**: 333-347

Peter, K., Jaroslav, L., Adrian, B. and Juraj Z. (2010). Gold mineralization and associated alteration zones of the Biely vrch Au-porphyry deposit. Slovakia, Mineralia Slovaca, **42**: 33-56

Peter, K., Jaroslav, L., Adrian, B. and Juraj, Z. (2010). Gold mineralization and associated alteration zones of the Biely vrch Au-porphyry deposit. Comenius University, Slovakia. **42**: 33-56.

Peter, R. and Beraki Woldehayimanot. (2014). Development of the Arabian Nubian Shield perspective on accretion and deformation in the North-East African Orogen and the Assembly of Gonduwana.

Plimer, R. (2013). Exploration and discoveries in the Arabian-Nubian Shield; Kefi Minerals. Unpublished technical report, 211pp.

Robert F., Brommecker,R., Bourne B. T., Dobak P. J., McEwan C.J., Rowe R. R. and Zhou, X. 2007. Models and Exploration Methods for Major Gold Deposit Types, In Proceedings of Exploration. Fifth Decennial International Conference on Mineral Exploration. **07**: 691-711.

Rollinson, R. (1993). Evaluation, Presentation, Interpretation Using Geochemical Data, Pearson Education limited, England, 380pp

Samuel Abraham, Bheema, K. and Solomon Gebreselassie. (2015). Geology of volcanogenic massive sulfide deposit near Meli, northwestern Tigray, northern Ethiopia. Momona Ethiopian Journal of Science (MEJS), Mekelle University, Mekelle, Ethiopia, **7(1):**85-104,

Shackleton, R.M., (1986). Precambrian collision tectonics in Africa. collision tectonics-Geological Society of London,. **19**: 329-341.

Solomon Tadesse, (2009). Mineral resource potential of Ethiopia, Addis Ababa University press, 293pp

Solomon Tadesse, Pierre. J.M. and Deschamps. Y. (2004). Geology and mineral potential of Ethiopia,. A not on the Geology and mineral map of Ethiopia, Journal of African Earth Sciences, 36:273-313

Stern, R.J, Peter, K., Alfred, K. and Bisrat Yibas. (2004). Neoproterozoic Ophiolites of the Arabian-Nubian Shield, Developments in Precambrian Geology. **13**:221-234

Stern, R.J. (1994). Arc assembly and continental collision in the Neoproterozoic east African orogeny: Implication for the consolidation of Gondwanaland, Annual review Earth planetary science. **22**: 319-351

Stern, R.J. (2002). Crustal evolution in the East African Orogen, a neodymium isotope Perspective. Journal of African Earth Sciences **34**: 109-117.

Stern, R.J., and Abdelsalam, M.G. (1998). Formation of juvenile continental crust in the Arabian-Nubian Shield: Evidence from granitic rocks of the Nakasib suture, NE Sudan. Geologische Rundschau. **87**: 150-160.

Stoeser, D.B, Frost, C.D. (2006). Nd, Pb, Sr, and O isotopic characterization of Saudi Arabian Shield terranes. Chem Geol. **226**: 163-88.

Sun, S.S. and McDonough, W.F. (1989). Chemical and isotopic systematics of oceanic basalts: implication for mantle composition and processes: Magmatism in the ocean basins. Geological Society Special Publication **42**, 313-345.

Tarekegn Tadesse, Hoshino, M., and Sawada, Y. (1999). Geochemistry of low-grade metavolcanic rocks, the Pan-African of the Axum area, northern Ethiopia. Precambrian Research **99**:101-124.

Tarekegn Tadesse, Hoshino, M., Suzuki, K., Iisumi, S. (2000). Sm–Nd, Rb–Sr and Th–U–Pb zircon ages of synand post-tectonic granitoids from the Axum area of northern Ethiopia: Journal of African Earth Sciences, **30**: 313–327.

Tarekegn Tadesse. (1996). Geological map of the Axum sheet, Northern Ethiopia, Ethiopian Mapping Authority, Addis Ababa Ethiopia.

Tarekegn Tadesse. (1996). Structures across a possible intra-oceanic suture zone in low-grade Pan African rocks of northern Ethiopia. Journal of African Earth Sciences **23**, 575-381.

Tarekgn Tadesse. (1997). The geology of Axum area, Ethiopian institute of Geological Survey. Addis Ababa, Ethiopia, 192pp

Tomkins, A.G, Pattison, D.R and Frost, B.R. (2007). On the initiation of metamorphic sulfide anatexis, Journal of Petrolology **48**: 511–535.

Tomkins, A.G, Pattison, D.R and Zaleski E. (2004). The Hemlo gold deposit, Ontario: an example of melting and mobilization of a precious metal-sulfosalt assemblage during amphibolites facies metamorphism and deformation. Economic Geology **99**: 1063–1084.

Vail, J.R. (1985). Pan-African (late Precambrian) tectonic terranes and the reconstruction of the Arabian-Nubian Shield. **13**: 839-842.

Vokes F.M, Marshall, B and Spry P.G. (1997). Metamorphic and metamorphogenic ore deposits: Society of Economic Geologists, Inc. Reviews in Economic Geology. Society of Economic Geologists, America, **11**. 356-365.

Vokes, F.M., (1969). A review of the metamorphism of sulphide deposits: Earth Science Reviews, **5:** 99–143.

Vokes, F.M., (2000). Ores and metamorphism, Introduction and historical perspectives: Reviews in Economic Geology, **11**:1–18.

Warden, A. and Horkel, A. (1984). The Geological Evolution of the NE-Branch (Kenya, Somalia, Ethiopia) of the Mozambique Belt, 174pp.

Wilson, M. (1989). Igneous petrogenesis: a global tectonic approach. Harper Collins Academic, London. 566pp

Winter, D. (2011). An introduction to igneous and metamorphic petrology, New Jersey, United States of America , Library of Congress Cataloging-in-Publication Data, 796pp

World Bank. (1988). Industry and Energy Operations Division, Ethiopia Mineral Sector Review, Unpublished technical report, Eastern Africa Department, 175pp

Yardley, W.D., Mackenzie W.S. and Guilford C. (1990). Atlas of metamorphic rock and their textures, Longman Scientific and Technical, Longman Group UK Ltd, Great Britain, England,126pp

Appendix

Appendix-1 Concentration of Au, Ag, Cu, Pb and Zn in VMS deposits at different depth interval.

Role no.	Hole ID	From (m)	To (m)	Interval (m)	Copper %	Gold g/t	Silver g/t	Zinc %	Local azimuth of hole	Dip of hole
1	09HTD001	39.00	42.00	3.00	3.75	0.39	11	0.01	260	-75
2	09HTD002	42.00	54.00	12.00	1.06	0.88	24	4.11	275	-65
		75.00	92.00	17.00	0.33	0.38	10	1.10		
3	09HTD003	17.00	22.00	5.00	0.61	0.70	41	1.51	275	-75
		41.00	52.20	11.20	0.34	0.37	3	0.15		
4	09HTD004	69.00	76.00	7.00	0.30	0.37	11	4.21	275	-70
5	09HTD005	66.30	69.90	3.60	3.05	1.58	30	1.68	260	-75
		77.00	90.90	13.90	2.67	1.17	22	3.42		
6	10HTD001	85.30	93.80	8.50	0.41	0.32	5	0.59	275	-70
7	10HTD002	28.80	42.00	13.20	0.16	2.84	300	0.02	275	-65
8	10HTD003	45.60	97.70	52.10	4.10	1.55	26	0.13	261	-76
		54.20	93.70	39.50	5.35	1.74	21	0.15		
9	10HTD005	164.60	167.80	3.20	0.83	1.57	8	5.02	275	-65
10	10HTD006	149.20	154.00	4.80	0.32	0.35	13	2.43	260	-65
11	TD001	44.00	46.00	2.00	1.63	1.41	23	1.70	270	-60
		53.30	55.40	2.10	2.80	1.09	12	0.19		
		90.15	95.75	5.60	1.11	0.54	17	4.96		
		138.40	140.00	1.60	2.89	2.54	16	0.99		
		148.00	152.20	4.20	1.51	0.43	5	0.03		
12	TD002	106.00	110.25	4.25	0.12	0.26	6	4.708	270	-69
13	TD003	104.80	106.10	1.30	1.95	3.42	23	0.08	270	-60
14	TD004	78.65	115.10	36.45	6.01	1.70	19	1.31	270	-60
		162.50	163.75	1.25	0.68	0.68	15	4.76		
15	TD005	71.40	90.10	18.70	2.12	0.96	18	3.58	270	-60
		77.60	90.10	12.50	3.04	1.24	24	4.55		
16	TD006	99.00	102.50	3.50	0.99	0.59	8	0.16	270	-75
		111.00	113.75	2.75	0.40	1.02	14	0.19		
		129.50	131.45	1.95	1.18	2.56	25	2.79		
17	TD007	0.00	22.50	22.50	0.05	1.48	2	0.07	270	-60
		6.30	21.50	15.20	0.05	2.00	3	0.06		
		42.85	49.40	6.55	0.78	2.83	0	0.00		
		44.50	48.70	4.20	0.85	4.27	0	0.00		
18	TD008	38.75	59.60	20.85	5.67	1.49	18	0.77	270	-60
		40.70	54.45	13.75	7.49	2.07	24	1.09		
19	TD009	82.50	84.40	1.90	1.18	0.33	5	0.04	270	-60
20	TD010	56.00	70.75	14.75	0.17	1.29	37	0.00	270	-63
21	TD011	181.75	196.95	15.20	2.61	2.53	43	6.79	270	-90
		181.75	193.45	11.70	3.26	3.10	53	8.40		
		220.10	224.25	4.15	1.82	1.53	29	1.06		
		229.70	232.10	2.40	1.36	1.02	15	2.00		

22	TD012	40.28	44.75	4.47	0.03	4.26	77	0.02	270	-71
23	TD013	14.10	23.60	9.50	0.09	3.40	3	0.05	270	-60
24	TD014	57.45	94.45	37.00	3.53	1.21	26	1.32	270	-65
		58.20	80.50	22.30	5.35	1.65	40	2.08		
25	TD015	40.25	43.75	3.50	0.02	1.24	23	0.01		
26	TD016	80.40	98.15	17.75	2.98	1.61	20	0.03	270	-45
27	TD017	54.85	63.95	9.10	0.24	1.40	65	0.03	270	-60
		80.00	82.90	2.90	1.59	1.14	8	0.07		
		121.30	141.70	20.40	0.13	0.30	7	1.63		
		138.40	141.70	3.30	0.29	0.62	14	4.89		
28	TD018	85.90	89.90	4.00	0.04	0.06	0	2.42	270	-58
		93.90	96.00	2.10	3.58	1.22	20	2.04		
		124.05	154.80	30.75	2.55	0.99	9	1.52		
		124.05	130.75	6.70	1.09	0.45	3	0.12		
29	TD019	160.00	161.40	1.40	0.64	1.04	13	0.42	270	-60
30	TD020	38.00	39.20	1.20	0.01	1.10	7	0.00	270	-60
31	TD021	47.95	65.95	18.00	0.62	0.02	0	0.43	270	-70
		139.20	152.00	12.80	0.29	0.70	6	0.34		
		146.90	152.00	5.10	0.42	1.11	9	0.40		
		250.00	252.00	2.00	0.28	0.28	13	3.63		
32	TD022	87.35	116.30	28.95	2.99	0.83	23	3.56	270	-51
		87.35	94.65	7.30	3.55	1.05	31	6.43		
		100.80	115.45	14.65	4.05	1.05	28	3.52		
		199.50	209.50	10.00	0.22	0.73	9	2.23		
		204.00	209.50	5.50	0.29	0.74	10	3.11		
33	TD023	51.20	63.20	12.00	0.01	2.18	68	0.00	270	-60
		51.20	55.20	4.00	0.01	5.48	157	0.01		
34	TD025	74.70	80.50	5.80	3.52	1.20	23	0.72	270	-58
		93.85	125.60	31.75	1.84	0.86	17	7.03		
		106.50	123.20	16.70	2.37	0.93	19	9.16		
		110.50	122.40	11.90	3.08	1.11	20	9.54		
35	TD026	98.80	102.40	3.60	0.91	1.01	28	4.34	267	-70
36	TD027	55.95	66.80	10.85	1.26	1.21	13	0.02	270	-63
		55.95	57.80	1.85	4.56	1.71	34	0.04		
		81.10	84.90	3.80	1.19	1.32	10	0.03		
37	TD027	55.95	66.80	10.85	1.26	1.21	13	0.02	270	-63
		55.95	57.80	1.85	4.56	1.71	34	0.04		
		81.10	84.90	3.80	1.19	1.32	10	0.03		
38	TD028	29.35	34.25	4.90	0.91	0.61	4	0.10	270	-60
		32.15	34.25	2.10	2.09	0.62	3	0.24		
39	TD029	36.45	45.25	8.80	0.01	9.19	78	0.00	270	-60
		38.30	41.90	3.60	0.01	21.88	168	0.00		
		55.75	62.80	7.05	1.19	0.01	0	0.31		
40	TD030	7.20	17.70	10.50	0.08	6.30	16	0.05	274	-60
41	TD031	21.80	23.60	1.80	0.03	0.82	0	0.00	270	-60
42	TD032	4.70	8.00	3.30	0.09	1.08	20	0.02	270	-60
43	TD033	25.10	27.10	2.00	0.03	0.71	25	7.35	270	-60
		52.00	56.00	4.00	0.16	0.34	9	2.86		

		20.20	29.00	8.80	0.29	8.77	34	0.12		
44	TD035	0.00	29.00	29.00	0.14	3.40	11	0.08	270	-61
		20.20	29.00	8.80	0.29	8.77	34	0.12		
45	TD036	52.00	59.80	7.80	3.31	1.45	9	1.46	270	-55
		70.80	77.50	6.70	1.61	2.32	10	0.49		
		81.40	89.10	7.70	2.32	1.23	21	2.71		
		220.10	228.00	7.90	0.19	0.39	9	4.70		
		256.55	263.60	7.05	0.34	0.72	13	5.01		
46	TD037	53.15	69.85	16.70	1.23	2.37	36	8.07	270	-75
		59.80	66.70	6.90	1.08	3.86	57	15.39		
47	TD038	14.50	20.00	5.50	0.02	5.94	9	0.02	264	-55
		-55	52.80	3.00	0.75	0.42	11	0.01		
		114.70	115.40	0.70	1.57	3.61	9	0.60		
48	TD040	58.70	61.20	2.50	1.22	1.13	21	0.20	268	-60
		83.60	98.50	14.90	0.18	0.72	15	3.95		
		215.00	242.70	27.70	0.26	0.50	7	4.40		
		239.20	242.70	3.50	1.41	2.09	31	23.03		
49	TD041	28.50	31.65	3.15	0.02	5.32	9	0.00	270	-60
		50.90	54.35	3.45	0.55	0.02	0	0.01		
50	TD042	82.10	83.20	1.10	0.11	0.48	6	5.75	270	-60
51	TD043	147.70	195.50	47.80	1.01	0.70	6	0.72	270	-61
		174.20	191.65	17.45	2.15	1.11	10	0.42		
		174.95	186.10	11.15	3.05	1.28	14	0.56		
52	TD044	0.00	33.95	33.95	0.06	1.43	2	0.03	270	-60
		17.20	30.60	13.40	0.10	2.92	2	0.03		
53	TD045	140.00	146.30	6.30	0.53	0.20	2	0.06	270	-70
54	TD047	0.00	4.90	4.90	0.14	0.43	0	0.07	270	-60
55	TD048	81.85	87.35	5.50	1.51	0.83	31	13.26	270	-60
56	TD049	38.90	58.00	19.10	0.01	0.57	42	0.00	270	-61
57	TD050	169.35	173.00	3.65	0.02	0.78	1	0.09	270	-76
58	TD051	211.55	225.75	14.20	0.55	0.73	13	0.32	270	-67
		233.35	263.30	29.95	1.29	1.09	19	1.87		
		242.95	256.25	13.30	2.52	1.95	36	3.48		
59	TD053	10.88	17.00	6.12	0.19	27.17	13	0.08	270	-60
60	TD054	0.00	4.95	4.95	0.11	1.94	0	0.04	270	-60
61	TD053	10.88	17.00	6.12	0.19	27.17	13	0.08	270	-60
62	TD054	0.00	4.95	4.95	4.95	1.94	0	0.04	270	-60
		27.65	33.05	5.40	2.26	1.72	20	1.46		
63	TD055	98.50	104.65	6.15	1.37	0.29	5	0.30	270	-45
64	TD056	77.65	80.45	2.80	2.60	1.26	19	3.46	270	-60
		90.45	97.93	7.48	2.87	1.19	24	2.98		
		148.80	153.85	5.05	2.97	2.77	20	2.36		
65	TD058	134.70	136.10	1.40	0.01	1.01	30	9.27	270	-73
		144.80	147.45	2.65	0.45	4.33	58	10.00		
		158.95	161.35	2.40	0.06	2.50	33	3.13		
		173.95	188.70	14.75	0.44	0.94	17	0.84		
		178.10	181.65	3.55	0.93	2.22	42	2.12		
66	TD059	56.00	67.05	11.05	0.08	0.18	2	0.70	270	-60

67	TD060	99.15	107.45	8.30	0.45	1.32	19	2.41	270	-60
		104.90	107.45	2.55	1.05	3.25	47	4.60		
68	TD061	45.25	47.35	2.10	1.34	0.34	7	0.01	270	-57
69	TD065	233.55	241.05	7-Jan-00	0.02	0.06	0.00	0.51	280	-60
		238.00	241.05	3-Jan-00	0.03	0.08	0.00	0.82		
70	TD068	182.20	188.80	6.60	0.26	0.82	10.00	2.48	282	-60
		186.45	188.80	2.35	0.60	1.21	18.00	3.22		

Appendix.2 Drill log data for the quartz porphyry intrusions at different drill holes and different depth intervals.

Role no.	Hole ID	DD or RC	From	To	Mineralization	Characteristic features of the quartz porphyry bodies
1	TD025	DD	90	94	Barren	Surrounded by massive sulfides
2	TD024	DD	0	32	weak Cu & Zn	under laid by dolerite body
3	TD024	DD	171.5	175	weak Zn only	under laid by silica and sericite rich intermediate volcanic and overlaid by altered & rich silica intermediate volcanic
4	TD018	DD	135	139	Weak Au, Zn	Found In large massive sulfide
5	TD001	DD	142	145	weak Au, Cu, Zn	Surrounded by massive sulfide above and below
6	TRC123	RC	0	5	weak Au, Cu, Pb & Zn	found in the first 5m depth
7	TRC123	RC	12	18	weak Au, Cu, Zn	bounded above and below by altered unit
8	TRC073	RC	0	5	weak Au, Pb & Zn	found in the first five meter depth
9	TRC073	RC	7	17	weak Au, Cu, & Zn	Bounded by altered material below & above
10	TRC113	RC	1	7	weak Au, Pb, Zn	located at shallow depth and under laid by the gossans
11	TRC099	RC	11	17	weak Au, Cu, Pb & Zn	overlaid by altered material and under laid by massive sulfide
12	TRC099	RC	27	31	weak Au, Cu, Pb & Zn	Overlaid and under laid by massive sulfide ore.
13	TRC070	RC	0	32	weak Au, Ag, Cu, Pb, Zn	From 29m-31m separated interrupted by the massive sulfide. A continuation of the TRC099
14	TRC069	RC	0	7	weak Au, Ag, Cu, Pb, Zn	outcrop at the surface & under laid by the massive sulfide & part of the TRC099
15	TD045	TD	0	11.5	weak Au, Cu & Pb	under laid by dolerite unit
16	TD043	TD	0	10.5	weak Cu & Zn	from 3m-8m intruded by dolerite
17	TD040	TD	0	12.5	weak Cu & Zn	under laid by lithic tuff with quartz grain & it is a continuation of the TD043 QPOR no VMS around
18	TD040	TD	35.5	45.5	weak Au, Cu & Zn	overlaid by felsic tuff with quartz grains & weathered sulfide zone
19	TD027	TD	26	40	weak Cu, Pb & Zn	Overlaid by maffic tuff and under laid by silt stone. A continuation of the other QPOR
20	TD023	TD	10	16.5	weak Au, Cu, Pb, Zn	Under laid by felsic tuff with quartz grains & overlaid by lithic tuff with lapili grains. Interrupted from the large QPOR below by the felsic tuff.
21	TD023	TD	21	51	weak Au, Cu, Pb, Zn	underlaid and overlaid by massive sulfides
22	TRC068	RC	0	16	weak Au, Cu, Pb, Zn	Exposed at the surface and under laid by the massive sulfide body. Also continued from 29-32m & 40-42 m depth with altered QPOR from

						32-40m depth
23	TRC067	RC	0	3	weak Au, Cu, Pb, Zn	continued up to 34m depth where it is interrupted by massive sulfide body from 3m-12m
24	TRC066	RC	0	36	weak Au, ag, Cu, Pb, Zn	The upper 28m are barren of Ag. From 20-24m, 30-32m interrupted by massive sulfide bodies. It is under laid by the massive sulfide body and from 18-19m it is intruded by Quartz vein.
25	TRC066	RC	55	65	weak Au & Zn, Ag, Rich Cu & Pb	overlaid and under laid by altered pyrite rich material rich in Au and Ag
26	TRC065	RC	0	30	weak Au, Cu, Pb, Zn	from 16-17m interrupted by the quartz vein and from 19-22m interrupted by altered material
27	TRC065	RC	36	42	weak Au, Ag, Cu & Pb	Under laid by altered QPOR and overlaid by altered unit
28	TRC064	RC	0	21	weak Au, Cu, Pb, Zn	From 7-8m interrupted by hematite dominated gossans with quartz vein and from 8-13m massive sulfide.
29	10HTD007	TD	7.5	19	weak Pb	very far away from the next drill hole of TRC063 under laid by quartz vein and overlaid by intermediate tuff
30	10HTD007	TD	31	38	weak Pb	Overlaid by intermediate volcanic and under laid by felsic rhyolite flow banded
31	10HTD007	TD	127.5	129.8	weak Pb	overlaid by intermediate volcanic and under laid by felsic material
32	10HTD007	TD	139.8	142.2	weak Pb	overlaid by dolerite and under laid by altered felsic volcanic
33	TRC063	TD	0	30	weak Au, Cu, Pb, Zn	under laid by altered intermediate volcanic and from 24-25m interrupted by massive limonite dominated
34	TRC072	RC	0	2	weak Au, Cu, Pb & Zn	thin and under laid by altered unit original rock unknown
35	TRC074	RC	44	46	weak AU, Cu Pb & Zn	very small alteration
36	TD001	DD	61	71	weak Au, Cu, Pl & Zn	interrupted by massive sulfide b/n 63 & 64m depth
37	TD001	DD	132	134	Weak Au & Zn	Overlaid by Stringer S and Under laid by SD
38	TD022	DD	40	42	weak Zn	Overlaid by unit and under laid by siltstone
39	TD022	DD	44	54	weak Au , Cu & Zn	Sandwiched between two siltstone units
40	TD004	DD	66	68	Weak Au,Ag,Cu,Pb & Zn	thin body situated above the massive sulfides
41	TD047	DD	46	58.5	weak Cu & Zn	it is thick & bounded above and below by ALT rocks
42	TD047	DD	64	69	weak Au, Cu & Zn	none assayed units above & under laid by intermediate volcanic
43	TD047	DD	72	80	weak Au, Cu & Zn	the last 98 depth is sampled as intermediate volcanic
44	TD021	DD	74.5	75	weak Au & Zn	very thin within the altered rock
45	TD021	DD	84	84.5	weak Zn	it is thin body within the ALT
46	TD021	DD	134	135.5	Weak Au & Zn	overlaid by ALT and under laid by brecciate

						sulfide matrix (SBX)
47	TD018	DD	57	61.5	weak Cu & Zn	from 61.5 to 64.5 depth it is interrupted by altered siltstone
48	TRC001	RC	35	42	weak Au, Cu & Pb	under laid by altered material and overlaid by intermediate tuff
49	TRC001	RC	64	67	weak Au, k Cu & Zn	Bounded by altered materials
50	TRC083	RC	33	37	weak Au, Cu & Zn	it is altered and bounded by altered materials
51	TRC083	RC	42	43	rich Ag weak others	It is very thin and found within the altered material
52	TD019	RC	24	31	weak Zn	under laid by dolerite and overlaid by intermediate volcanic
53	TD019	RC	65.4	82	weak Cu & weak Zn	it is interrupted by aplite in the mid and by quartz vein below
54	TD003	TD	49	61	weak Ag, Cu & & Zn	Characterized by Quartz vein and overlaid by Chrystal tuff
55	TD 003	DD	22.4	28.4	weak Ag, Cu & Zn	overlaid and under laid by maffic tuff
56	TD 004	DD	21	22.6	weak Ag, Cu & Zn	Overlaid by dolerite and under laid by intermediate volcanic
57	TD004	DD	37	44	weak Ag, Cu & Zn	overlaid and interrupted by mafic tuff and under laid by silt stone and chert
58	TD004	DD	65	71	weak Au & Cu	Located between the massive sulfide bodies
59	TRC084	RC	30	37	weak Au, Cu, Pb & Zn	Shallow depth and overlaid by altered material
60	TD026	DD	19.5	26.5	weak Zn	sandwiched between two mafic bodies
61	TD026	DD	29.5	35.5	weak Cu & Zn	under laid by lithic tuff and overlaid by mafics
62	TD026	DD	130	132	weak Au, Cu & Zn	Located between the two extended massive bodies and bounded above by brachiated sulfide and below by altered unit
63	TD025	DD	24.5	32.5	weak Zn	overlaid by mafics and under laid by lithic tuff with Quartz grains
64	TD025	DD	90	94	Weak Zn	located between the two massive bodies
65	TRC087	RC	25	31	weak Au, Cu & Pb	found below the alteration zone and the altered material is found inside it
66	10HTD006	DD	10	12	weak Au, Ag, Cu, & Zn	Overlaid by intermediate volcanic and under laid by felsics
67	10HTD006	DD	32.5	46.5	weak Cu & Zn	bounded above by mafic tuff and basalt below it
68	10HTD006	DD	78.2	72.5	Barrel	found between the basaltic units
69	10HTD006	DD	87.5	94	Barrel	overlaid and under laid by basaltic units
70	TRC118	RC	28	43	weak Au,Cu,Pb & Zn	interlayered by altered rock units
71	TRC109	RC	22	27	weak Au, Cu, Pb & Zn	found below the VMS body
72	TD053	DD	0	9	weak Au, Cu, Pb & Zn	found above the VMS body
73	TD053	DD	20	73	weak Cu, Pb, Zn &Ag	very massive
74	TRC007	RC	0	10	weak Au,Cu,Pb,&	overlaying the VMS

					Zn	
75	TRC007	RC	19	31	weak Au, Cu, Pb & Zn	Overlaid and under laid by the massive sulfides
76	TD034	DD	4	7	weak Au, Cu, Pb & Zn	located within the massive bodies
77	TD034	DD	32	80	weak Au, Cu, Pb & Zn	very massive, overlaid by massive sulfide
78	TD036	DD	24	26	Au rich, others weak	found at the lower zone of the VMS body
79	TD036	DD	34.5	81.5	Poor Au, Cu, Pb & Zn	Intruded by quartz vein and under laid by VMS
80	TD036	DD	89.5	91	weak Au, Cu & Zn	under laid by altered sulfide and overlaid by massive sulfide, and it is green
81	TRC060	RC	37	46	weak Au, Ag, Cu, Pb, Zn	bounded above by VMS and below by oxide zones
82	TRC116	RC	25	39	Weak Au, Cu, Pb & Zn	Overlaid by felsic rock and under laid by altered units
83	TD055	DD	12	36	Weak Cu & Zn	overlaid by felsic rock and under laid by lithic tuff
84	TD055	DD	53	98	weak Au, Cu, Pb & Zn	Under laid by VMS units at its base,
85	TD055	DD	107	109	Weak Au, Cu & Zn	above by intermediate volcanic and below by alt unit
86	TD055	DD	131.8	143	weak Zn	overlaid silica, chlorite altered VMS
87	TD055	DD	152.5	170.3	weak Zn only	Overlaid by altered intermediate volcanic rich in chalcopyrite and pyrite
88	TD056	DD	8	66	weak cu, rich Zn & Ag	Rich in Ag at some selected depth intervals
89	TD056	DD	80.5	90.5	weak Zn	found between two large VMS bodies
90	TD056	DD	98	101	weak Au, Zn	overlaid and under laid by VMS bodies
91	TD057	DD	1	18	Ag rich, weak Zn	Under laid by the altered mafics
92	TD057	DD	19.5	23.5	Ag rich, weak Zn	Bounded by mafic below and above
93	TD057	DD	33.5	86.5	Ag rich, Poor Cu & Zn	from 44.5 to 50.5 and 82.5 to 84.5 it is interlayered by Mafics
94	TD057	DD	104	149	Rich Ag & Poor Zn	at depth 38 to 39 & 41 to 43 it is interrupted by VMS body and massive sulfides rich Au, Ag, Cu & Zn
95	TD058	DD	1.5	24.5	weak Cu & Zn	under laid by altered Massive sulfide units
96	TD058	DD	34	45	Weak Zn	under laid by crystal tuff with Quartz eye & overlaid by mafic units
97	TD058	DD	92	115.5	weak Zn	overlaid by alt intermediate volcanic and under laid by mafics
98	TRC004	RC	0	2	Au rich, others weak	Under laid by the Massive sulfide.
99	TRC004	RC	13	31	weak Au, Cu, Pb & Zn	massive body below the VMS and continue below this depth
100	TRC005	RC	0	5	Poor Au, Cu, Pb & Zn	just above the VMS Body
101	TRC005	RC	9	11	weak Au, Ag, Cu, Pb & Zn	found beneath the massive sulfide interrupted from the upper one by VMS
102	09HTD005	TD	10.8	41.5	weak Cu, Pb Zn &	overlaid by intermediate volcanic and under

					Au	laid by felsic volcanic
103	09HTD005	TD	52	61	weak Cu & Zn	overlaid by massive sulfide and under laid by altered felsic volcanic
104	TRC062	RC	16	31	weak Au,Ag,Cu, Pb & Zn	overlaid by altered felsic volcanic and from19-20m it is interrupted by gossans
105	TRC003	RC	0	37	weak Au,Ag,Cu, Pb & Zn	From 0.5-1m depth quartz vein and from 1m-2m by gossans. From 11-14m and from 19-20m it is intruded by quartz vein
106	TRC061	RC	6	19	Poor Au, Cu, Pb & Zn	Overlaid by gossanous material and from 12-15m intruded by quartz vein
107	TRC104	RC	0	16	weak Au,Cu, & Zn	Under laid by the massive sulfide
108	TRC104	RC	23	37	weak Au,Cu, & Zn	Overlaid by the altered and gossanous body
109	TRC058	RC	0	9	Weak Au, Cu, Pb & Zn	Under laid by thick massive sulfide deposit
110	TRC058	RC	39	49	weak of Au, Cu & Zn	overlaid by altered quartz porphyry and massive sulfide
111	TRC008	RC	0	16	weak of Au, Cu & Zn	Under laid by the massive sulfide deposit
112	TRC008	RC	29	37	Ag rich, weak Au,Cu &Pb	Overlaid by the massive sulfide and the gossanous materials
113	TRC009	RC	0	3	weak Au, Ag, Cu, Pb & Zn	Under laid by altered quartz porphyry
114	TRC009	RC	14	18	weak Au, Ag, Cu, Pb & Zn	Overlaid and under laid by VMS deposits
115	TRC009	RC	23	43	Ag rich others weak	Overlaid by the massive sulfide and a continuation of the other quartz porphyry bodies
116	TRC010	RC	28	42	weak Au, Ag, Cu, Pb & Zn	from 33-34m it is rich in Au and Ag
117	TRC059	RC	20	37	weak Au, Cu, Pb & Zn	Overlaid by intensely altered and weathered intermediate volcanic and from 27-30m it is intense altered QPOR
118	TRC011	RC	0	25	weak Au,Cu, & Zn	Very large body possibly extend beyond this depth limit
119	TRC012	RC	0	5	weak Au, Ag, Cu, Pb & Zn	Relatively rich in those metals than the others and under laid by altered materials
120	TRC012	RC	16	20	weak Au, Cu, Pb & Zn	Overlaid by the quartz vein and under laid by the altered material
121	TRC013	RC	46	49	weak Au, Ag, Cu & Pb	Overlaid by altered pyrite material and continued from the other holes in the sections
122	TRC014	RC	0	4	weak Au,Cu, & Zn	Under laid by altered sericite altered porphyries
123	TRC014	RC	36	43	rich Ag others weak	Overlaid and under laid by massive sulfides
124	TRC056	RC	0	25	weak Au,Cu, & Zn	Overlaid by pyrite rich mafic volcanic and under laid by the intermediate volcanic. below IV is massive sulfide
125	TRC056	RC	50	75	weak Au & rich Cu , Zn	Overlaid by the massive sulfide and intruded by the pyrite altered quartz vein
126	TRC110	RC	3	6	weak Au,Cu, & Zn	Overlaid and under laid by altered material;

						also found from 8-9m depth in the same drill hole
127	TRC057	RC	13	16	weak Au,Cu, & Zn	Overlaid and under laid by the massive sulfides.
128	TRC057	RC	21	38	rich Cu, & weak Au, Zn	Overlaid by the massive sulfide and under laid by pyrite altered material
129	TRC016	RC	27	35	weak Au & Cu	Overlaid and under laid by the massive sulfides.
130	TRC017	RC	10	14	weak Au, Cu & Zn	Overlaid by intermediate volcanic and under laid by intensely altered materials
131	TRC017	RC	43	49	Ag rich others weak	Overlaid and under laid by the massive sulfides.
132	TRC018	RC	8	17	Ag rich others weak	Under laid by mafic rocks and overlaid by intermediate tuff
133	TRC018	RC	47	51	Weak Au, Ag, Cu, Pb, Zn	overlaid and under laid by the massive sulfide body
134	TRC018	RC	55	65	Rich Au, Cu, Ag, weak Pb & Zn	Overlaid and under laid by the massive sulfide body
135	TRC018	RC	69	79	Rich Au, Cu, Ag, weak Pb Zn	Overlaid by the quartz vein and possibly continued at greater depth beyond the limit of the drill hole
136	TRC006	RC	8	31	weak Au,Ag,Cu, Pb & Zn	Overlaid & under laid by massive sulfide
137	TD007	DD	28	29	weak Au, Cu & Zn	Bounded between the two massive sulfides
138	TD007	DD	22	28	weak Au, Cu & Zn	bounded by the massive sulfides, just above it there is altered silica
139	TD007	DD	37	42.5	Weak Au & Pb	overlaid by Massive body and under laid by the intermediate volcanic
140	TD007	DD	60.5	93	Rich in Ag, Cu & Zn	overlaid by the intermediate volcanic (IV)
141	TD008	DD	25.2	34	Ag rich, weak Cu & Zn	under laid by altered material and overlaid by the intermediate volcanic
142	TD009	DD	29.5	43	Ag rich, weak Zn	Bounded by two small mafics above and below it
143	TD009	DD	55.6	57	weak Zn	Overlaid by lithic tuff and under laid by the intermediate volcanic
144	TD009	DD	65	67.2	Ag rich and poor Zn	bounded by dolomite
145	TD009	DD	68.4	72	Ag rich, poor Zn & Cu	under laid by mafic and overlaid by crystal tuff
146	TD009	DD	88	90	weak Au, Cu & Zn	under laid by altered bodies & overlaid by the mafic tuff
147	TD009	DD	92	95	weak Au & Cu	Under laid by mafics and overlaid by altered zone.
148	TD009	DD	100	132	Ag Rich & weak Zn	Overlaid and under laid by the mafics.
149	TD011	DD	43	61	Ag Rich & weak Zn	Overlaid by lithic tuff and under laid by dolomite; below the dolomite there is lithic tuff with the lapili grains and altered & from 63.2 to 63.6 Dolomite is interlayered
150	TD011	DD	73.5	97	Ag rich	Overlaid and under laid by Dolomite
151	TD011	DD	111	113	Ag rich	Under laid by dolomite and overlaid by dacite
152	TD011	DD	126.5	131.5	Ag rich	Overlaid by mafics with chlorite alteration and chalcopyrite grains

153	TD011	DD	135	147.4	Ag Rich & weak Zn	Overlaid and under laid by the altered basalt
154	TRC019	RC	1	8	weak Au, Cu, Pb & Zn	Overlaid by intermediate volcanic and under laid by gossanous massive sulfide.
155	TRC019	RC	25	27	weak Au, Ag, Cu & Zn	Overlaid and under laid by pyrite altered materials
156	TRC019	RC	44	49	weak Cu & Zn	Only partially assayed and overlaid by altered materials. The section is dominated by the QPOR where at the center it is massive sulfide body
157	MET09	DD	1	25	weak Au, Cu, Zn	From 7-9m it is interrupted by altered gossanous materials with limonite dominated
158	MET09	DD	33	38	weak Au, Cu, Zn	Overlaid by altered gossans with hematite dominated and under laid by quartz vein
159	MET09	DD	42	45	weak Au, Cu	under laid by pyrite altered material and overlaid by altered intermediate volcanic
160	TRC020	RC	36	48	weak Au, Zn & Cu	overlaid and under laid by two massive sulfide bodies
161	TRC020	RC	62	67	weak Ag, Cu, Pb, Au & Zn	overlaid by pyrite altered material and intrudes the small massive sulfide bodies
162	TRC021	RC	37	40	Rich Au, Ag,& poor Cu& Pb	Overlaid by thick quartz vein and under laid by pyrite rich massive sulfide body. It is within the large massive sulfide body
163	TRC022	RC	0	13	weak Au,Ag,Cu, Pb & Zn	under laid by the altered material and the massive sulfide body
164	TRC100	RC	8	15	weak Cu, Pb & Zn, rich Au	Overlaid and under laid by the massive sulfide.
165	TRC023	RC	0	17	weak Au,Ag,Cu, Pb & Zn	It is under laid by the intermediate volcanic
166	TRC023	RC	48	61	Weak Au, Cu, Pb, Zn & Ag rich	Overlaid by the massive sulfide and possibly continued at depth and under laid by the massive sulfide
167	TRC024	RC	46	48	rich Au, Cu, Ag, weak Pb & Zn	Under laid by the quartz vein and overlaid by the massive sulfide.
168	TRC024	RC	51	53	weak Au, Ag, Cu, Pb & rich Zn	Under laid by the massive sulfide and overlaid by the pyrite altered QPOR
169	TRC025	RC	0	4	Weak Au,Ag,Cu, Pb & Zn	under laid by altered intermediate volcanic like
170	TRC027	RC	7	43	weak Au,Ag,Cu, Pb & Zn	From 10-12m and 28-29m it is rich in Au, Ag & Cu and at this depth interrupted by the massive sulfides. Overlaid by altered QPOR and under laid by pyrite altered material.
171	TRC028	RC	17	24	weak Au,Ag,Cu, Pb & Zn	Overlaid and under laid massive sulfide bodies
172	TRC028	RC	59	65	weak of Au, Cu & Zn	overlaid and under laid by altered intermediate volcanic
173	TRC026	RC	0	7	weak Au,Ag,Cu, Pb & Zn	under laid by the quartz vein and below it is the massive sulfide
174	TRC026	RC	21	32	rich Au weak Ag, Cu, Pb, & Zn	overlaid and under laid by the massive sulfides

175	TRC029	RC	27	36	weak Au,Ag,Cu, Pb	In the upper part partially rich In Au and Ag. overlaid and under laid by the massive bodies
176	TRC029	RC	46	51	Rich Au, Cu, Ag, Weak Pb, Zn	Inserted within the massive sulfide body. Characterized by pyrite altered bodies
177	TRC029	RC	68	73	Weak Au, Cu, Pb, Zn & rich Ag	overlaid by pyrite altered material and below the massive sulfide bodies
178	TRC033	RC	66	67	rich Au, Ag; weak Cu, Pb & Zn	Under laid by sub massive sulfide and overlaid by altered sub massive sulfide ore
179	TRC033	RC	70	73	Au rich, weak Ag, Cu, Pb & Zn	under laid by 2m quartz vein with pyrite and overlaid by massive sulfide
180	TRC033	RC	75	97	Rich in Au, Ag, Cu & Zn poor Pb	From 73-75m it is Intrude by the quartz vein and inserted within the massive sulfide bodies
181	TRC032	RC	0	20	weak Au, Ag, Cu, Pb & Zn	highly weathered and under laid by altered material
182	TRC032	RC	34	44	weak Au, Cu & Zn	bounded by the two massive bodies
183	TRC031	RC	22	33	weak of all	Overlaid and under laid by massive sulfides
184	TRC031	RC	43	58	weak Au, Cu, Zn	Under laid by intermediate volcanic and overlaid by the massive body
185	TRC030	RC	26	49	weak Au, Cu, Zn	overlaid and under laid by the intermediate volcanic
186	10HTD001	DD	78	86	Ag rich & weak Zn	overlaid by sub massive sulfide and under laid by silica and pyrite altered disseminated sulfide
187	TD037	DD	70	99.4	weak au, Cu, Zn	Overlaid by the mineralized massive sulfide and under laid by the andesite volcanic with silica alteration.
188	TD035	DD	36	52	weak Cu & Zn	under laid by the massive sulfide and overlaid by altered massive sulfide
189	TRC036	RC	0	29	weak of all	under laid by the massive sulfide
190	TRC036	RC	37	76	weak all	From 55-77m it its intruding the massive sulfide and rich in Au, Cu & Ag others are poor in All. From 63-65m it is interrupted by the massive sulfide body.
191	09HTD003	DD	23	37	weak Cu & Zn; rich in Ag	Under laid by pyrite altered disseminated sulfide volcanic and overlaid by mineralized massive sulfide.
192	09HTD003	DD	52	64	Weak Cu, Zn & rich Ag	Under laid by pyrite rich mafic volcanic and overlaid by mineralized massive sulfide
193	09HTD003	DD	81	126	Ag rich & weak cu & Zn	Overlaid by the quartz vein
194	TRC035	DD	48	49	poor of all	Possibly continued at depth. Overlaid by pyrite altered material
195	TD054	DD	43	48.9	barren	very small anomaly of Cu & Zn
196	TRC055	RC	0	11	weak Au, Ag, Cu, Pb, & Zn	Under laid by thick and altered intermediate volcanic. Continued dipping to the east
197	TRC055	RC	52	74	Rich Au, Ag, Cu, Zn & Pb	it intrudes the massive sulfide body and under laid by the pyrite altered intermediate volcanic
198	TD039	DD	10	63.5	weak Cu & Zn	Overlaid by chlorite altered mafic material and under laid by oxide gossans
199	TD039	DD	80.5	87	weak Au, Cu, Pb &	Overlaid by silica altered breccias and under

					Zn	laid by massive sulfide
200	TD039	DD	10.5	114	Weak all	Overlaid by silica altered stringer sulfide body and under laid by the thin and highly mineralized massive sulfide up to 3.61 Au
201	TD033	DD	97	107.5	weak Zn	overlaid by the maffic tuff and under laid by the silicified tuff
202	TD038	DD	110.5	120	weak Zn	overlaid by pyrite intermediate tuff and under laid by chlorite intermediate tuff
203	TD028	DD	97.5	108.5	weak Zn	Chloritized QPOR. Overlaid by chlorite altered material and under laid by disseminated sulfide rich chlorite altered maffic tuff
204	TD028	DD	141.2	148.5	weak Zn	overlaid by silica, chlorite and pyrite altered maffic material
205	09HTD002	DD	116	127.5	Ag rich and weak Zn	overlaid by silica and pyrite rich stringer sulfide